Skeletal muscle BMAL1 is necessary for transcriptional adaptation of local and peripheral tissues in response to endurance exercise training.

Author Information

Mark R Viggars[1,2], Hannah E Berko[1,2], Stuart J Hesketh[1,2,3], Christopher A Wolff[1,2], Miguel A Gutierrez-Monreal[1,2], Ryan A Martin[1,2], Isabel G Jennings[1,2], Zhiguang Huo[4], Karyn A Esser[1,2].

Affiliations

[1]Department of Physiology and Aging, University of Florida, Gainesville, Florida, United States.

[2]Myology Institute, University of Florida, Gainesville, Florida, United States.

[3]School of Medicine, University of Central Lancashire, United Kingdom.

[4]Department of Biostatistics, University of Florida, Gainesville, Florida, United States.

Author contributions

M.R.V, S.J.H, K.A.E conceived and designed research. M.R.V, S.J.H, M.A.G, C.A.W, R.A.M, H.E.B, I.G.J performed experiments. M.R.V, M.A.G, Z.H analysed data. M.R.V, R.A.M, M.A.G, K.A.E interpreted results of experiments. M.R.V prepared figures, M.R.V, K.A.E drafted manuscript. M.R.V, K.A.E edited and revised manuscript, M.R.V, S.J.H, M.A.G, C.A.W, R.A.M, H.E.B, I.G.J, Z.H, K.A.E approved final version of manuscript.

Declaration of Interests: The authors declare no competing interests.

Keywords: Exercise, circadian, skeletal muscle, metabolism, inflammation, transcription.

Corresponding author

Correspondence to: Karyn A Esser kaesser@ufl.edu ORCID 0000-0002-5791-1441.

Mark R Viggars m.viggars@ufl.edu ORCID: 0000-0002-0722-7051.

Physical Address: Department of Physiology and Aging, University of Florida, Gainesville, Florida, USA.

Abstract:

Objectives: In this investigation, we addressed the contribution of the core circadian clock factor, BMAL1, in skeletal muscle to both acute transcriptional responses to exercise and transcriptional remodelling in response to exercise training. Additionally, we adopted a systems biology approach to investigate how loss of skeletal muscle BMAL1 altered peripheral tissue homeostasis as well as exercise training adaptations in iWAT, liver, heart, and lung of male mice.

Methods: Combining inducible skeletal muscle specific BMAL1 knockout mice, physiological testing and standardized exercise protocols, we performed a multi-omic analysis (transcriptomics, chromatin accessibility and metabolomics) to explore loss of muscle BMAL1 on muscle and peripheral tissue responses to exercise.

Results: Muscle-specific BMAL1 knockout mice demonstrated a blunted transcriptional response to acute exercise, characterized by the lack of upregulation of well-established exercise responsive transcription factors including *Nr4a3* and *Ppargc1a*. Six weeks of exercise training in muscle-specific BMAL1 knockout mice induced significantly greater and divergent transcriptomic and metabolomic changes in muscle. Surprisingly, liver, lung, inguinal white adipose and heart showed divergent exercise training transcriptomes with less than 5% of 'exercise-training' responsive genes shared for each tissue between genotypes.

Conclusion: Our investigation has uncovered the critical role that BMAL1 plays in skeletal muscle as a key regulator of gene expression programs for both acute exercise and training adaptations. In addition, our work has uncovered the significant impact that altered exercise response in muscle plays in the peripheral tissue adaptation to exercise training. We also note that the transcriptome adaptations to steady state training suggest that without BMAL1, skeletal muscle does not achieve the expected homeostatic program. Our work also demonstrates that if the muscle adaptations diverge to a more maladaptive state this is linked to increased inflammation across many tissues. Understanding the molecular targets and pathways contributing to health vs. maladaptive exercise adaptations will be critical for the next stage of therapeutic design for exercise mimetics.

Keywords: Circadian Biology; Exercise; Transcription; Metabolism; Signal Transduction; Inflammation.

1. Introduction:

Circadian transcription factors and their autoregulatory transcription-translation feedback loops (TTFL) regulate skeletal muscle homeostasis through both transcriptional and epigenetic regulation [1–3]. The daily gene expression program regulated by the clock mechanism, called clock output, contributes to temporal patterning of a wide range of biological processes including skeletal muscle metabolism and proteostasis [4], as we and others have previously published [5–8].

A clear interaction between exercise and the circadian TTFL has been established in recent years. Genes encoding the negative limb of the TTFL have been shown to be responsive to acute exercise/muscle contraction (e.g., *Pers*, *Nfil3*) [9–16] and exercising at different times of the day is known to lead to unique metabolomic and transcriptional outcomes [17–20]. Exercise training also directly impacts the circadian transcriptome, by increasing the number of clock output genes [21,22]. Various exercise performance measures such as strength and endurance capacity also present time-of-day differences, highlighting a likely role of the muscle clock in overall muscle function [21–27]. While it is clear that exercise and the skeletal muscle circadian TTFL are linked [4], the question of whether the muscle clock has any impact on either the acute response or training induced adaptations in skeletal muscle is yet to be elucidated.

Here we asked whether the core clock factor, *Bmal1* is necessary in skeletal muscle for either the acute exercise response and/or adaptations to exercise training. Additionally, we probed the systemic impact of the loss of muscle *Bmal1* on the adaptations in other peripheral tissues. Our results determined that the core clock factor *Bmal1*, is necessary for the acute molecular response to exercise with notable loss of up-regulation of well-known exercise response genes including *Ppargc1a* and *Nr4a3* [28,29]. We also determined that muscle *Bmal1* is required for the expected transcriptional and metabolomic response to treadmill training in muscle. We found less than 5% of the exercise training induced changes in gene expression were identified in the absence of muscle *Bmal1*. Lastly, we found that loss of muscle *Bmal1* also contributes to a significant divergence in the exercise training transcriptional changes in all peripheral tissues studied including the heart, lung, liver, and white adipose tissue. Importantly these divergent transcriptional outcomes with acute exercise and following training were apparent even though the exercise workloads, speed, grade, and duration, were equivalent between genotypes. Our results identify the core circadian clock factor, *Bmal1*, in skeletal muscle as an integral transcriptional modulator for acute exercise and training adaptations. In addition, these results highlight the importance of the muscle for peripheral tissue transcriptome changes in response to exercise training.

2. Materials & Methods:

2.1. Ethical Approval

84 All animal and experimental procedures in this study were conducted in accordance with the
85 guidelines of the University of Florida for the care and use of laboratory animals (IACUC #202100000018).
86 The use of animals for exercise protocols was in accordance with guidelines established by the US Public
87 Health Service Policy on Humane Care and Use of Laboratory Animals.

88 2.2. Skeletal Muscle Specific *Bmal1* Knockout Mouse Model

89 Male inducible skeletal muscle-specific *Bmal1* knockout mice were generated as previously
90 described [5,6]. Activation of Cre recombination was performed by intraperitoneal injections of tamoxifen
91 (2 mg/day) dissolved in sunflower seed oil for five consecutive days when the HSA-Cre+/-; Bmal1 fl/fl mice
92 reached ~4 months of age. These mice are referred to as iMSBmal1KO mice henceforth. Controls were
93 $Cre^{+/-}$:$Bmal1^{fl/fl}$ mice treated with a vehicle (15 % ethanol in sunflower seed oil) and are referred to as
94 Vehicle treated mice.

95 To assess recombination specificity within the gastrocnemius DNA was extracted from ~1-5mg of
96 muscle post-mortem, lysed in tail lysis buffer (10mM Tris pH 8, 100mM NaCl, 10mM EDTA, 0.5% SDS
97 and 20mg/ml of Proteinase K) and DNA purified using the DNeasy Blood and Tissue Kit (Qiagen, Venlo,
98 Netherlands). PCR was performed with extracted DNA and primers for the recombined and non-
99 recombined alleles as previously described [5]. For the training study, lack of recombination was confirmed
100 in the inguinal white adipose tissue, liver, heart, and lung. Recombination specificity for tissues in this
101 cohort is provided in Supplementary Figure 1.

102 A total of 40 mice were used in this experiment, (n=20 vehicle and n=20 iMSBmal1KO mice).
103 Mice were randomly assigned to a control or an acute exercise group (Vehicle Control n=10, Vehicle
104 Exercise n=10, iMSBmal1KO Control n=10, iMSBmal1KO Exercise n=10). Mice assigned to the acute
105 exercise bout experiment were group housed (2-5 per cage) at 23 ± 1.5°C, 58 ± 5.8% relative humidity
106 within temperature and humidity controlled light boxes. Light schedules were maintained on a 12:12 h
107 light: dark schedule with *ad libitum* access to standard rodent chow (Envigo Teklad 2918, Indianapolis, IN,
108 USA) and water. The macronutrient content of this chow is 24% protein, 18% fat and 58% carbohydrate,
109 presented as a percent of calorie intake. Experiments were performed in two cohorts that differed
110 significantly by age (30 weeks vs. 77 weeks, p<0.0001) (Supplementary Figure 2A), but were randomly
111 and evenly distributed across the vehicle and iMSBmal1KO groups. Following randomization, no
112 differences in age were observed between ages of vehicle and iMSBmal1KO mice, (p=0.86),
113 (Supplementary Figure 2B).

114 An additional 21 mice were used for exercise training experiments. 21 male mice were randomly
115 assigned to tamoxifen or vehicle treatment, with or without exercise training at ~11 months of age (7-
116 months post tamoxifen treatment). For clarity, these groups will be referred to in future text as Vehicle
117 Control (n=5), Vehicle Exercise Trained (n=5), iMSBmal1KO Control (n=6), and iMSBmal1KO Exercise

Trained (*n*=5). Mice were single housed in conditions of 23 ± 1.5°C, 58 ± 10% relative humidity within temperature and humidity controlled light boxes. Light schedules were maintained on a 12:12 h light: dark schedule with *ad libitum* access to standard rodent chow (Envigo Teklad 2918, Indianapolis, IN, USA) and water. To maintain standardised nomenclature for this study, we will reference time through use of zeitgeber time (ZT), where ZT0 refers to time of lights on and ZT12 refers to time of lights off. The active period of the day for mice is from ZT12-ZT24 and their rest period is ZT0-ZT12. All physiological testing, treadmill familiarization and exercise/training sessions were performed in the active phase so transportation of mice from housing to the treadmill room was in a light tight cart and the treadmill room was dark with red lights.

2.3. Treadmill Familiarization, Graded Exercise Test, Grip Strength & Rotarod

Mice from all groups/experiments were first subjected to treadmill familiarization under red light on a Panlab treadmill (Harvard Apparatus, Holliston, MA) at ZT13. Familiarization consisted of 3 sessions performed on 3 consecutive days. The first familiarization session started at 10 cm/s for 5 min at 0° incline. The incline was then adjusted to 5° and speed was increased by 2 cm/s every 2 min up to 20 cm/s (15 minutes total). The second day consisted of an increase in speed every 3 min by 3 cm/s from 10 cm/s to 24 cm/s at an incline of 10°, (18 minutes total). The final familiarization session was the same as the second but performed at a 15° incline, (18 minutes total).

Following 1 day of rest, mice were subject to a graded treadmill exercise test to serve as a baseline performance measure, conducted at ZT13 under red light. For the graded exercise test, animals began at a speed of 10 cm/s at 10° incline for a 5 min warm-up. From which the incline was increased to 15° and the treadmill speed increased by 3 cm/s every 2 min until exhaustion. The treadmill was operated with the electrical shock grid turned off and mice gently encouraged by a compressed air canister when needed. Mice were deemed to be exhausted when they remained in contact with the back of the treadmill >15 s and could not be encouraged to move away by the compressed air.

Mice in groups assigned to an acute exercise bout were given ~1-week of rest before their acute exercise bout. This consisted of a 30-minute treadmill bout at ZT13 in which the mice would complete 70% of the work done within the graded exercise test (group mean), calculated according to previous work [30], work done = (M·D· sin q). M is the mass (g) of the animal, D is the distance (m) ran in the graded exercise test and sin q is the slope (15°) of the treadmill. Work done is measured in arbitrary units (AU).

Mice in groups assigned to exercise training were given 2-weeks of rest post familiarization before their 6-weeks of exercise training commenced. Exercise training was always completed at ZT13 under red light, 5 times per week for a total of 30 individual exercise training bouts. Each bout consisted of 1 hour of treadmill running in which mice would complete 100% of the work done in their prior graded exercise test (group mean). Additional graded exercise tests were conducted at the end of 2 and 4 weeks of training to account for increases in performance and adjustment of exercise speed during training sessions. As a result,

152 treadmill speed was set to 18cm/s for weeks 1-2, 25.5cm/s for weeks 3-4 and 29cm/s for weeks 5-6 for both
153 groups. At the end of 6-weeks training a final maximal capacity test was performed to serve as a post
154 training comparison.

155 Forelimb grip strength (N/gBW) measures were performed between ZT13-14 on mice from the
156 acute exercise cohort using a Harvard Apparatus grip strength meter (average of 5 trials). Rota Rod (Panlab)
157 performance was also measured in 3 trials and averaged, data is presented in Supplemental Figure 1.

158 2.4. Body Composition Analysis (Echo-MRI)

159 Body composition was assessed by nuclear magnetic resonance (Echo MRI-100 Body Composition
160 Analyzer; Echo Medical Systems, Houston, TX) prior to treadmill familiarization at ZT13. For the exercise
161 training cohort, measurements were taken in the week prior to starting exercise training, after 3 weeks and
162 after 6 weeks of exercise training. Lean and fat mass (grams) are presented as percentage changes over time
163 as well as a percentage of total body weight over time.

164 2.5. Food Intake & Cage Activity Measurements

165 As described above, mice were individually housed to track food intake and cage activity. Food
166 and body mass were weighed on a weekly basis to assess changes in food intake relative to body weight.
167 The daily activity of the mice in their home cages were continuously recorded throughout the entire
168 experiment using wireless infrared activity monitoring (Actimetrics, Wilmette, IL, USA) and analysed
169 using ClockLab software 7. Average counts per week were calculated for the 4-weeks prior to training,
170 weeks 1-2, 3-4 and 5-6. The hour during treadmill running +/- 30 minutes was excluded from each
171 individual's analysis.

172 2.6. Tissue Collection

173 All animals were humanely sacrificed following the experiments using isoflurane anaesthesia (2-
174 3%) in oxygen followed by cervical dislocation performed under red light. For the acute exercise bout
175 experiments, tissue was collected 1-hour post the end of their acute exercise bout (ZT14.5). Control,
176 unexercised mice were collected alongside the acute exercise groups as time-of-day matched controls.
177 Gastrocnemius muscles from the hindlimbs were dissected, cleaned of excess fat and connective tissue and
178 flash frozen in liquid nitrogen before storage at -80°C. For the training study, animals were humanely
179 sacrificed as above, 47 hours after the exercise trained mice final maximal capacity test at ZT13. Hindlimb
180 muscles, iWAT, liver, heart and lungs were dissected and cleaned of excess fat and connective tissue. The
181 heart and lungs were gently perfused with phosphate buffered saline. Muscles from the left hindlimb were
182 weighed and flash frozen in liquid nitrogen and muscles from the right hindlimb embedded in optimal
183 cutting temperature compound (OCT) before snap freezing in isopentane pre-cooled by liquid nitrogen.
184 Muscles were stored at -80°C until biochemical analysis or cryo-sectioning.

185 ## 2.7. Blood/plasma collection & Analysis

186 For the training study, blood samples ~50ul were collected from the tail veins of all mice at ZT13
187 prior to the maximal exercise test, 48 hours prior to tissue collection. Blood glucose levels were measured
188 at this point using the OneTouch® UltraMini system (OneTouch Solutions, UK). A whole blood aliquot
189 was kept on ice for assessment of glycosylated hemoglobin content (Hba1c%) (#80310, Crystal Chem High
190 Performance Assays, IL, USA) as per manufacturer's instructions. Endpoint colorimetric measurements
191 were made using the Molecular Devices Spectramax i3X system (Molecular Devices LLC, CA, USA). The
192 remaining blood was collected in EDTA coated plasma tubes before centrifugation at 4°C for 10 mins at
193 2000RCF. The plasma was frozen and stored at -20°C. Insulin concentration was measured using a
194 commercially available kit (#90080, Crystal Chem High Performance Assays, IL, USA) as per
195 manufacturer's instructions.

196 ## 2.8. Gastrocnemius Muscle & Liver Glycogen/Triglyceride Content Analysis

197 Small (~15mg) snap-frozen pieces from the gastrocnemius muscle and liver (n=5 per group) were
198 used to detect glycogen/triglyceride content. Care was taken to ensure the same location of each tissue was
199 sampled across replicates. For glycogen, tissue samples were weighed and homogenized in 100µl of
200 glycogen hydrolysis buffer in a bullet blender (BBY24M, Next Advance, NY, USA), at speed 10 for two,
201 2-min sets, at 4°C using 0.5mm stainless steel beads. Homogenates were boiled at 95°C for 5 mins to
202 inactivate enzymes, then centrifuged at 12,000 rpm for 5 mins at 4°C to remove insoluble material. Muscle
203 glycogen concentrations were then quantified from the supernatant using a commercially available kit
204 (Sigma-Aldrich-MAK016) according to manufacturer's instructions. Glycogen concentrations were
205 normalized to input tissue weight. For triglyceride analysis, tissue was homogenized as above in
206 chloroform: methanol (2:1). Samples were incubated for 30 mins at 20°C with shaking at 1,400rpm.
207 Samples were then centrifuged at 13,000rpm for 30 mins at 20°C. The liquid phase was mixed with 0.9%
208 NaCl and centrifuged at 2,000rpm for 5 mins. Chloroform: Triton X-100 (1:1) was added to the organic
209 phase and solvents evaporated. Triglycerides were then measured using a commercially available kit
210 (Abcam, (ab65336), according to manufacturer's instructions. Triglyceride concentrations were normalized
211 to input tissue weight.

212 ## 2.9. Fibre Morphology Analysis

213 Histological samples were transversely sectioned (10µm thick) from the mid-belly of the
214 gastrocnemius, soleus and plantaris muscles and labelled with a cocktail of antibodies against isotype-
215 specific anti-mouse primary antibodies for types IIA (SC-71) and IIB (BF-F3) (1:100) from Developmental
216 Studies Hybridoma Bank (DSHB) (Iowa City, Iowa, USA), and an antibody against dystrophin (1:100,
217 ab15277, Abcam, St. Louis, MO, USA) overnight as previously described [31,32]. Following overnight

218 incubation, sections were washed for 3x5 mins with phosphate buffered saline (PBS) before AlexaFluor
219 secondary antibodies against Rabbit IgG H&L, Mouse IgG1, Mouse IgG2B (Invitrogen/Thermofisher,
220 USA) were added for 2 hours before 3x5 min washes with PBS. Sections were post-fixed in methanol for
221 5 mins before 3x5 min washes with PBS. Sections were carefully dried to remove excess PBS before
222 mounting in Vectashield Antifade Mounting Medium (Vector Laboratories, UK). For nuclei counting,
223 sections were just labelled with dystrophin and counterstained for nuclei with DAPI. Additional labelling
224 was performed as above using an antibody against embryonic myosin (BF-G6, DSHB). Embryonic myosin
225 positive fibers were counted manually using Image Jv1.53, excluding intrafusal muscle fibers of muscle
226 spindles, and expressed as a percentage of total fibers identified. Manual counting of central nuclei was
227 also performed in this manner. Whole labelled cross sections were imaged at 20x using a Leica TCS SPE
228 microscope equipped with a DFC7000 camera (Leica, Germany). LAS Navigator software was used to
229 generate a merged image of the whole muscle cross-section. Fiber type distribution, overall muscle fibre
230 cross-sectional area (CSA) and total nuclei/myonuclei per fiber was characterised using MyoVision 2.2
231 automated software [31]. For succinate dehydrogenase (SDH) staining, cryosections were incubated at
232 37°C for 1 hour with a sodium succinate buffer (50mM sodium succinate, 50mM phosphate buffer and
233 0.5mg/ml nitroblue tetrazolium) before washing in distilled water and imaged as above. Colorimetric
234 images were converted to greyscale 8-bit image and SDH labelling intensity quantified using the polygon
235 selection tool to select within the muscle cross-section and raw intensity density measurement tool as
236 standard in Image Jv1.53.

237 ## 2.10. RNA Isolation, Library Preparation & RNA-sequencing

238 For the acute exercise bout experiment, gastrocnemius muscles were powdered under liquid
239 nitrogen and ~20mg weighed and placed in 500 µl of Trizol (Invitrogen 15596018). Tissue samples were
240 homogenized in a bullet blender using 0.5mm stainless steel beads (BBY24M, Next Advance, NY, USA)
241 for 2 mins at 4°C. RNA was isolated using the RNeasy Mini Kit (Qiagen 74104) according to the
242 manufacturer's protocol. DNase digest was performed on column using the RNase-Free DNase Set (Qiagen
243 79254). RNA concentration and purity were assessed by UV spectroscopy at ODs of 260 and 280 nm using
244 a Nanodrop (ThermoFisher One/One UV spectrophotometer, USA). RNA integrity numbers (RIN) were
245 subsequently determined on an Agilent TapeStation 2200 (Agilent, CA, USA), and all samples prepared
246 for sequencing had RIN values of at least 8. Preparation of poly-A tail selected RNA libraries (Illumina
247 mRNA Prep kit (Illumina, Inc. CA, USA)) and whole transcriptome sequencing (Novaseq 6000 (Illumina,
248 Inc. CA, USA)), was conducted by Novogene Co., LTD (Durham, NC) in a 2x150bp format for the acute
249 exercise bout study. A total of 20 samples were sequenced with a read depth of around ~25 million paired
250 end reads per sample, *n*=5 per group (~30 weeks of age).

251 For the exercise training experiment, RNA was extracted and sequenced in the same format as
252 above but was performed by the University of Florida ICBR Gene Expression and Genotyping Core
253 Facility, RRID:SCR_019145 and the University of Florida ICBR NextGen DNA Sequencing Core Facility,
254 RRID:SCR_019152 for gastrocnemius muscle, liver and heart (*n*=5 per group). iWAT and lung, (*n*=3 per
255 group) were completed as above by Novogene Co., LTD (Durham, NC).

256 2.11. RNA-seq Bioinformatic Analysis

257 FastQ files were imported to Partek® Flow® Genomic Analysis Software (Partek Inc. Missouri,
258 USA) for pipeline processing. Pre-alignment QA/QC was performed on all reads prior to read trimming
259 below a Phred quality score of 25 and adapter trimming. STAR alignment 4.4.1d was used to align reads
260 to the Mus Musculus, mm10 genome assembly. Aligned reads were then quantified to the Ensembl
261 transcriptome annotation model associated with Mus Musculus mm10, release 99_v2. Gene expression was
262 normalized using DESeq2 median of ratios within tissues. Differentially expressed genes (DEGs) were
263 identified through the Partek® Flow® DESeq2 binomial generalized linear model with Wald testing for
264 significance between conditions. In Supplementary Figure 3, we overlapped the queried vehicle exercise
265 responsive DEGs with a previously published BMAL1:CLOCK chromatin immunoprecipitation with
266 sequencing dataset from our lab to identify directly bound genes within murine gastrocnemius muscle (any
267 genomic region, FDR <0.001) [33].

268 2.12. Assay For Transposase-Accessible Chromatin Using Sequencing (ATAC-seq)

269 A whole gastrocnemius muscle was diced and then homogenized using a Polytron homogenizer in
270 homogenization buffer (Homogenization buffer (10mM HEPES, pH 7.5, 10mM MgCl2, 60mM KCl,
271 300mM sucrose, 0.1mM EDTA, 0.1% Triton, 1mM DTT, complete with mini protease inhibitor mix).
272 Homogenates were spun at 300rpm for 3 minutes and supernatant containing nuclei moved to a new tube.
273 This was repeated 3 times. The supernatant was then filtered through a 40µm cell strainer before
274 centrifugation at 1000g for 10 minutes. The nuclei pellet was then resuspended in 1.2ml of homogenization
275 buffer, gently triturated and 200µl loaded on top of 2.15M sucrose cushions (10mM HEPES, pH 7.5, 10mM
276 MgCl2, 60mM KCl, 2.15M sucrose, 0.1mM EDTA, 0.1% Triton, 1mM DTT, complete with mini protease
277 inhibitor mix). Nuclei samples were centrifuged at 13,500g at 4°C for 1.5 hours. Samples were aspirated
278 and washed leaving a nuclei pellet, free of cytoplasmic fragments. Nuclei were quality checked using light
279 microscopy (intact nuclei, no blebbing, free of cytoplasmic fragments) and then counted. 50,000 nuclei
280 were used for input into a commercially available ATAC-seq kit which includes library preparation
281 (#53150, Active Motif, Inc., CA, USA). We have previously determined that this isolation technique yields
282 ~70% myosin heavy chain expressing nuclei through RNA-sequencing, (unpublished data). Libraries were
283 assessed via Bioanalyzer to compare library fragments ranging from 250-1000bp with an oscillation period

284 at ~150bp. were sequenced by the UF ICBR Nextgen DNA Sequencing facility RRID:SCR_019152 with
285 ~70 million paired-end reads per sample in a 2x150bp format.

286 2.13. ATAC-seq Bioinformatic Analysis

287 Fastq files were imported to Partek® Flow® Genomic Analysis Software (Partek Inc. Missouri,
288 USA) for processing. Pre-alignment QA/QC was performed on all reads prior to read trimming below a
289 Phred quality score of 30 and adapter trimming. Alignment was performed using Bowtie2 to the mm10
290 genome, and peak detection/calling performed using MACS2. Peaks were quantified, normalized using
291 Deseq2 (median of ratios) before differential analysis to identify differentially accessible regions (DARs)
292 between conditions (significant differences in peak heights P= 0.01). ATAC peaks mapping to any genomic
293 region were included in the differential analysis. 24.3% of peaks corresponded to the transcription start site,
294 5.2% aligned to the transcription termination site, 4% to exons, 8.5% to 5' untranslated regions (UTR),
295 3.1% to 3'UTR regions, 29.3% to intronic regions and 25.6% to intergenic regions.

296 2.14. Pathway & Motif Analysis

297 Biological interpretation of filtered/selected gene lists was performed using DAVID [34] to identify
298 associated Kyoto Encyclopedia of Genes and Genomes (KEGG), Reactome and Biological Processes
299 pathways. HOMER (v4.11) motif analysis was performed on DEGs, to identify enrichment of known motifs
300 (6-12bp long) in the gene body and up to 2kb upstream of the transcription start site. Upset plots were
301 created using Intervene, a publicly available software [35].

302 2.15. LC-MS Metabolomics

303 Gastrocnemius muscle samples (n=5 per group) underwent cellular extraction procedures
304 (Southeast Center for Integrated Metabolomics, SECIM). Global metabolomics profiling was performed
305 on a Thermo Q-Exactive Orbitrap mass spectrometer with Dionex UHPLC and autosampler. All samples
306 were normalized by total protein content prior to extraction. Samples were analyzed in positive and negative
307 heated electrospray ionization with a mass resolution of 35,000 at m/z 200 as separate injections. Separation
308 was achieved on an ACE 18-pfp 100 x 2.1 mm, 2 µm column with mobile phase A as 0.1% formic acid in
309 water and mobile phase B as acetonitrile. This is a polar embedded stationary phase that provides
310 comprehensive coverage but does have some limitations in coverage of very polar species. The flow rate
311 was 350 µL/min with a column temperature of 25°C. 4µL was injected for negative ions and 2 µL for
312 positive ions. MZmine (freeware) was used to identify features, deisotope, and align features. All adducts
313 and complexes were identified and removed from the data set. The mass and retention time data was
314 searched against SECIMs internal metabolite library, and known metabolites were mapped to KEGG IDs.
315 Blank feature filtering was performed using inner-quartile range filtering as implemented in the R package
316 MetaboAnalystR (https://github.com/xia-lab/MetaboAnalystR). Missing data were imputed by k-nearest

neighbour imputation and peak intensities were normalized sample-wise using sum normalization followed by log^{10} transformation and pareto scaling as implemented R package MetaboAnalystR. Univariate ANOVA was performed using the R package stats (R Core Team 2023) to determine whether there was a significant effect of variable Class on metabolite peak intensity, and post-hoc pairwise comparisons were performed using least-squares means method as implemented in the R package emmeans (R.V. Lenth 2023). Adjusted p-values are adjusted for multiple pairwise comparison testing, not testing of multiple metabolites. A significance threshold was set at an FDR of 5%. Metaboanalyst 5.0 [36] was used to perform enrichment analysis on annotated features against the KEGG metabolite set library.

2.16. Statistical Analysis

Unless otherwise stated, physiology data are presented as mean ± standard deviation (SD) and statistical analyses conducted in GraphPad Prism 9.4.1. For multiple comparisons, data were analysed using one, or two factor analysis of variance (ANOVA) followed by Tukey's multiple comparisons test. Repeated measures ANOVA were performed on measures where the same subjects were measured over time. To assess differences between exercise training groups only, two-tailed independent student t-tests were performed to evaluate statistical differences. All statistically significant thresholds were considered at the level of $P < 0.05$. Corresponding symbols to highlight statistical significance are as follows; $*P \leq 0.05$, $**P \leq 0.01$, $***P \leq 0.001$, $****P \leq 0.0001$.

2.17. Data Availability

RNA-seq data is available in Supplementary File 1 and raw data can be found at the GEO accessions GSE255280 (acute exercise), GSE240653 (gastrocnemius training), GSE253735 (peripheral tissue training). Chromatin accessibility data (ATAC-seq is available in Supplementary File 1 and raw data can be found at GSE255376. LCMS metabolomics data is available in Supplementary File 2.

3. Results:

3.1 Loss of the skeletal muscle clock significantly alters the acute exercise transcriptional response.

Previous work has identified that acute exercise performed at different time of the day leads to divergent transcriptional responses [18] suggesting that the acute response to exercise is modulated by the muscle circadian clock. To directly test this, we exposed vehicle treated and iMSBmal1KO mice to a workload-matched 30-minute treadmill exercise bout and performed transcriptional analysis on the gastrocnemius muscles at 1-hour post completion of the bout, (Figure 1A). Physiological phenotyping is available in Supplementary Figure 2. Despite vehicle and iMSBmal1KO mice completing the same amount of treadmill work (Figure 1B), the acute transcriptional response was significantly different in many

349 parameters. First, we noted the iMSBmal1KO muscle exhibited a 48% reduction in the number of exercise
350 responsive genes with 517 genes changed (250 upregulated and 267 downregulated: $q < 0.05$) compared to
351 the 989 genes that changed in the muscle of vehicle mice (600 upregulated and 389 downregulated), (Figure
352 1C). Only 117 of these genes were common as exercise response genes in both genotypes, (Figure 1D).
353 Within this shared group of exercise responsive genes 'Biological rhythms' was the most enriched pathway
354 (Figure 1E), driven by changes in expression of genes in the negative limb of the E-box feedback loop
355 (*Per1*, *Per2*) and RORE element/D-box feedback loop (*Nfil3*) which are still responding to the exercise
356 bout despite the absence of BMAL1, (Figure 1F)[37], previously shown to be downstream of CREB[38].
357 This observation confirms that the negative limb circadian genes can be directly regulated downstream of
358 the exercise bout in skeletal muscle and do not require *Bmal1* or a functioning TTFL clock mechanism.
359 Analysis of the exercise DEGs unique to vehicle muscle identified the robust up-regulation of well-
360 known exercise transcription factors and co-activators, including *Nr4a3*, *Fosb* and *Ppargc1a (PGC1a)*. In
361 contrast, this cluster of well-defined exercise responsive factors did not change following exercise in
362 iMSBmal1KO muscle. This was unexpected as these genes have been shown to be very responsive to an
363 acute exercise bouts in preclinical rodent models, in muscle of healthy human subjects and in muscle from
364 subjects with T2D [9,10,28,39], (Figure 1F). These results identify that muscle BMAL1 is necessary for
365 the acute up-regulation of *Ppargc1a*, *Nr4a3* and other exercise responsive transcription factors in skeletal
366 muscle. We suggest that the lack of up-regulation of these factors, in the absence of muscle BMAL1, likely
367 contributes to the divergent transcriptional program post-acute exercise.
368 We next asked if the divergent exercise gene expression patterns reflected similar or different
369 functional pathways, (Figure 1G-H). Consistent with many studies, the vehicle exercise response pathway
370 enrichment contained 'Oxidative Phosphorylation,' 'Stress Response,' and signaling pathways such as
371 'insulin receptor, 'PI3K-Akt', 'Nuclear Receptor', Receptor Tyrosine Kinase', 'MAPK' and 'PPAR'.
372 Additionally, there were 85 'Immune System' associated genes also differentially regulated specifically in
373 vehicle treated mice. Pathway analysis of the iMSBmal1KO specific exercise DEGs revealed very different
374 pathways and noticeably lacked the pathways seen in the vehicle muscle response. The primary pathways
375 identified were enriched for 'Immunity' (22 genes) and the 'Innate Immune System' (33 genes), (Figure
376 1H). We noted that 109 'signal transduction' associated genes were altered post exercise, (61% upregulated)
377 in the vehicle mice, but were unchanged in the iMSBmal1KO, (Figure 1G). This included the absence of
378 several well-known exercise responsive signaling pathways including 'insulin receptor, PI3K-Akt, nuclear
379 receptor, receptor tyrosine kinase, MAPK and PPARG.
380 Mechanistically, we asked if the altered exercise response in the iMSBmal1KO mice could be due
381 to epigenetic changes after loss of BMAL1. We performed an assay for transposase accessible chromatin
382 with sequencing (ATAC-seq) on gastrocnemius muscle from sedentary vehicle and iMSBmal1KO mice to

383 determine chromatin accessibility. We identified a number of changes in chromatin accessibility between
384 vehicle and iMSBmal1KO mice that may contribute to some of the altered exercise responses, including
385 1837 more accessible DNA regions and 1973 less accessible regions, (Supplementary Figure 3A-H). We
386 note that 'Signal transduction' was the most enriched pathway in the less accessible DNA regions,
387 comprising 152 genes. Furthermore, 28 of those genes also had decreased gene expression suggesting that
388 loss of BMAL1 alters chromatin accessibility in muscle with reduced availability of many signal
389 transduction genes which could be directly impacting their response to exercise, or their upstream
390 regulators. A further 73 'Signal transduction' associated genes were not affected at the chromatin level but
391 were downregulated at the gene expression level with loss of BMAL1 indicating altered transcriptional
392 regulation. We next queried muscle ChIP-Seq data and identified that 31.5% of acute exercise responsive
393 DEGs are bound by BMAL1:CLOCK within the promoter and/or gene body including *Nr4a1*, *Nr4a2*,
394 *Nr4a3*, *Fosb*, *Irs2*, *Fosl2* and *Ppargc1a* which we highlight are unresponsive in the iMSBmal1KO,
395 (Supplementary Figure 3F-H). These observations highlight that the core clock gene, *Bmal1* contributes to
396 both the epigenetic and direct transcriptional network that is a necessary for the acute exercise response in
397 skeletal muscle.

398 INSERT FIGURE 1

399 3.2 Loss of skeletal muscle BMAL1 does not impact exercise training workloads, 400 body composition, or muscle size and fiber type.

401 We next asked whether muscle *Bmal1* contributes to endurance training adaptations
402 (Supplementary Figure 4-6). We followed a progressive treadmill training approach, performing graded
403 exercise tests before training to set the relative training intensity for each group of mice and then we
404 repeated testing at 2 and 4 weeks to prescribe increases in workload, followed by a post-intervention test at
405 6 weeks, Figure 2A. Important for interpretations of this training study, we found that the total treadmill
406 work done (AU) across the timecourse of training was not different between genotypes and both groups
407 demonstrated increased performances with training ($P < 0.0001$), (Figure 2B).

408 We observed no differences in body mass between groups, (Supplementary Figure 4C). Following
409 6-weeks training there was no significant differences between body mass for both of the exercise trained
410 groups vs. their respective controls (Vehicle: 32.3 ± 2.7g vs. 29.8 ± 0.8g, $P = 0.13$ and iMSBmal1KO: 34.1
411 ± 2.5g vs. 30.5 ± 2.4g, $P = 0.09$), (Figure 2C/Supplementary Figure 4C). Food intake measured per week
412 (g, p/w) per bodyweight (g) did not change over time, or between groups across the experimental
413 timecourse, equaling ~0.8-1 times bodyweight per week, (Supplementary Figure 4D). We also note that
414 there were no significant differences between the 4 groups in cage activity measures, suggesting that neither
415 loss of muscle *Bmal1* nor exercise training affected behavioral cage activity (Supplementary Figure 4E-G).

416 Run training has been shown to modify body composition. In this study, MRI body composition
417 measurements identified no significant differences in total fat mass, or percent fat mass as a proportion of
418 total body mass prior to training between genotypes, (Supplementary Figure 4C). We identified a
419 progressive decline in total fat mass in both the vehicle exercise trained (P = 0.006) and iMSBmal1KO
420 exercise trained mice, (P = 0.03), with no genotype effect (P = 0.5), (Figure 2D-G). Similar progressive
421 reductions in lean mass (g) were observed between vehicle exercise trained (P = 0.01), equivalent to a 4.8
422 ± 1.7% reduction in lean mass. A similar percent reduction (4.98 ± 6.1% reduction) was observed in
423 iMSBmal1KO exercise trained mice (Figure 2F), but this was not statistically significant (P = 0.07), (Figure
424 2F). These reductions occurred in the absence of changes in the ratio of lean-to fat mass, (Figure 2D-G).
425 In general, 6-weeks of run training does not normally induce significant changes in muscle fiber
426 size or fiber type. We performed histological analysis on cross-sections of the gastrocnemius muscle to ask
427 if the muscle of the iMSBmal1KO mice exhibited any unique training induced features. Overall, we found
428 no differences in the main measures of muscle phenotype either in the vehicle mice with training or in the
429 sedentary iMSBmal1KO mice at rest or following training. Supplementary Figure 5. We highlight that there
430 were no significant differences in muscle weight, fiber cross-sectional area, myonuclei per fiber cross-
431 section or proportion of fiber types with either muscle specific *Bmal1* knockout, or exercise training
432 (Supplementary Figure 4A-F). We observed similar increases in SDH staining intensity after exercise
433 training but there was no effect based on genotype, (Supplementary Figure 5D). However, we did notice a
434 small but statistically significant increase in central nuclei (0.92 ± 0.86% fibers vs. 3.9 ± 1.7% fibers, P <
435 0.001) and embryonic positive fibers (0.16 ± 0.13% fibers vs. 1.76 ± 0.84% fibers, P < 0.001) after exercise
436 training in the *Bmal1* knockout, which was not present in the vehicle treated group after exercise training,
437 (Supplementary Figure 5G-H). This suggests some small, but reproducible, muscle damage the
438 iMSBmal1KO trained mice. Representative immunohistochemistry images of gastrocnemius muscles are
439 available in Supplementary Figure 5I-J.
440 INSERT FIGURE 2

441 ## 3.3. Loss of skeletal muscle BMAL1 alters core clock factor gene expression and
442 disrupts the transcriptional regulation of metabolism.

443 To assess the response to training we first had to define, in this cohort of mice, the differential gene
444 expression in the muscles of vehicle control vs. iMSBmal1KO. We identified 1217 DEGs; (q < 0.05)
445 between the groups; 535 genes that were upregulated and 682 that were downregulated with muscle specific
446 *Bmal1* knockout respectively, similarly to our reports in Figure 1C. As seen in the volcano plot
447 (Supplementary Figure 6A) and consistent with prior studies [4–6], many of the clock output genes, such
448 as *Dbp*, *Mylk4*, and *Tcap* were significantly down-regulated [40,41]. Motif analysis of the promoters of the

682 down-regulated genes in the iMSBmal1KO determined that there was significant enrichment for E-boxes, and these include several circadian clock (CLOCK, NPAS2) specific E-boxes, as well as MYC specific E-box sequences. Other represented motifs in the down-regulated genes include MEF2 or MADS elements and sites for NFAT which are well recognized pathways in skeletal muscle, (Supplementary Figure 6B). Subsequent KEGG pathway analysis of the DEGs confirmed significant dysregulation of genes associated with 'circadian rhythms' (14 genes), as well as a large number of pathways relating to substrate metabolism, (Supplementary Figure 6C). Within this pathway, we identified dysregulation of transcripts essential for glucose and glycogen homeostasis including (*Hk2*, *Rab10*, *Slc2a3*, *Slc2a4*, *Tbc1d1*, *Aldoc*, *Fbp2*, *Gbe1*, *Pgm1*, *Pgm2*, *Phka1*, *Pygm*) as previously reported [4–6].

3.4. Identification of BMAL1-dependent and BMAL1-independent transcriptional adaptation to 6-weeks of exercise training in gastrocnemius muscle.

While there were few phenotypic differences between the muscles of trained vehicle and iMSBmal1KO mice, we did find that the transcriptional adaptations to training were largely divergent. For this analysis, we performed RNA-seq on gastrocnemius muscle 47 hours after their last exercise bout. Analysis of the transcriptome in muscle from vehicle control and vehicle trained mice identified only 142 DEGs after training which is consistent with prior studies with up-regulation of *Fabp1* and down regulation of *Hadha* [10,42], Figure 3A. Enrichment of DNA binding motifs within the promoter or gene body of the small number of upregulated DEGs included MEF2C, SIX1, Androgen receptor half sites and NFAT, (Figure 3B). Downregulated DEGs were also enriched for DNA motifs relating to EGR1, SMAD4 and NFAT, suggesting the latter contributes to both activation/suppression of exercise DEGs. Pathway analysis revealed the expected exercise adaptations pathways including 'PPAR signaling' (11 genes), 'protein digestion and absorption' (8 genes), 'fatty acid metabolism/degradation' (7 genes), 'ECM-receptor' (7 genes), 'focal adhesion' (5 genes), 'calcium signaling' (7 genes), 'PI3K-Akt signaling' (5 genes) and 'HIF-1 signaling' (5 genes), Figure 3C. As expected, a number of these DEGs included fatty acid metabolism regulators (*Hadha, Hadhb, Acaa2, Cpt2, Acsl1, Scd2, Acadm, Cd36, Fabp1, Apoa1 and Apoa2*).

In contrast, analysis of the gene expression changes with training in the iMSBmal1KO mice identified a much larger, >5-fold increase in the number of DEGs in the KO muscle following training. We identified 780 DEGs, of which 283 were downregulated and 497 upregulated with exercise training, Figure 3D-F. Similar to our findings following acute exercise, there was little overlap in the exercise DEGs between genotypes. Analysis of the DNA motifs associated with the iMSBmal1 exercise DEGS predicts that exercise adaptation in the iMSBmal1KO muscle relies on vastly different sets of upstream transcription factors, (Figure 3E). Within the genes upregulated by exercise training in the iMSBmal1KO mouse, motif enrichment analysis identified sites for YY1, ESRRA/B, SP1, NRF/1, SMAD2/4 and P53. In the down-

482 regulated genes, we identified XBP1 sites were enriched which was interesting as XBP1 is a transcription
483 factor that functions as a regulator of the unfolded protein response and is known as a key part of the ER
484 stress pathway. For the training study, we collected tissues at 48hrs after the last exercise bout so the
485 observation that many of the DEGs have regulatory elements that indicate a stress pathway was unexpected.
486 We also noted that several of these motifs represent transcription factors normally associated with an acute
487 response to exercise (e.g., ESRRA, NRF1, P53). However, they are not commonly identified as motifs
488 enriched in steady state training induced changes in gene expression [10,43–48], (Figure 3E). The results
489 from the DEG motif analysis suggest a vastly different transcriptional mechanism for muscle adaptation
490 with exercise training that relies on inclusion of known acute response pathways. We suggest that without
491 muscle BMAL1, exercise training results in activation of a chronic stress set of pathways coupled with an
492 inability of the muscle to return to homeostasis following exercise.

493 While the exercise adaptations were largely divergent, there was a small overlap in the
494 transcriptomes with training between genotypes. Initial analysis identified only 23 common exercise
495 adaptation genes (1.6% of DEGs) using an FDR cut-off of $q = 0.05$. To increase the number of genes for
496 this analysis, we decreased the stringency to $P = 0.01$ and found 63 overlapping genes (2.99%), (Figure
497 3G). We probed the 63 common genes to ask if they represented a common, non-BMAL1 dependent,
498 training response, Figure 3H. We determined that only 25 (39.7%) of the 63 genes were upregulated in both
499 genotypes, with 6 (9.5%) were downregulated in both. We identify these as BMAL1-independent exercise
500 training genes. Interestingly, 22 (34.9%) of the shared genes were up in vehicle but down in the KO exercise
501 trained muscle and these were associated with the extracellular matrix (*Col3a1, Col4a1, Col5a2, Tnxb,*
502 *Emilin2, Fn1, Lama2, Nid1* and *Nid2*) and insulin regulation (*Pappa* and *Irs2*). We also identified 10 genes
503 (15.9%) including *Coq10a, Cyc1* and *Esrra* that where downregulated with training in the vehicle but were
504 upregulated in the iMSBmal1KO, (Figure 3H). Thus, while there are shared genes between the two
505 genotypes, over 50% of the 63 shared genes are regulated in opposite directions. This indicates this set of
506 shared genes are exercise responsive, but the directionality is dependent muscle BMAL1.

507 We also asked whether exercise training can function to restore the dysregulated gene expression
508 in the iMSBmal1KO muscle toward levels seen in vehicle control muscle. For this analysis we compared
509 the DEGs dysregulated by loss of BMAL1 in sedentary mice (1217) to the exercise training DEGs in the
510 iMSBmal1KO muscle (780) and found only 94 DEGs are shared suggesting that the majority of disrupted
511 transcripts in the sedentary iMSBmal1KO muscle are not rescued by exercise training. To visualize this,
512 we plotted Log^2 fold changes of these genes comparing vehicle control and exercise trained iMSBmal1KO
513 muscle and calculated Pearson's correlation coefficient. As seen in Figure 3I we identified that 73.4% of
514 the genes disrupted with initial loss of *Bmal1* were directionally closer to vehicle control levels following
515 training. However, the correlation coefficient of determination was weak (R^2=0.24) indicating that the

levels of gene expression were not close to sedentary values. This provides additional evidence that the exercise adaptations work with BMAL1 and are not occurring through separate transcriptional pathways. A heatmap for all 94 genes is presented in Supplementary Figure 7A. Recent results from cardiac *Bmal1* knockout mice have demonstrated that cardiac dysfunction caused by loss of BMAL1 cannot be attenuated with a similar exercise training paradigm [49].

Lastly, we wanted to ask if exercise training impacted core circadian clock genes or genes associated with glucose and glycogen metabolism in muscle. As illustrated in the heatmap in Figure 3J, 6 weeks of training in vehicle mice resulted in changes in many circadian clock related genes such as *Nfil3*, *Per1, Per3*, *Cry2*, and *Dbp*. In contrast, in the iMSBmal1KO mouse there were no changes in any of the factors following training. Since we found that acute exercise can modify expression of clock genes, like *Per1* and *Nfil3*, in the absence of muscle Bmal1 (Figure 1E), the lack of changes in these circadian clock genes with training suggests that it is BMAL1 and the core clock mechanism, that is required for the clock factor changes with training. Analysis of glucose and glycogen metabolism genes found that several of these genes changed expression with training in the muscle, including increases in *Hk2*, *Pgm2* and decreased expression of *Slc2a4* (Glut4). In contrast there were little to no significant changes in gene expression of this cluster of genes in iMSBmal1KO mice post-training. These observations reinforce that BMAL1 and/or a functional circadian clock is required for regulating expression of genes critical for glucose homeostasis in skeletal muscle. Plots with individual data points are provided within Supplementary Figure 8A.

INSERT FIGURE 3

3.5. Elevated gene expression of TCA-cycle components, β-oxidation, mitochondrial constituents and mito-ribosomes is a distinct feature of iMSBmal1KO exercise adaptation in gastrocnemius muscle.

Analysis of the unique training genes for the iMSBmal1KO muscle identified oxidative metabolic adaptations were a highly enriched category, well beyond any oxidative changes in the vehicle muscle adaptation. We found that a number of these DEGs are shared across pathways relating to pyruvate metabolism, the tricarboxylic acid cycle (TCA cycle), fatty acid β-oxidation and genes relating to mitochondrial complex constituents and their associated mitochondrial ribosomal subunits. A schematic of these pathways is provided in Figure 4A, and the changes in genes within each pathway are presented in Figure 4B-C. It is striking that most genes were upregulated in response to exercise training in the iMSBmal1KO mice, in contrast, muscle from vehicle treated mice showed limited changes for these genes in response to training.

548 Most strikingly in the iMSBmal1KO training response was the robust up-regulation across almost
549 all genes relating to the TCA cycle, β-oxidation and mitochondrial components encoded by both nuclear
550 and mitochondrially encoded genes, (Figure 4B-C). Interestingly, 12 genes (*Acaa2, Aco2, Crat, Cs, Dlst,*
551 *Fh1, Idh3a, Idh3b, Idh3g, Ogdh, Suclg1 and Suclg2*) encoding proteins involved in TCA cycle intermediate
552 and anaplerotic reactions were significantly upregulated in the iMSBmal1KO mouse in response to exercise
553 training, whereas they were downregulated with training in the vehicle treated mice. This result suggests
554 that exercise training without muscle BMAL1 pushed increased reliance on alternate substrates to support
555 the energy demand of exercise training. This trend was also observed for a large family of genes associated
556 with Acyl-CoA hydrolysis to fatty acids and coenzyme A and β-oxidation. Genes including *Acadl, Acadm,*
557 *Acads, Acadv1, Acat1, Acot7* were largely down regulated with exercise training in the muscle of vehicle
558 treated but were uniformly upregulated with training in the iMSBmal1KO muscle. This observation is
559 consistent with a greater requirement for the use of fatty acids for energy metabolism, Figure 4B. We note
560 that there were very few changes in genes involved in triglyceride biosynthesis with exercise training in the
561 iMSBmal1KO indicating that the primary adaptation with exercise was to enhance fat oxidation.
562 We also observed upregulation of a large network of both nuclear and mitochondrial encoded genes
563 that were largely unique to the iMSBmal1KO training adaptation. These related to mitochondrial complexes
564 I (n=44), II (n=4), III (n=11), IV (n=15), V (n=18), as well as 22 nuclear and mitochondrial encoded genes
565 related specifically to the large and small mitochondrial ribosomal subunits, (Figure 4C). The majority of
566 these genes were significantly upregulated relative to both vehicle control and vehicle exercise trained mice,
567 as well as iMSBmal1KO control mice. The uniformity of this training response suggests a common
568 transcriptional program for these genes in the absence of BMAL1. Analysis of upstream motifs within these
569 genes identifies sites for *Esrra, Esrrb, Nrf/1* and *p53* and we did identify that expression of *Esrra* was
570 elevated with training in the iMSBmal1KO but downregulated with vehicle exercise trained muscle. As
571 noted earlier, these transcription factors are most seen with the acute exercise response in muscle but not
572 normally associated with steady state training responses, (Figure 3E).
573 INSERT FIGURE 4

574 3.6. Exacerbated amino acid availability, further depletion of TCA cycle 575 intermediates suggests inefficient energy status with exercise training in the 576 iMSBmal1KO mouse.

577 Transcriptomic data indicated divergent metabolic programs in the muscle of trained vehicle vs.
578 trained iMSBmal1KO mice. We performed untargeted metabolomics to assess potential steady state
579 changes in muscle metabolites following training in the vehicle vs. iMSBmal1KO mouse. Comparing
580 vehicle controls to iMSBmal1KO sedentary mice, we found 46 differentially abundant metabolites, (Figure

581 5A), a comparison that has previously been reported [25]. In response to training, we observed only 19
582 differentially abundant known metabolites in vehicle exercise trained mice, which is similar to the small
583 transcriptomic response. In contrast, we identified 116 differentially abundant metabolites in the
584 iMSBmal1KO exercise trained mice. Comparisons between genotypes identified only 8 common
585 metabolites in the exercise training response and they showed enrichment in lysine degradation and
586 glutathione metabolism pathways, (Figure 5B).

587 The differentially abundant metabolites in the iMSBmal1KO exercise trained muscle were enriched
588 amongst amino acid and TCA cycle pathways including 'Tyrosine metabolism', 'Alanine, aspartate and
589 glutamate metabolism', 'Pyruvate metabolism', (Figure 5D-H). Since exercise training does not restore
590 glucose metabolic genes in the iMSBmal1KO muscle we suggest that these metabolite changes reflect the
591 need for TCA cycle substrates via amino acid metabolism. For example, threonine, leucine, tryptophan,
592 phenylalanine and tyrosine are significantly elevated with loss of skeletal muscle BMAL1 but levels were
593 reduced following exercise training. Consistent with this pattern, fumarate, a TCA cycle intermediate
594 metabolized from aromatic amino acids is also significantly upregulated with loss of BMAL1 in sedentary
595 mice and is significantly reduced following training to levels below vehicle controls, (Figure 5E/G). The
596 changes in these metabolites are consistent with the increased reliance on amino acids to support TCA
597 metabolism in the iMSBmal1 muscle with exercise training.

598 We were surprised that despite our samples being taken 47 hours after their last exercise bout,
599 pyruvate levels were significantly lower by ~180% in the iMSBmal1KO mice with exercise training,
600 (Figure 5G). This finding falls in line with our transcriptome analysis, that the genes encoding the enzymes
601 required for glucose transport and metabolism are not rescued with exercise training, which may lead to
602 pyruvate availability being a limiting factor. However, we noted above that there is a compensatory increase
603 in genes involved in pyruvate metabolism and TCA cycle components, likely resultant of diminished steady
604 state levels of pyruvate with training. Despite the reduction in pyruvate, acetyl-CoA levels were
605 significantly increased in the iMSBmal1KO mice after exercise training, suggesting that other substrates
606 (likely lipid) contribute more to the increase in acetyl-CoA levels.

607 Further evidence of disrupted glycolytic metabolism was found when we measured tissue glycogen
608 content in gastrocnemius and liver with exercise training, Supplementary Figure 9D-G. Vehicle treated
609 mice had greater concentrations ($P = 0.008$) and achieved larger increases in muscle glycogen with exercise
610 training (262.8% vs. 66.5%, 1.85 ± 0.13μg/mg vs. 1.43 ± 0.31μg/mg). Similarly in liver, training
611 significantly increased glycogen content in both vehicle treated (16.28 ± 1.81μg/mg, $P < 0.0001$) and
612 iMSBmal1KO mice (13.26 ± 1.64μg/mg, $P < 0.0001$), yet glycogen content was significantly lower in the
613 trained iMSBmal1KO liver, ($P = 0.036$). As the magnitude of improvement in muscle and liver glycogen

614 with training are reduced, it suggests ongoing glycolytic dysregulation within iMSBmal1KO muscle
615 requires higher triglyceride utilization with a systemic impact on the liver glycogen stores.
616 Glycosylated haemoglobin was lower post exercise training in both groups, $P < 0.001$, with no
617 detected genotype effect, (Supplementary Figure 9A-B). Exercise training significantly reduced plasma
618 insulin levels in both genotypes, however the levels in the exercise trained iMSBmal1KO mice remained
619 significantly higher than vehicle control (~41%, $P = 0.0196$) and vehicle exercise trained mice (~135%, P
620 <0.0001), Supplementary Figure 9C. While these circulating markers of glucose homeostasis are improved
621 with exercise training in the iMSBmal1KO mouse we note that the effect is partial. We suggest that these
622 partial systemic improvements in blood glucose and insulin are mediated by other peripheral tissue
623 adaptations, such as liver and iWAT, to exercise training.

624 INSERT FIGURE 5

625 3.7. Loss of skeletal muscle BMAL1 disrupts the transcriptome of peripheral tissues.

626 Exercise is well recognized to induce healthy systemic adaptations and virtually all bodily tissues
627 exhibit significant transcriptome changes following exercise training [50,51]. Since our exercise workloads
628 were the same between genotypes across training, we asked if the peripheral tissue adaptations to exercise
629 would be independent of the divergent muscle adaptations in the iMSBmal1KO mice. For this analysis we
630 chose to investigate highly metabolic tissues and organs that are known to be important for exercise capacity
631 (iWAT, liver, heart and lung). We defined the transcriptomic changes in the vehicle vs. iMSBmal1KO
632 mouse tissues to allow for clear delineation of the exercise training responses. In the control iMSBmal1KO
633 mice we identified a large number of genes (1029) specifically dysregulated in the heart, 511 in iWAT, 159
634 in liver and 87 DEGs in the lung illustrating unique tissue disruption in gene expression with loss of muscle
635 BMAL1. We did not identify any DEGs shared across all 5 tissues in response to iMSBmal1KO, but we
636 found minor overlap with DEGs specifically dysregulated in muscle and heart (81 genes), muscle and
637 iWAT (58 genes), muscle and liver (21 genes), Figure 6A.
638 In iWAT, loss of muscle *Bmal1* was associated with 684 DEGs (425 upregulated, 259
639 downregulated) that were associated with pathways relating to collagen/extra-cellular matrix terms and
640 insulin signaling/resistance related terms which were largely upregulated. *Srebf1*, a key transcription factor
641 responsible for regulation of de novo lipogenesis and glycolysis, as well as *Acacb* which encodes the gene
642 responsible for the carboxylation of acetyl-CoA to malonyl-CoA, a rate-limiting step in fatty acid synthesis
643 and pro-glycogenic genes, *Gys1* and *Ppp1r3d* were significantly downregulated in the iWAT with loss of
644 skeletal muscle BMAL1. This was concomitant with significant upregulation of *Creb3l1*, a master regulator
645 of fibrosis in adipose and liver tissue [52], changes that have previously been associated with insulin
646 resistance and obesity [53–55], (Figure 6B).

647 The liver transcriptome was also significantly affected by loss of skeletal muscle BMAL1 with 199
648 DEGs (86 upregulated, 114 downregulated) associated with dysregulation of 'fatty acid/cholesterol
649 metabolism', 'AMPK signaling' and 'glucagon signaling', (Figure 6C). This included significant
650 downregulation of several genes regulating lipid transport/homeostasis and glycolysis including *Elovl6*,
651 *Scd1*, *Apoa4*, Pfkfb1, *Slc2a4* and fatty acid synthesis rate limiting enzyme, *Acaca*. Conversely, *Abcg8*,
652 *Lrp1*, *Lipg* were significantly upregulated along with *Pparg*, known as a master regulator of lipogenesis
653 and glucose uptake [56–59], suggesting a shift of fuel preference to fatty acid metabolism in the liver.
654 Surprisingly, a large remodeling of the transcriptome was identified in the heart with alteration of
655 1177 genes (665 upregulated, 512 downregulated). We confirmed that there was no *Bmal1* recombination
656 in the heart tissue of these mice, Supplementary Figure 3. These transcriptional changes included
657 upregulation of genes associated with ribosomal, mito-ribosomal and mitochondrial constituents,
658 proteasomal subunits, but also genes associated with cardiac muscle structure and function. This included
659 upregulation of *Myl2*, *Myl3*, *Tnnc1*, *Tnni3*, *Tpm4*, *Actb* and downregulation of *Dmd*, *Lama2*, *Ryr2*, and *Ttn*,
660 (Figure 6D). More minor changes in gene expression were identified in the lung with 110 DEGs (82
661 upregulated, 28 downregulated) largely relating to angiogenesis and Ras signaling, (Figure 6E).
662 INSERT FIGURE 6

663 3.8. Exercise training adaptations are altered in peripheral tissues in mice lacking 664 skeletal muscle BMAL1.

665 We next tested whether exercise training adaptations in peripheral tissues were impacted in the
666 iMSBmal1KO mice. As evidenced by the upset plot, (Figure 7A), we found that all peripheral tissues
667 studied in the iMSBmal1KO mouse exhibited significantly larger numbers of post exercise training DEGs
668 (iWAT 441 vs. 455 DEGs, Liver 336 vs. 571 DEGs, Heart 261 vs. 798 DEGs and Lung 208 vs. 633 DEGs).
669 These changes were also qualitatively different and tissue specific with only ~3% of the exercise training
670 responsive changes shared between genotypes, (iWAT 32 DEGs, Liver 30 DEGs, Heart 33 DEGs and Lung
671 16 DEGs), (Figure 7B,E,H,K). Furthermore, predicted upstream transcription factor analysis of the exercise
672 training responsive DEGs, similarly to skeletal muscle, showed largely different putative upstream
673 regulators, Supplementary Figure 10. The magnitude and breadth of these differences were unexpected and
674 point to the impact that training adaptations in skeletal muscle have on systemic adaptations to exercise.
675 In vehicle exercise trained iWAT, we observed an expected transcriptional remodeling with
676 exercise training which included genes enriched in pathways associated with 'PPAR signaling', 'Lipid
677 Metabolism' and 'Inflammatory Response'. This included downregulation of *Pparg* itself along with other
678 factors involved in lipid metabolism/storage, insulin sensitivity and inflammation. Analysis of the liver
679 transcriptome of exercise trained vehicle mice demonstrated a synergy with the iWAT transcriptome, with

680 downregulation of pathways including 'Lipid/cholesterol biosynthesis/metabolism', (Figure 7F). This
681 common pathway enrichment between iWAT and liver was lost in the iMSBmal1KO training response. In
682 iMSBmal1KO iWAT the exercise-responsive genes were associated with insulin resistant signatures and
683 inflammation, included within 'insulin-like growth factor transport/binding protein' pathways. One
684 example was the upregulation of the transcription factor *Srebf1*, known to promote cholesterol and fatty
685 acid biosynthesis and downregulation of the glycolytic enzyme *Pkm*, (Figure 7C-D). Uniquely, liver of
686 iMSBmal1KO exercise trained mice showed alterations in 'RNA Polymerase II Transcription', pathways
687 associated with ubiquitin mediated proteolysis, and upregulation of a number of TGF-beta receptor
688 signaling associated pathway genes including *Smad4*, *Smurf2*, *Itgav* and *Tgfbr1*, (Figure 7G). These results
689 suggest that exercise training in the iMSBmal1KO mice leads to abnormal transcriptional remodeling in
690 iWAT and liver including many biological signatures that could be considered 'maladaptive'.

691 The exercise training response in the lung of the vehicle mice corroborated outcomes recently
692 published investigations by the MoTrPAC consortium and were broadly related to decreased inflammation
693 [50]. We identified 208 DEGs that are changed in the lung following training including 37 genes associated
694 with the Reactome pathway 'immune system', over ~83% of which were downregulated with exercise
695 training. There were 633 training induced DEGs in the iMSBmal1KO lung which was a surprise as the
696 transcriptomes of the sedentary vehicle and iMSBmal1KO lungs were not very different. This adaptation
697 included 69 different 'immune system' associated genes were found to be enriched in the iMSBmal1KO
698 exercise training response, 72% of which were upregulated with exercise training indicating a discordance
699 in the inflammatory response with training between genotypes, (Figure 7K-M).

700 In the vehicle exercise trained heart we observed modest changes to the transcriptome associated
701 with 'Immunity', 'Lipid Metabolism' and 'Collagen Degradation', (Figure 7H-I). Conversely, a majority
702 of the exercise training responsive genes in the iMSBmal1KO heart were directionally opposite to the
703 features identified in the loss of BMAL1 sedentary mice, see Figure 6D. This indicates that unlike the other
704 peripheral tissues, exercise training rescued the dysregulation of these genes in the iMSBmal1KO heart,
705 (Figure 6D/7J). This is supported by data presented in Supplementary Figure 11, where we highlight that
706 97% of genes in the heart that are disrupted by loss of muscle BMAL1 in sedentary mice, are exercise
707 training responsive in iMSBmal1KO hearts and return closer to vehicle control expression levels, R^2=0.67.
708 The mechanism(s) through which exercise training restores the heart transcriptome in the iMSBmal1KO
709 mouse is unclear and requires additional study.

710 INSERT FIGURE 7

711 ## 3.9. Exercise training in the abence of skeletal muscle BMAL1 alters the steady state
712 immune system and metabolic pathways of peripheral tissues.

713 Since inflammation and metabolism pathways were the most common differences among the
714 transcriptional changes, we computed Z-scores for each pathway by averaging the Z-score of every gene
715 found within each pathway. Specifically, we included 'Immune System', 'Carbohydrate Metabolism',
716 'Lipid Metabolism', 'Amino Acid Metabolism' and the 'Endocrine System' to characterize between
717 genotype changes in the exercise trained state. As visualized in Figure 8A, genes associated with the
718 'Immune System' pathways were generally expressed at a higher level with exercise training in skeletal
719 muscle and iWAT and decreased in liver heart and lung in the vehicle mice, a signature that has been linked
720 to increased immune cell recruitment [50]. In contrast, this pattern is reversed in the iMSBmal1KO tissues
721 following training with expression of these immune pathway genes lower in the muscle and iWAT and
722 much higher in liver, lungs and heart with training. These observations indicate that the altered tissue
723 environment(s) and/or altered immune cells in circulation results in recruitment or retention of different
724 amounts, or types of immune cell populations in these tissue and organs with targeted loss of muscle
725 BMAL1 and warrants further investigation.

726 The endocrine system pathways were also differentially modified by exercise training between
727 genotypes. One recognized exercise feature is the 'PPAR signaling pathway' which was signficiantly lower
728 across tissues in the vehicle mice but was higher across all 5 tissues in the iMSBmal1KO exercise trained
729 mice, Figure 8B. This likely reflects the altered energy homeostasis resulting from loss of skeletal muscle
730 BMAL1 promoting systemic increases in fatty acid metabolism [60–62]. As expected from our muscle
731 transcriptome and metabolomic data, we observed strong upregulation of pathways associated with amino
732 acid metabolism that are generally expressed at a higher levels in all peripheral tissues in the iMSBmal1KO
733 exercise trained mice, compared with their vehicle trained counterparts, Figure 8C. In particular, we identify
734 the lung as a tissue that gets brought into substrate metabolism in a much bigger way with exercise in the
735 iMSBmal1KO mouse. This is a unique observation that highlights the potential for lung metabolism to
736 contribute to systemic energy homeostasis with exercise training. Together, analysis of these pathways
737 emphasise that skeletal muscle BMAL1, and likely a functional skeletal muscle clock, is essential for
738 systemic tissue homeostasis and peripheral tissue transcriptional remodelling in response to exercise
739 training, pertaining to metabolic and immune components and these warrant further investigation.

740 4. Discussion:

741 In this investigation, we addressed the contribution of the core circadian clock factor, BMAL1, in
742 skeletal muscle to both acute transcriptional responses to exercise and transcriptional remodelling in
743 response to exercise training. Additionally, we adopted a systems biology approach to investigate how loss
744 of skeletal muscle BMAL1 altered peripheral tissue homeostasis as well as exercise training adaptations in
745 iWAT, liver, heart, and lung of male mice.

746 Mice deficient in muscle BMAL1 failed to mount a 'normal' transcriptional response to acute
747 exercise despite performing the same amount of treadmill work. iMSBmal1KO mice demonstrated a
748 blunted transcriptional response to acute exercise and this was associated with the lack of up-regulation of
749 *Ppargc1a*, *Fos*, and orphan nuclear receptors, *Nr4a1* and *Nr4a3*. This was concomitant with the lack of
750 activation of genes within well-known exercise responsive pathways, e.g., PI3k-Akt, MAPK and PPAR.
751 We also identified that signal transduction associated genes were significantly altered at both the chromatin
752 accessibility level and transcript level, consistent with reports in liver[63], that BMAL1 plays an important
753 role in epigenetic regulation as well as transcriptional regulation.
754 We next tested the exercise training response in the mice lacking BMAL1 specifically in skeletal
755 muscle. As with the acute response studies, the mice were able to perform the same training paradigm so
756 that the treadmill work for both vehicle and iMSBmal1KO mice was the same over a 6-week period.
757 Analysis of the transcriptome identified a novel BMAL1 -dependent program of gene expression in skeletal
758 muscle in response to chronic exercise training. Despite the same exercise training volumes, the adaptation
759 of the transcriptome in skeletal muscle resulted in a quantitatively larger reprogramming with very few
760 genes in common (~3%), representing very different enriched pathways and putative upstream
761 transcriptional networks. It is important to note that of the subset of common exercise responsive genes
762 between the two genotypes (n=63), only half of them change in the same direction. These outcomes indicate
763 that the well-defined molecular responses to a set exercise training paradigm in skeletal muscle requires
764 BMAL1 and/or a functional circadian clock mechanism, but in its absence requires a far larger network of
765 genes to elicit adaptations. We also note that although the transcriptome was largely divergent between
766 genotypes, classic markers of muscle, such as fiber size and fiber type, were not different indicating that
767 these parameters of muscle are not under BMAL1 control.
768 Our multi-omic analyses identified that the skeletal muscle without BMAL1 did adapt but the
769 steady state responses within the transcriptome and metabolome were quantitatively larger and importantly,
770 fundamentally divergent. This included the observation that exercise training is not sufficient to rescue the
771 dysregulation of genes essential for glucose metabolism in the iMSBmal1KO skeletal muscle
772 demonstrating that exercise training is not sufficient to restore metabolic flexibility in the absence of
773 BMAL1. To support the increased energy demand of exercise training the iMSBmal1KO muscle exhibited
774 a uniform up-regulation of genes, likely regulated by *Esrra*, to support the TCA cycle, beta oxidation and
775 electron transport complexes. These divergent transcriptomic changes in the iMSBmal1KO muscle were
776 supported by the divergent metabolomic responses to training, with amino acids being an important source
777 for TCA substrates to support oxidative metabolism. These studies uncover that in response to the increased
778 energy demand with exercise the iMSBmal1KO muscle that adaptation can occur, but it does not resemble
779 the expected molecular and metabolic adaptations seen in the vehicle treated mice.

780 Our findings have similarities to recent work demonstrating the contribution of muscle specific
781 *Ppargc1a* to the exercise training response [42]. This is not surprising as it has been shown previously that
782 *Ppargc1a* is a circadian clock output gene in skeletal muscle. In support of this, our acute exercise studies
783 extend this relationship as a clock output gene and demonstrate that up-regulation of *Ppargc1a* requires
784 muscle BMAL1. This places muscle BMAL1, and likely the core clock mechanism, as an upstream
785 regulator of *Ppargc1a* expression in response to exercise. Recent work has demonstrated similar
786 relationships between the core clock and time-of-day exercise activation of HIF1A/HIF1A target genes
787 [17]. We suggest that this loss of the exercise expression of *Ppargc1a* and the other acute exercise
788 transcription factors are significant contributors to the divergent exercise training transcriptome in the
789 iMSBmal1KO mouse. We found that only 3% of the differentially expressed genes were shared between
790 vehicle treated and iMSBmal1KO muscle. This is a significant reduction compared to the 32% shared
791 differentially expressed genes defined following training in the muscle specific *Ppargc1a* KO mice. Thus,
792 our findings establish the importance of muscle BMAL1 as an upstream regulator of *Ppargc1a* and other
793 transcription factors, including *Nr4a3*. We suggest that the loss of the ability of exercise to induce these
794 transcription factors result in a largely divergent molecular adaptation to exercise training [42].
795 There is growing recognition that exercise is a lifestyle intervention that contributes to systemic
796 health with beneficial impacts on virtually all organs studied to date. While this is commonly recognized,
797 the molecular mechanisms for these broad adaptations are still poorly understood. A key finding from this
798 work is that we have identified that muscle specific adaptations with exercise are significant contributors
799 to molecular adaptations in peripheral tissues. We were surprised to find that peripheral tissue remodelling,
800 similarly, to skeletal muscle was greater in magnitude in every tissue in the iMSBmal1KO mouse. The
801 changes in gene expression were largely unique to each tissue with <4% overlap in the exercise training
802 responsive genes across iWAT, liver, heart, and lung between the vehicle and iMSBmal1KO mice.
803 Importantly, while exercise training is known to be beneficial to the resilience of most tissues, the analysis
804 of the functional groups of genes that change with training in the iMSBmal1KO mice suggest several
805 organs, including lungs, liver and iWAT may be exhibiting a maladaptive response. Since the loss of
806 BMAL1 only occurred in skeletal muscle these outcomes highlight the systemic tissue cross talk induced
807 by skeletal muscle in response to exercise training. We speculate that these systemic changes are a result
808 of two factors, or the combination of both. One factor is the systemic metabolic changes which result from
809 the metabolic inflexibility of the BMAL1 deficient skeletal muscles exacerbated by the energetic demands
810 of exercise training. Changes in metabolite/substrate availability/abundance may subsequently influence
811 the transcriptomic state of the cells within the peripheral tissues. Secondly, our data indicate that loss of
812 skeletal muscle BMAL1 changes the inflammatory transcriptome both within the muscle and as well as
813 peripheral tissues, and this altered status may interfere with the adaptive processes within these tissues. Our

work adds further evidence to the growing body of literature demonstrating the importance of BMAL1 in maintaining homeostasis and facilitating adaptive processes in different and across organ systems [64–70].

In conclusion, our investigation has uncovered the critical role that BMAL1 plays in skeletal muscle as a key regulator of the gene expression programs for both acute exercise and training adaptations. In addition, our work has uncovered the significant impact that altered exercise response in muscle plays in the peripheral tissue adaptation to exercise training. Specifically, we propose that muscle BMAL1 acts upstream and is necessary for the well-defined acute exercise induction of key transcription factors including *Ppargc1a*. We also note that the transcriptome adaptations to steady state training suggest that without BMAL1 the muscle does not achieve the expected homeostatic program. Lastly, we propose that the peripheral tissue adaptations to exercise training are tightly coupled to the adaptations in skeletal muscle. In fact, if the muscle adaptations diverge to a more maladaptive state this is also linked to increased inflammation across many tissues. Understanding the molecular targets and pathways contributing to health vs. maladaptive exercise adaptations will be critical for the next stage of therapeutic design for exercise mimetics.

Acknowledgements:

We would like to thank Dr. Daniel Kopinke at the University of Florida for the use of his microscope. We also extend our thanks to the Gene Expression & Genotyping (GE) core, RRID:SCR_019145, and NextGen DNA Sequencing (NS) core, RRID:SCR_019152 and the Southeast Center for Integrated Metabolomics, (SECIM) at the University of Florida for library preparation, DNA sequencing and metabolomics respectively. We would like to thank Dr. Jerome Menet for constructive feedback and discussions on our data. This work was supported by NIH R01AR079220 to KAE.

References:

[1] Dyar, K.A., Ciciliot, S., Wright, L.E., Biensø, R.S., Tagliazucchi, G.M., Patel, V.R., et al., 2014. Muscle insulin sensitivity and glucose metabolism are controlled by the intrinsic muscle clock. Molecular Metabolism 3(1): 29–41, Doi: 10.1016/j.molmet.2013.10.005.

[2] Ripperger, J.A., Schibler, U., 2006. Rhythmic CLOCK-BMAL1 binding to multiple E-box motifs drives circadian Dbp transcription and chromatin transitions. Nature Genetics 38(3): 369–74, Doi: 10.1038/ng1738.

[3] Menet, J.S., Pescatore, S., Rosbash, M., 2014. CLOCK:BMAL1 is a pioneer-like transcription factor. Genes & Development 28(1): 8–13, Doi: 10.1101/gad.228536.113.

[4] Martin, R.A., Viggars, M.R., Esser, K.A., 2023. Metabolism and exercise: the skeletal muscle clock takes centre stage. Nature Reviews Endocrinology: 1–13.

[5] Hodge, B.A., Wen, Y., Riley, L.A., Zhang, X., England, J.H., Harfmann, B.D., et al., 2015. The endogenous molecular clock orchestrates the temporal separation of substrate metabolism in skeletal muscle. Skeletal Muscle 5(1): 1–16.

[6] Harfmann, B.D., Schroder, E.A., Kachman, M.T., Hodge, B.A., Zhang, X., Esser, K.A., 2016. Muscle-specific loss of Bmal1 leads to disrupted tissue glucose metabolism and systemic glucose homeostasis. Skeletal Muscle 6(1): 12, Doi: 10.1186/s13395-016-0082-x.

[7] Zitting, K.-M., Vujovic, N., Yuan, R.K., Isherwood, C.M., Medina, J.E., Wang, W., et al., 2018. Human resting energy expenditure varies with circadian phase. Current Biology 28(22): 3685-3690. e3.

[8] Wolff, C.A., Gutierrez-Monreal, M.A., Meng, L., Zhang, X., Douma, L.G., Costello, H.M., et al., 2022. Defining the age-dependent and tissue-specific circadian transcriptome in male mice. Genomics.

[9] Viggars, M.R., Sutherland, H., Cardozo, C.P., Jarvis, J.C., 2023. Conserved and species-specific transcriptional responses to daily programmed resistance exercise in rat and mouse. The FASEB Journal 37(12): e23299.

[10] Viggars, M.R., Sutherland, H., Lanmüller, H., Schmoll, M., Bijak, M., Jarvis, J.C., 2023. Adaptation of the transcriptional response to resistance exercise over 4 weeks of daily training. The FASEB Journal 37(1): e22686, Doi: 10.1096/fj.202201418R.

[11] Akashi, M., Tsuchiya, Y., Yoshino, T., Nishida, E., 2002. Control of Intracellular Dynamics of Mammalian Period Proteins by Casein Kinase I ε (CKIε) and CKIϛ in Cultured Cells. MOL. CELL. BIOL. 22: 11.

[12] Camacho, F., Cilio, M., Guo, Y., Virshup, D.M., Patel, K., Khorkova, O., et al., 2001. Human casein kinase Iδ phosphorylation of human circadian clock proteins period 1 and 2. FEBS Letters 489(2–3): 159–65, Doi: 10.1016/S0014-5793(00)02434-0.

[13] Etchegaray, J.-P., Machida, K.K., Noton, E., Constance, C.M., Dallmann, R., Di Napoli, M.N., et al., 2009. Casein Kinase 1 Delta Regulates the Pace of the Mammalian Circadian Clock. Molecular and Cellular Biology 29(14): 3853–66, Doi: 10.1128/MCB.00338-09.

[14] Thomas, J.M., Kern, P.A., Bush, H.M., McQuerry, K.J., Black, W.S., Clasey, J.L., et al., 2020. Circadian rhythm phase shifts caused by timed exercise vary with chronotype. JCI Insight 5(3): e134270, Doi: 10.1172/jci.insight.134270.

[15] Kemler, D., Wolff, C.A., Esser, K.A., 2020. Time-of-day dependent effects of contractile activity on the phase of the skeletal muscle clock. The Journal of Physiology 598(17): 3631–44, Doi: 10.1113/JP279779.

[16] Wolff, C.A., Esser, K.A., 2020. Exercise sets the muscle clock with a calcium assist. The Journal of Physiology 598(24): 5591–2, Doi: 10.1113/JP280783.

[17] Sato, S., Basse, A.L., Schönke, M., Chen, S., Samad, M., Altıntaş, A., et al., 2019. Time of Exercise Specifies the Impact on Muscle Metabolic Pathways and Systemic Energy Homeostasis. Cell Metabolism 30(1): 92-110.e4, Doi: 10.1016/j.cmet.2019.03.013.

[18] Sato, S., Dyar, K.A., Treebak, J.T., Jepsen, S.L., Ehrlich, A.M., Ashcroft, S.P., et al., 2022. Atlas of exercise metabolism reveals time-dependent signatures of metabolic homeostasis. Cell Metabolism 34(2): 329-345.e8, Doi: 10.1016/j.cmet.2021.12.016.

[19] Savikj, M., Gabriel, B.M., Alm, P.S., Smith, J., Caidahl, K., Björnholm, M., et al., 2019. Afternoon exercise is more efficacious than morning exercise at improving blood glucose levels in individuals with type 2 diabetes: a randomised crossover trial. Diabetologia 62(2): 233–7, Doi: 10.1007/s00125-018-4767-z.

[20] Savikj, M., Stocks, B., Sato, S., Caidahl, K., Krook, A., Deshmukh, A.S., et al., 2022. Exercise timing influences multi-tissue metabolome and skeletal muscle proteome profiles in type 2 diabetic patients – A randomized crossover trial. Metabolism 135: 155268, Doi: 10.1016/j.metabol.2022.155268.

[21] Dyar, K.A., Ciciliot, S., Tagliazucchi, G.M., Pallafacchina, G., Tothova, J., Argentini, C., et al., 2015. The calcineurin-NFAT pathway controls activity-dependent circadian gene expression in slow skeletal muscle. Molecular Metabolism 4(11): 823–33.

[22] Casanova-Vallve, N., Duglan, D., Vaughan, M.E., Pariollaud, M., Handzlik, M.K., Fan, W., et al., 2022. Daily running enhances molecular and physiological circadian rhythms in skeletal muscle. Molecular Metabolism 61: 101504, Doi: 10.1016/j.molmet.2022.101504.

[23] Douglas, C.M., Hesketh, S.J., Esser, K.A., 2021. Time of Day and Muscle Strength: A Circadian Output? Physiology 36(1): 44–51, Doi: 10.1152/physiol.00030.2020.
[24] Ab Malik, Z., Bowden Davies, K.A., Hall, E.C., Barrett, J., Pullinger, S.A., Erskine, R.M., et al., 2020. Diurnal differences in human muscle isometric force in vivo are associated with differential phosphorylation of sarcomeric M-band proteins. Proteomes 8(3): 22.
[25] Dyar, K.A., Hubert, M.J., Mir, A.A., Ciciliot, S., Lutter, D., Greulich, F., et al., 2018. Transcriptional programming of lipid and amino acid metabolism by the skeletal muscle circadian clock. PLOS Biology 16(8): e2005886, Doi: 10.1371/journal.pbio.2005886.
[26] Fernández-Martínez, J., Ramírez-Casas, Y., Aranda-Martínez, P., López-Rodríguez, A., Sayed, R.K.A., Escames, G., et al., n.d. iMS-Bmal1−/− mice show evident signs of sarcopenia that are counteracted by exercise and melatonin therapies. Journal of Pineal Research n/a(n/a): e12912, Doi: 10.1111/jpi.12912.
[27] Adamovich, Y., Dandavate, V., Ezagouri, S., Manella, G., Zwighaft, Z., Sobel, J., et al., 2021. Clock proteins and training modify exercise capacity in a daytime-dependent manner. Proceedings of the National Academy of Sciences 118(35): e2101115118, Doi: 10.1073/pnas.2101115118.
[28] Pillon, N.J., Gabriel, B.M., Dollet, L., Smith, J.A.B., Sardón Puig, L., Botella, J., et al., 2020. Transcriptomic profiling of skeletal muscle adaptations to exercise and inactivity. Nature Communications 11(1): 470, Doi: 10.1038/s41467-019-13869-w.
[29] Egan, B., Sharples, A.P., 2022. Molecular Responses to Acute Exercise and Their Relevance for Adaptations in Skeletal Muscle to Exercise Training. Physiological Reviews.
[30] Avila, J.J., Kim, S.K., Massett, M.P., 2017. Differences in Exercise Capacity and Responses to Training in 24 Inbred Mouse Strains. Frontiers in Physiology 8: 974, Doi: 10.3389/fphys.2017.00974.
[31] Viggars, M.R., Wen, Y., Peterson, C.A., Jarvis, J.C., 2022. Automated cross-sectional analysis of trained, severely atrophied, and recovering rat skeletal muscles using MyoVision 2.0. Journal of Applied Physiology 132(3): 593–610, Doi: 10.1152/japplphysiol.00491.2021.
[32] Murach, K.A., Mobley, C.B., Zdunek, C.J., Frick, K.K., Jones, S.R., McCarthy, J.J., et al., 2020. Muscle memory: myonuclear accretion, maintenance, morphology, and miRNA levels with training and detraining in adult mice. Journal of Cachexia, Sarcopenia and Muscle 11(6): 1705–22, Doi: 10.1002/jcsm.12617.
[33] Gabriel, B.M., Altıntaş, A., Smith, J.A., Sardon-Puig, L., Zhang, X., Basse, A.L., et al., 2021. Disrupted circadian oscillations in type 2 diabetes are linked to altered rhythmic mitochondrial metabolism in skeletal muscle. Science Advances 7(43): eabi9654.
[34] Huang, D.W., Sherman, B.T., Tan, Q., Kir, J., Liu, D., Bryant, D., et al., 2007. DAVID Bioinformatics Resources: expanded annotation database and novel algorithms to better extract biology from large gene lists. Nucleic Acids Research 35(suppl_2): W169–75.
[35] Khan, A., Mathelier, A., 2017. Intervene: a tool for intersection and visualization of multiple gene or genomic region sets. BMC Bioinformatics 18(1): 1–8.
[36] Pang, Z., Zhou, G., Ewald, J., Chang, L., Hacariz, O., Basu, N., et al., 2022. Using MetaboAnalyst 5.0 for LC–HRMS spectra processing, multi-omics integration and covariate adjustment of global metabolomics data. Nature Protocols 17(8): 1735–61.
[37] Laothamatas, I., Rasmussen, E.S., Green, C.B., Takahashi, J.S., 2023. Metabolic and chemical architecture of the mammalian circadian clock. Cell Chemical Biology.
[38] Small, L., Altıntaş, A., Laker, R.C., Ehrlich, A., Pattamaprapanont, P., Villarroel, J., et al., 2020. Contraction influences Per2 gene expression in skeletal muscle through a calcium-dependent pathway. The Journal of Physiology 598(24): 5739–52, Doi: 10.1113/JP280428.
[39] Sabaratnam, R., Pedersen, A.J., Eskildsen, T.V., Kristensen, J.M., Wojtaszewski, J.F., Højlund, K., 2019. Exercise induction of key transcriptional regulators of metabolic adaptation in muscle is preserved in type 2 diabetes. The Journal of Clinical Endocrinology & Metabolism 104(10): 4909–20.

[40] Liu, C., Li, S., Liu, T., Borjigin, J., Lin, J.D., 2007. Transcriptional coactivator PGC-1α integrates the mammalian clock and energy metabolism. Nature 447(7143): 477–81.

[41] Andrews, J.L., Zhang, X., McCarthy, J.J., McDearmon, E.L., Hornberger, T.A., Russell, B., et al., 2010. CLOCK and BMAL1 regulate MyoD and are necessary for maintenance of skeletal muscle phenotype and function. Proceedings of the National Academy of Sciences 107(44): 19090–5.

[42] Furrer, R., Heim, B., Schmid, S., Dilbaz, S., Adak, V., Nordström, K.J.V., et al., 2023. Molecular control of endurance training adaptation in male mouse skeletal muscle. Nature Metabolism, Doi: 10.1038/s42255-023-00891-y.

[43] Dings, M.P., van der Zalm, A.P., Bootsma, S., van Maanen, T.F., Waasdorp, C., van den Ende, T., et al., 2022. Estrogen-related receptor alpha drives mitochondrial biogenesis and resistance to neoadjuvant chemoradiation in esophageal cancer. Cell Reports Medicine 3(11).

[44] Tripathi, M., Yen, P.M., Singh, B.K., 2020. Estrogen-related receptor alpha: an under-appreciated potential target for the treatment of metabolic diseases. International Journal of Molecular Sciences 21(5): 1645.

[45] Kan, J., Hu, Y., Ge, Y., Zhang, W., Lu, S., Zhao, C., et al., 2021. Declined expressions of vast mitochondria-related genes represented by CYCS and transcription factor ESRRA in skeletal muscle aging. Bioengineered 12(1): 3485–502.

[46] Billon, C., Sitaula, S., Banerjee, S., Welch, R., Elgendy, B., Hegazy, L., et al., 2023. Synthetic ERRα/β/γ Agonist Induces an ERRα-Dependent Acute Aerobic Exercise Response and Enhances Exercise Capacity. ACS Chemical Biology 18(4): 756–71.

[47] Baar, K., Wende, A.R., Jones, T.E., Marison, M., Nolte, L.A., Chen, M.A.Y., et al., 2002. Adaptations of skeletal muscle to exercise: rapid increase in the transcriptional coactivator PGC-1. The FASEB Journal 16(14): 1879–86.

[48] Xia, H., Scholtes, C., Dufour, C.R., Guluzian, C., Giguère, V., 2023. ERRα fosters running endurance by driving myofiber aerobic transformation and fuel efficiency. Molecular Metabolism: 101814, Doi: 10.1016/j.molmet.2023.101814.

[49] Yusifova, M., Yusifov, A., Polson, S.M., Todd, W.D., Schmitt, E.E., Bruns, D.R., 2023. Voluntary wheel running exercise does not attenuate circadian and cardiac dysfunction caused by conditional deletion of Bmal1. Journal of Biological Rhythms: 07487304231152398.

[50] Group, M.S., Amar, D., Gay, N.R., Jean Beltran, P.M., Adkins, J.N., Almagro Armenteros, J.J., et al., 2022. Temporal dynamics of the multi-omic response to endurance exercise training across tissues. BioRxiv: 2022.09. 21.508770.

[51] Smith, G.R., Zhao, B., Lindholm, M.E., Raja, A., Viggars, M., Pincas, H., et al., 2023. Multi-omic identification of key transcriptional regulatory programs during endurance exercise training. bioRxiv.

[52] Wang, Z.-Y., Keogh, A., Waldt, A., Cuttat, R., Neri, M., Zhu, S., et al., 2021. Single-cell and bulk transcriptomics of the liver reveals potential targets of NASH with fibrosis. Scientific Reports 11(1): 19396.

[53] DeBari, M.K., Abbott, R.D., 2020. Adipose tissue fibrosis: mechanisms, models, and importance. International Journal of Molecular Sciences 21(17): 6030.

[54] Jääskeläinen, I., Petäistö, T., Mirzarazi Dahagi, E., Mahmoodi, M., Pihlajaniemi, T., Kaartinen, M.T., et al., 2023. Collagens Regulating Adipose Tissue Formation and Functions. Biomedicines 11(5): 1412.

[55] Sun, K., Li, X., Scherer, P.E., 2023. Extracellular matrix (ECM) and fibrosis in adipose tissue: overview and perspectives. Comprehensive Physiology 13(1): 4387.

[56] Ruschke, K., Fishbein, L., Dietrich, A., Klöting, N., Tönjes, A., Oberbach, A., et al., 2010. Gene expression of PPARγ and PGC-1α in human omental and subcutaneous adipose tissues is related to insulin resistance markers and mediates beneficial effects of physical training. European Journal of Endocrinology 162(3): 515–23.

[57] Nigro, P., Vamvini, M., Yang, J., Caputo, T., Ho, L.-L., Carbone, N.P., et al., 2023. Exercise training remodels inguinal white adipose tissue through adaptations in innervation, vascularization, and the extracellular matrix. Cell Reports 42(4).
[58] Dreher, S.I., Irmler, M., Pivovarova-Ramich, O., Kessler, K., Jürchott, K., Sticht, C., et al., 2023. Acute and long-term exercise adaptation of adipose tissue and skeletal muscle in humans: a matched transcriptomics approach after 8-week training-intervention. International Journal of Obesity 47(4): 313–24.
[59] Ma, X., Wang, D., Zhao, W., Xu, L., 2018. Deciphering the roles of PPARγ in adipocytes via dynamic change of transcription complex. Frontiers in Endocrinology 9: 473.
[60] Youssef, J., Badr, M., 2004. Role of peroxisome proliferator-activated receptors in inflammation control. BioMed Research International 2004: 156–66.
[61] Bensinger, S.J., Tontonoz, P., 2008. Integration of metabolism and inflammation by lipid-activated nuclear receptors. Nature 454(7203): 470–7.
[62] Moller, D.E., Berger, J.P., 2003. Role of PPARs in the regulation of obesity-related insulin sensitivity and inflammation. International Journal of Obesity 27(3): S17–21.
[63] Qu, M., Qu, H., Jia, Z., Kay, S.A., 2021. HNF4A defines tissue-specific circadian rhythms by beaconing BMAL1::CLOCK chromatin binding and shaping the rhythmic chromatin landscape. Nature Communications 12(1): 6350, Doi: 10.1038/s41467-021-26567-3.
[64] Bass, J., 2024. Interorgan rhythmicity as a feature of healthful metabolism. Cell Metabolism.
[65] Smith, J.G., Koronowski, K.B., Mortimer, T., Sato, T., Greco, C.M., Petrus, P., et al., 2023. Liver and muscle circadian clocks cooperate to support glucose tolerance in mice. Cell Reports 42(6): 112588, Doi: 10.1016/j.celrep.2023.112588.
[66] Greco, C.M., Koronowski, K.B., Smith, J.G., Shi, J., Kunderfranco, P., Carriero, R., et al., 2021. Integration of feeding behavior by the liver circadian clock reveals network dependency of metabolic rhythms. Science Advances 7(39), Doi: 10.1126/sciadv.abi7828.
[67] Ehlen, J.C., Brager, A.J., Baggs, J., Pinckney, L., Gray, C.L., DeBruyne, J.P., et al., 2017. Bmal1 function in skeletal muscle regulates sleep. Elife 6: e26557.
[68] McDearmon, E.L., Patel, K.N., Ko, C.H., Walisser, J.A., Schook, A.C., Chong, J.L., et al., 2006. Dissecting the functions of the mammalian clock protein BMAL1 by tissue-specific rescue in mice. Science 314(5803): 1304–8.
[69] Smith, J.G., Molendijk, J., Blazev, R., Chen, W.H., Zhang, Q., Litwin, C., et al., 2023. Impact of Bmal1 rescue and time-restricted feeding on liver and muscle proteomes during the active phase in mice. Molecular & Cellular Proteomics 22(11).
[70] Sun, S., Ma, S., Cai, Y., Wang, S., Ren, J., Yang, Y., et al., 2023. A single-cell transcriptomic atlas of exercise-induced anti-inflammatory and geroprotective effects across the body. The Innovation 4(1).

Supplemental Files:

Supplementary File 1: RNA/ATAC-seq Data

Supplementary File 2: LCMS Metabolomics Data

Figure Legends:

Figure 1: Loss of skeletal muscle *Bmal1* alters the transcriptional response to acute exercise.

(A) Experiment 1. Vehicle and iMSBmal1KO mice completed a 30-minute, 15° inclined treadmill bout at 70% of their maximum work done and gastrocnemius muscles were collected 1-hour post. (B) Exercise

1037 bout work was matched between genotypes. (C) RNA-sequencing was used to assess the number of DEGs
1038 1-hour post exercise in vehicle and iMSBmal1KO mice. (D) Venn overlap of vehicle and iMSBmal1KO
1039 mice exercise responses. (E) Pathway analysis of shared exercise response genes. (F) Z-scores of exercise
1040 responsive clock factors and common exercise response genes shown between genotypes. Associated
1041 pathway databases are indicated by (R) Reactome, (K) KEGG, and (BP) Biological Processes. Pathway
1042 analysis of vehicle exercise responsive genes (G) and iMSBmal1KO exercise responsive genes (H).
1043 Figure 2: Graded exercise performance and body composition analysis of vehicle and iMSBmal1KO mice.
1044 The experimental design is illustrated in (A) which shows the timecourse and parameters of exercise
1045 training, physiological testing and tissue collection. At ~4 months of age, iMSBmal1$^{fl/fl}$ were treated with
1046 either a vehicle, or with tamoxifen for 5 days (2mg/day) to induce Cre-recombination and loss of *Bmal1*
1047 specifically in skeletal muscle. Both vehicle and iMSBmal1KO mice were randomly assigned to 6 weeks
1048 of exercise training performed at ZT13, or control groups. Graded exercise tests were performed prior to,
1049 after 2, 4 and 6-weeks of training with the speed adjusted accordingly to make training progressive. MRIs
1050 were performed before, after 3 and 6 weeks of training. Mice from all groups were euthanised, and tissue
1051 was collected at ZT13, 47 hours after their final graded exercise test. (B) illustrates the weekly work done
1052 (AU) during exercise training. (C) Measurements of body mass were taken before, after 3 and 6 weeks of
1053 training and the subsequent percentage change calculated for each individual. (D) Total fat mass (g)
1054 measured before, after 3 and 6 weeks of training. (E) Percent changes in fat mass (g) were calculated from
1055 the beginning of the training period to the middle and end of the training period. (F) Total lean mass (g)
1056 measured before, after 3 and 6 weeks of training. (G) Percent changes in lean mass (g) were calculated from
1057 the beginning of the training period to the middle and end of the training period.

1058 Figure 3: iMSBmal1KO gastrocnemius muscles present a larger and divergent transcriptional adaptation to
1059 6-weeks of exercise training. (A) Volcano plot illustrating DEGs between control and iMSBmal1 WT
1060 exercise trained mice. A total of 142 (75 downregulated, 67 upregulated) genes were differentially
1061 expressed using an FDR cut off of <0.05. (B) HOMER Motif analysis performed on up and downregulated
1062 DEGs identifies a number of transcription factors regulating the transcriptional response to normal exercise
1063 adaptation. (C) KEGG Pathway analysis of genes associated with the vehicle treated transcriptional
1064 response to exercise training. (D) Volcano plot illustrating DEGs between iMSBmal1KO control and
1065 iMSBmal1KO exercise trained mice. A total of 780 (283 downregulated, 497 upregulated) genes were
1066 differentially expressed using an FDR cut off of <0.05. (E) HOMER Motif analysis performed on up and
1067 downregulated DEGs identifies a number of transcription factors regulating the transcriptional response to
1068 exercise adaptation in the absence of skeletal muscle Bmal1. (F) KEGG Pathway analysis of genes
1069 associated with the iMSBmal1KO transcriptional remodeling to exercise training. (G) Venn diagram

1070 overlapping of DEG responses to vehicle and iMSBmal1KO exercise training at $P < 0.01$. Minimal overlap
1071 in the transcriptional exercise responses is present between vehicle treated and iMSBmal1KO mice using a
1072 lenient significance cut off (63 out of 2107, 2.99% overlap). (H) Pie chart of the 63 common exercise
1073 training responsive genes in both genotypes reveals common and oppositely regulated gene reprogramming.
1074 (I) Analysis of DEGs affected by loss of BMAL1 and exercise training responsive DEGs in the
1075 iMSBma1KO mice, reveals 94 common genes. Pearson's correlation of the 94 common DEGs (Log^2 fold
1076 changes) reveals that genes affected with Bmal1KO are not rescued with exercise training. (J) Heatmap
1077 presenting Log^2 Z-scores for core clock factors/clock output genes and genes associated with glucose
1078 handling and glycogen utilization. Exercise training does not rescue the downregulation of these genes in
1079 iMSBmal1KO mice.

1080 Figure 4: Upregulation of genes associated with pyruvate oxidation, TCA cycle, β-oxidation, mitochondrial
1081 complexes and mitoribosome subunits after exercise training in the iMSBmal1KO mouse. (A) Schematic
1082 of biological processes involved in providing acetyl-CoA from carbohydrates and lipids for the TCA cycle.
1083 Subsequently, the TCA cycle provides NADH and $FADH_2$ for the electron transport chain. Components
1084 are numbered/labelled for clarity of the associated genes presented in panels B and C. (B) Heatmaps
1085 presenting genes associated with pyruvate oxidation, TCA cycle and β-oxidation, (Log^2 Z-scores). (C)
1086 Heatmap presenting genes associated with mitochondrial complexes I-V and the mitochondrial ribosome
1087 (Log^2 Z-scores).

1088 Figure 5: Loss of *Bmal1* in skeletal muscle disrupts the metabolomic rewiring in response to exercise
1089 training and causes depletion of TCA cycle intermediates. (A) Table of differentially abundant metabolites
1090 ($q < 0.05$) with loss of skeletal muscle BMAL1, the vehicle exercise training response and the
1091 iMSBmal1KO exercise training response. (B) Venn diagram analysis of the different comparisons reveals
1092 little overlap and divergent metabolomic adaptations to exercise training. (C) Metaboanalyst KEGG
1093 metabolite pathway analysis of the iMSBmal1KO exercise training response. Numbers indicate the number
1094 of metabolites identified within the pathway. (D) Heatmap illustrating normalized metabolite abundance
1095 for amino acids. (E) Heatmap illustrating normalized metabolite abundance for metabolites relating to
1096 glycolysis and the TCA cycle. (F) Boxplots of highlighted amino acids changing with loss of BMAL1 and
1097 exercise training. (G) Boxplots of highlighted TCA cycle metabolites/phosphocreatine changing with loss
1098 of BMAL1 and exercise training. (H) Summary diagram of TCA cycle metabolites affected with exercise
1099 training in the iMSBmal1KO (Blue indicates higher abundance, red indicates lower abundance.
1100 Significance for one way ANOVA analysis is presented as $*P \leq 0.05$, $**P \leq 0.01$, $***P \leq 0.001$, $****P \leq$
1101 0.0001.

1102 Figure 6: Loss of skeletal muscle BMAL1 indirectly disrupts transcriptional homeostasis of peripheral
1103 tissues. (A) Upset plot of the differentially expressed genes affected by loss of skeletal muscle BMAL1
1104 across tissues. Set size indicates the total number of differentially expressed genes regulated by loss of
1105 BMAL1 in skeletal muscle in each tissue. Numbers above bars indicate the number of differentially
1106 expressed genes. Overlapping differentially expressed genes which are common between tissues are
1107 indicated by the connected points below bars. In summary when comparing vehicle control and
1108 iMSBmal1KO controls we identified 684 (425 upregulated, 259 downregulated) differentially expressed
1109 genes in inguinal white adipose tissue (iWAT), 199 (86 upregulated, 114 downregulated) in liver, 1177
1110 (665 upregulated, 512 downregulated) in the heart and 110 (82 upregulated, 28 downregulated) in lung
1111 tissue where identified. Pathway analysis for differentially expressed genes in inguinal white adipose tissue
1112 (B), liver tissue (C), heart tissue (D) and lung tissue (E). Red segments of bars indicate downregulation
1113 with loss of BMAL1, blue segments of bars indicate upregulation with loss of BMAL1. Associated pathway
1114 databases are indicated by (R) Reactome, (K) KEGG and (BP) Biological Processes.

1115 Figure 7: Divergent transcriptional reprogramming of peripheral tissues in response to endurance exercise
1116 training in the absence of skeletal muscle BMAL1. (A) Upset plot of the gene sets associated with the
1117 training response of each tissue in both genotypes. Set size indicates the total number of differentially
1118 expressed genes regulated by exercise training in each tissue in both genotypes. Numbers above bars
1119 indicate the number of differentially expressed genes. Overlapping differentially expressed genes which
1120 are common between tissues are indicated by the connected points below bars. Differentially expressed
1121 genes common between genotypes within the same tissue are indicated by red connected points. (B)
1122 Summary Venn diagram of genotype specific exercise training responsive genes in vehicle (409 DEGs) and
1123 iMSBmal1KO mice (423 DEGs) with shared features (32 DEGs) in inguinal white adipose tissue.
1124 Associated inguinal white adipose tissue pathway analysis for vehicle (C) and iMSBmal1KO mice (D). (E)
1125 Summary Venn diagram of genotype specific exercise training responsive genes in vehicle (316 DEGS)
1126 and iMSBmal1KO mice (541 DEGs) with shared features (30 DEGs) in liver tissue. Associated liver
1127 pathway analysis for vehicle (F) and iMSBmal1KO mice (G). (H) Summary Venn diagram of genotype
1128 specific exercise training responsive genes in vehicle (228 DEGs) and iMSBmal1KO mice (765 DEGs)
1129 with shared features (33 DEGs) in heart tissue. Associated heart pathway analysis for vehicle (I) and
1130 iMSBmal1KO mice (J). (K) Summary Venn diagram of genotype specific exercise training responsive
1131 genes in vehicle (192 DEGs) and iMSBmal1KO mice (617 DEGs) with shared features (16 DEGs) in lung
1132 tissue. Associated lung pathway analysis for vehicle (L) and iMSBmal1KO mice (M). Red segments of
1133 bars indicate downregulation with exercise training, whereas blue segments of bars indicate upregulation
1134 with exercise training. Associated pathway databases are indicated by (R) Reactome, (K) KEGG and (BP)
1135 Biological Processes.

1136 Figure 8: Loss of skeletal muscle BMAL1 causes rewiring of inflammatory and metabolic pathways across
1137 multiple tissues after exercise training. Deseq2 normalized counts were used to produce within tissue Z-
1138 scores for all expressed genes for all 4 experimental groups. Average Z-scores were then produced from all
1139 genes found within the given KEGG pathway for vehicle exercise trained (grey bars) and iMSBmal1KO
1140 exercise trained mice (dark blue bars) for each tissue. Tissues are indicated by green bars (Gastrocnemius
1141 Muscle), light blue bars (iWAT), yellow bars (Liver), red bars (Heart) and purple bars (Lung). Data is
1142 presented for KEGG pathways related to (A) the Immune System, (B) Endocrine System and (C) Amino
1143 Acid, Carbohydrate and Lipid Metabolism. Blue signifies relative upregulation of associated pathways and
1144 red signifies relative downregulation of the genes within the associated pathways.

1145 Supplemental Figure Legends:

1146 Supplementary Figure 1: (A) Confirmation of successful Bmal1 Cre-Recombination in gastrocnemius
1147 muscles and lack of recombination in heart (B), liver (C), inguinal white adipose tissue (D) and lung (E).

1148 Supplementary Figure 2: Physiological assessment of vehicle treated and iMSBmal1KO mice. (A)
1149 Differences in age (weeks) between cohorts 1 and 2 at termination. Mice in the older cohort are indicated
1150 by square data points, mice in the younger cohort are indicated by circle data points. (B) Age in weeks
1151 (termination). (C) Body Weight (g). (D) MRI measured lean mass as a percentage of total body weight. (E)
1152 MRI measured fat mass as a percentage of total body weight. (F) Forelimb grip strength (N/gBW). Rotarod
1153 time to fall assessment in seconds (average of 3 trials) (G) and maximal speed (RPM) (H). Cohort 1 is
1154 delineated by circles, cohort 2 is delineated by squares. Vehicle treated mice are delineated by blue circles,
1155 iMSBmal1KO mice are delineated by red circles. Significance was determined by use of an unpaired t-test
1156 where ns indicates $p>0.05$, * indicates $p<0.05$, ** indicates $p<0.01$, *** indicates $p<0.001$ and ****
1157 indicates $p<0.0001$.

1158 Supplementary Figure 3: Transcriptome and chromatin accessibility analysis of iMSBmal1KO mice.
1159 Vehicle treated and iMSBmal1KO mice underwent baseline physiological phenotyping including RNA and
1160 ATAC-sequencing analysis at ZT13 on gastrocnemius tissue. (B) Number of DEGs genes with loss of
1161 skeletal muscle *Bmal1* ($q = 0.05$). Numbers in bars indicate up or downregulation. (C) Pathway analysis of
1162 differentially expressed RNAs split by direction of change. Numbers in bars indicate the number of genes
1163 present within the pathway. (D) Number of differentially accessible regions as assessed by ATAC-seq.
1164 Numbers in bars indicate the number of DNA regions/peaks becoming more or less accessible with loss of
1165 *Bmal1*. (E) Pathway analysis of differentially accessible chromatin regions split by direction of change.
1166 Numbers in bars indicate the number of genes present within the pathway. (F) Venn overlap of vehicle
1167 acute exercise response DEGs and genes regulated by skeletal muscle BMAL1 (BMAL1:CLOCK ChIP-

1168 seq peaks, Gabriel *et al*. 2021 Sci Adv). (G) Pathway analysis of overlapping features. (H) Example
1169 BMAL1 ChIP-seq plots illustrating BMAL1 binding in promoter regions of *Nr4a3* and *Irs2*.

1170 Supplementary Figure 4: Panel (A/B) Maximum work-done tests were performed prior to, after 2, 4 and 6-
1171 weeks of training with the speed adjusted accordingly to make training progressive. (C) The amount of food
1172 consumed per week was measured and is presented as a proportion of body weight. (D) Measurements of
1173 body mass were taken weekly. Habitual cage activity as measured by infrared cage monitors revealed no
1174 change in total activity levels between groups. (E) Total Activity. (F) Activity restricted to the dark/active
1175 phase. (G) Activity restricted to the light/inactive phase. Significance for two-way ANOVA analysis is
1176 presented as $*p \leq 0.05$, $**p \leq 0.01$, $***p \leq 0.001$, $****p \leq 0.0001$.

1177 Supplementary Figure 5: Histological phenotyping of gastrocnemius muscle. (A) Gastrocnemius muscle
1178 wet weight is presented as milligrams per gram of body weight. Myovision 2.0 software was used to
1179 automatically assess the average fiber cross-sectional area (µm2) (B), the proportion of different fiber types
1180 (expressed as a percentage of all fibers) (C). (D) Gastrocnemius SDH intensity value (Log10 AU).
1181 Myovision 2.0 assessments of the total number of nuclei per fiber cross-section (E), the number of
1182 myonuclei per fiber cross-section (F). (G) illustrates the % of fibers with central nuclei and (H) illustrates
1183 the % of fibers that were embryonic myosin positive. (I) Representative dystrophin and DAPI images for
1184 each respective group. Scale bars indicate 100µm. (J) Representative immunofluorescent images depicting
1185 whole cross-section gastrocnemius muscles from each experimental condition labeled with Type IIA/Type
1186 IIX/B. Scale bars indicate 1800µm. Data are presented as mean ± standard deviation or min-max values for
1187 box plots. Significance for one-way ANOVA analysis is presented as $*P \leq 0.05$, $**P \leq 0.01$, $***P \leq 0.001$.

1188 Supplementary Figure 6: Training Study. Loss of Bmal1 in skeletal muscle causes transcriptional disruption
1189 of circadian rhythms, substrate metabolism and energy sensing pathways. (A) Volcano plot illustrating the
1190 DEGs between vehicle control and iMSBmal1KO controls. A total of 1217 (682 downregulated, 535
1191 upregulated) genes were differentially expressed using an FDR cut off of <0.05. (B) HOMER Motif analysis
1192 performed on up and downregulated DEGs (q=0.05), identifies a number of transcription factors regulating
1193 the transcriptional response to loss of BMAL11 in skeletal muscle. (C) KEGG Pathway analysis reveals
1194 disruption of circadian rhythms, metabolic pathways and cell cycle/energy sensing pathways with loss of
1195 BMAL1 in skeletal muscle.

1196 Supplementary Figure 7: (A) Heatmap representing the 94 genes overlapping the vehicle control vs.
1197 iMSBmal1KO Control statistical comparison and iMSBmal1KO Control vs. iMSBmal1KO exercise
1198 trained statistical comparison.

1199 Supplementary Figure 8: ZT13 core clock factor gene expression (Deseq2 normalized counts) in the
1200 gastrocnemius muscle in response to muscle specific Bmal1KO, exercise training and the combination of
1201 the two treatments. Data is presented as mean ± standard deviation. Significance for one way ANOVA
1202 analysis is presented as $*P \leq 0.05$, $**P \leq 0.01$, $***P \leq 0.001$, $****P \leq 0.0001$.

1203 Supplementary Figure 9: Metabolic indices of vehicle treated and iMSBmal1KO mice with and without 6-
1204 weeks exercise training taken at ZT13. (A) Blood hemoglobin A1C percentage (Hba1c%), (B) resting blood
1205 glucose (mg/dL), (C) resting plasma insulin (ng/dL), (D) gastrocnemius muscle glycogen concentration
1206 (µg/mg), (E) gastrocnemius muscle triglyceride concentration (nmol/mg), (F) liver glycogen concentration
1207 (µg/mg), (G) liver triglyceride concentration (nmol/mg). Significance for one way ANOVA analysis is
1208 presented as $*p \leq 0.05$, $**p \leq 0.01$, $***p \leq 0.001$, $****p \leq 0.0001$.

1209 Supplementary Figure 10: (A) HOMER transcription factor enrichment analysis of exercise responsive
1210 DEGs across genotypes and tissues presented as -Log10 *P*-values.

1211 Supplementary Figure 11: Rescue correlations for all genes affected by loss of skeletal muscle BMAL1 and
1212 their exercise trained responses in iMSBmal1KO mice for (A) gastrocnemius muscle, (B) inguinal white
1213 adipose tissue, (C) liver, (D) heart and (E) lung. iWAT and heart display relatively strong relationships (R^2=
1214 0.51-0.67) suggesting exercise training in the iMSBma1KO mice brings their transcriptomes closer to
1215 vehicle control mice. Muscle, liver and lung show weaker relationships (R^2= 0.04-0.22).

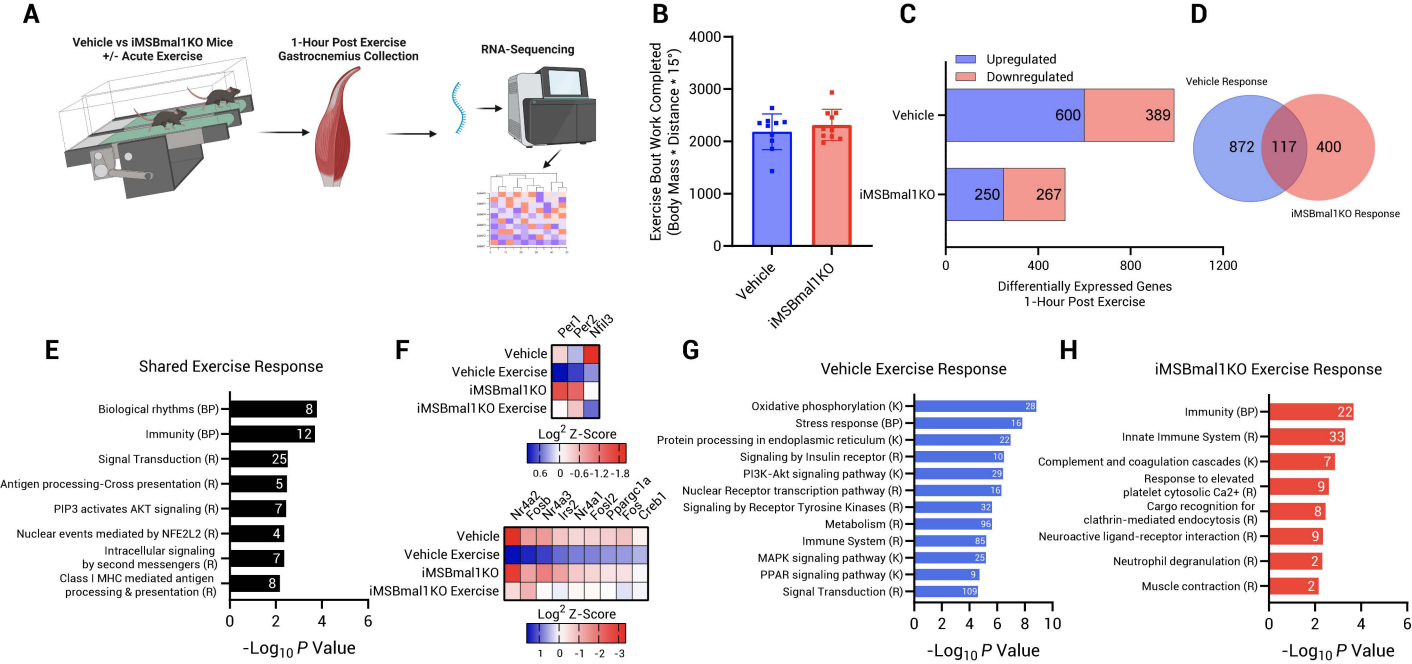
A
Vehicle vs iMSBmal1KO Mice
+/- Acute Exercise
1-Hour Post Exercise
Gastrocnemius Collection
RNA-Sequencing
B
Exercise Bout Work Completed
(Body Mass * Distance * 15°)
4000
3000
2000
1000
0
Vehicle
iMSBmal1KO
C
Upregulated
Downregulated
Vehicle
600
389
iMSBmal1KO
250
267
0
400
800
1200
Differentially Expressed Genes
1-Hour Post Exercise
D
Vehicle Response
872
117
400
iMSBmal1KO Response
E
Shared Exercise Response
Biological rhythms (BP) 8
Immunity (BP) 12
Signal Transduction (R) 25
Antigen processing-Cross presentation (R) 5
PIP3 activates AKT signaling (R) 7
Nuclear events mediated by NFE2L2 (R) 4
Intracellular signaling
by second messengers (R) 7
Class I MHC mediated antigen
processing & presentation (R) 8
0 2 4 6
-Log10 P Value
F
Per1 Per2 Nfil3
Vehicle
Vehicle Exercise
iMSBmal1KO
iMSBmal1KO Exercise
Log2 Z-Score
0.6 0 -0.6 -1.2 -1.8
Nr4a2 Fosb Nr4a3 Irs2 Nr4a1 Fosl2 Ppargc1a Fos Creb1
Vehicle
Vehicle Exercise
iMSBmal1KO
iMSBmal1KO Exercise
Log2 Z-Score
1 0 -1 -2 -3
G
Vehicle Exercise Response
Oxidative phosphorylation (K) 28
Stress response (BP) 16
Protein processing in endoplasmic reticulum (K) 22
Signaling by Insulin receptor (R) 10
PI3K-Akt signaling pathway (K) 29
Nuclear Receptor transcription pathway (R) 16
Signaling by Receptor Tyrosine Kinases (R) 32
Metabolism (R) 95
Immune System (R) 85
MAPK signaling pathway (K) 25
PPAR signaling pathway (K) 9
Signal Transduction (R) 109
0 2 4 6 8 10
-Log10 P Value
H
iMSBmal1KO Exercise Response
Immunity (BP) 22
Innate Immune System (R) 33
Complement and coagulation cascades (K) 7
Response to elevated
platelet cytosolic Ca2+ (R) 9
Cargo recognition for
clathrin-mediated endocytosis (R) 8
Neuroactive ligand-receptor interaction (R) 9
Neutrophil degranulation (R) 2
Muscle contraction (R) 2
0 2 4 6
-Log10 P Value

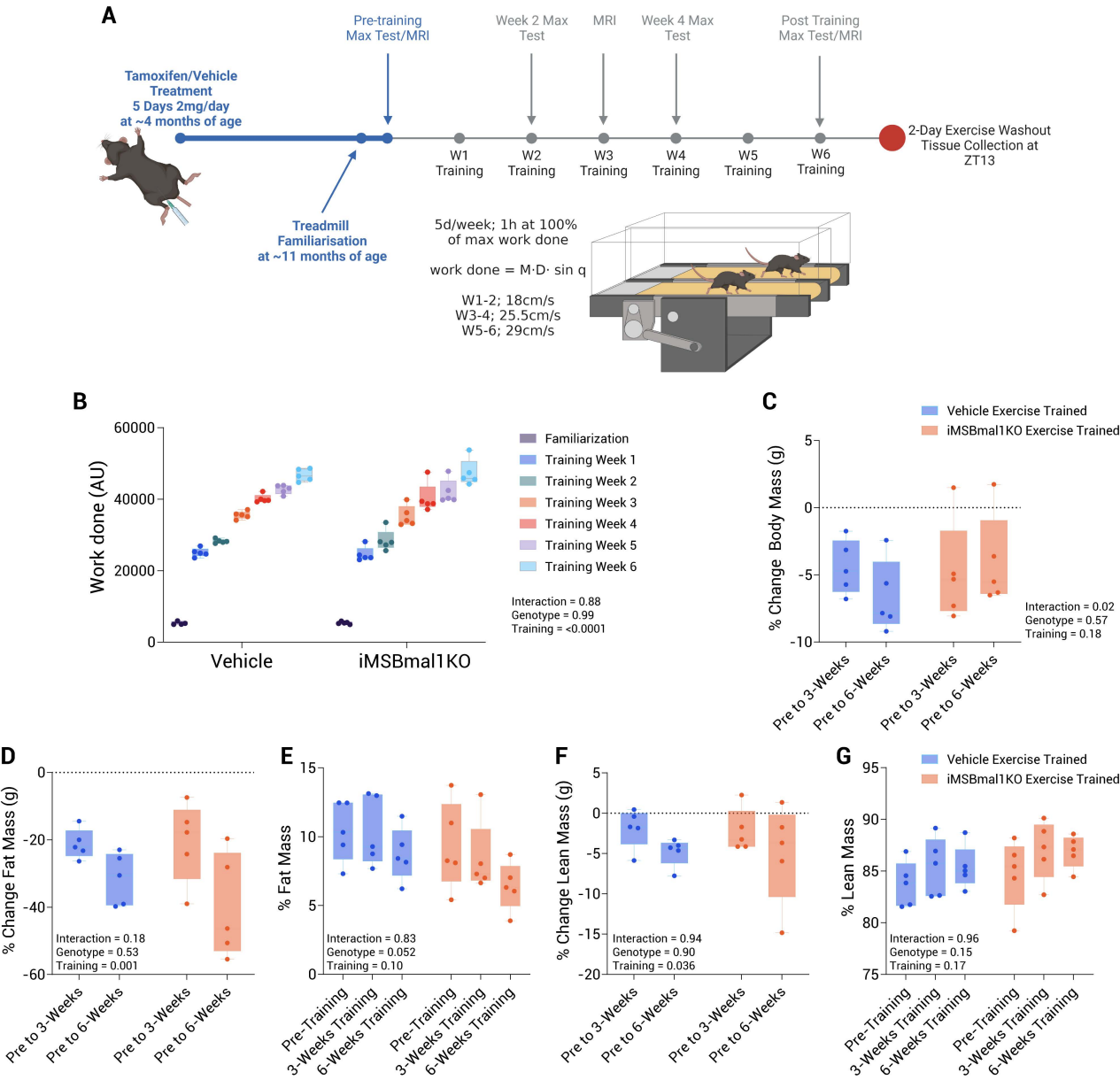
A
Pre-training Max Test/MRI
Week 2 Max Test
MRI
Week 4 Max Test
Post Training Max Test/MRI
Tamoxifen/Vehicle Treatment 5 Days 2mg/day at ~4 months of age
W1 Training
W2 Training
W3 Training
W4 Training
W5 Training
W6 Training
2-Day Exercise Washout Tissue Collection at ZT13
Treadmill Familiarisation at ~11 months of age
5d/week; 1h at 100% of max work done
work done = M·D· sin q
W1-2; 18cm/s
W3-4; 25.5cm/s
W5-6; 29cm/s
B
Work done (AU)
Vehicle
iMSBmal1KO
Familiarization
Training Week 1
Training Week 2
Training Week 3
Training Week 4
Training Week 5
Training Week 6
Interaction = 0.88
Genotype = 0.99
Training = <0.0001
C
Vehicle Exercise Trained
iMSBmal1KO Exercise Trained
% Change Body Mass (g)
Interaction = 0.02
Genotype = 0.57
Training = 0.18
Pre to 3-Weeks
Pre to 6-Weeks
D
% Change Fat Mass (g)
Interaction = 0.18
Genotype = 0.53
Training = 0.001
E
% Fat Mass
Interaction = 0.83
Genotype = 0.052
Training = 0.10
Pre-Training
3-Weeks Training
6-Weeks Training
F
% Change Lean Mass (g)
Interaction = 0.94
Genotype = 0.90
Training = 0.036
G
% Lean Mass
Interaction = 0.96
Genotype = 0.15
Training = 0.17

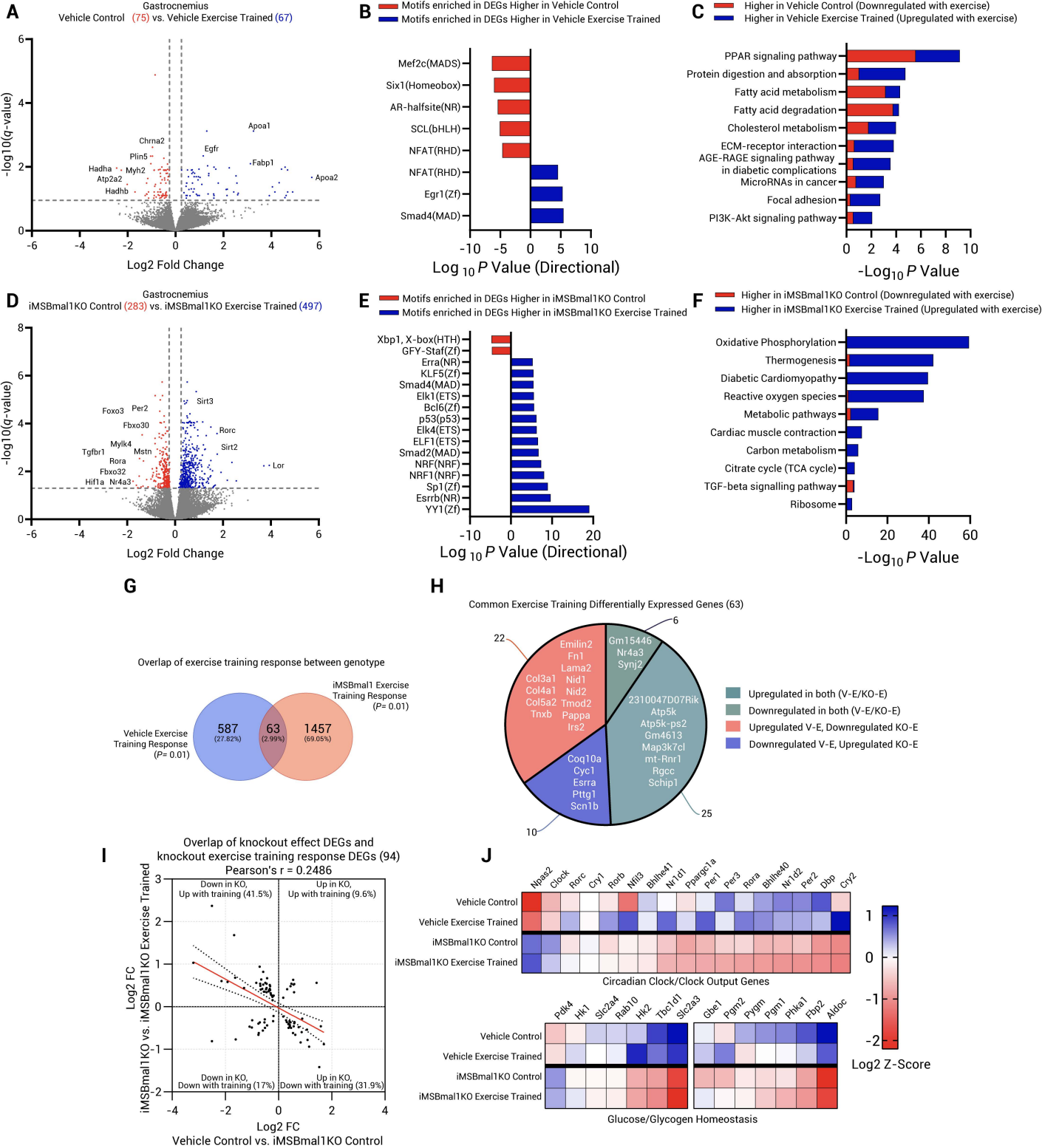
A
Gastrocnemius
Vehicle Control (75) vs. Vehicle Exercise Trained (67)
-log10(q-value)
Log2 Fold Change
Apoa1
Chrna2
Egfr
Plin5
Fabp1
Hadha
Myh2
Atp2a2
Apoa2
Hadhb
B
Motifs enriched in DEGs Higher in Vehicle Control
Motifs enriched in DEGs Higher in Vehicle Exercise Trained
Mef2c(MADS)
Six1(Homeobox)
AR-halfsite(NR)
SCL(bHLH)
NFAT(RHD)
NFAT(RHD)
Egr1(Zf)
Smad4(MAD)
Log 10 P Value (Directional)
C
Higher in Vehicle Control (Downregulated with exercise)
Higher in Vehicle Exercise Trained (Upregulated with exercise)
PPAR signaling pathway
Protein digestion and absorption
Fatty acid metabolism
Fatty acid degradation
Cholesterol metabolism
ECM-receptor interaction
AGE-RAGE signaling pathway in diabetic complications
MicroRNAs in cancer
Focal adhesion
PI3K-Akt signaling pathway
-Log10 P Value
D
Gastrocnemius
iMSBmal1KO Control (283) vs. iMSBmal1KO Exercise Trained (497)
-log10(q-value)
Log2 Fold Change
Sirt3
Foxo3
Per2
Fbxo30
Rorc
Mylk4
Sirt2
Tgfbr1
Mstn
Rora
Lor
Fbxo32
Hif1a
Nr4a3
E
Motifs enriched in DEGs Higher in iMSBmal1KO Control
Motifs enriched in DEGs Higher in iMSBmal1KO Exercise Trained
Xbp1, X-box(HTH)
GFY-Staf(Zf)
Erra(NR)
KLF5(Zf)
Smad4(MAD)
Elk1(ETS)
Bcl6(Zf)
p53(p53)
Elk4(ETS)
ELF1(ETS)
Smad2(MAD)
NRF(NRF)
NRF1(NRF)
Sp1(Zf)
Esrrb(NR)
YY1(Zf)
Log 10 P Value (Directional)
F
Higher in iMSBmal1KO Control (Downregulated with exercise)
Higher in iMSBmal1KO Exercise Trained (Upregulated with exercise)
Oxidative Phosphorylation
Thermogenesis
Diabetic Cardiomyopathy
Reactive oxygen species
Metabolic pathways
Cardiac muscle contraction
Carbon metabolism
Citrate cycle (TCA cycle)
TGF-beta signalling pathway
Ribosome
-Log10 P Value
G
Overlap of exercise training response between genotype
Vehicle Exercise Training Response (P= 0.01)
iMSBmal1 Exercise Training Response (P= 0.01)
587 (27.82%)
63 (2.99%)
1457 (69.05%)
H
Common Exercise Training Differentially Expressed Genes (63)
22
6
25
10
Emilin2 Fn1 Lama2 Nid1 Nid2 Tmod2 Pappa Irs2
Col3a1 Col4a1 Col5a2 Tnxb
Gm15446 Nr4a3 Synj2
2310047D07Rik Atp5k Atp5k-ps2 Gm4613 Map3k7cl mt-Rnr1 Rgcc Schip1
Coq10a Cyc1 Esrra Pttg1 Scn1b
Upregulated in both (V-E/KO-E)
Downregulated in both (V-E/KO-E)
Upregulated V-E, Downregulated KO-E
Downregulated V-E, Upregulated KO-E
I
Overlap of knockout effect DEGs and knockout exercise training response DEGs (94)
Pearson's r = 0.2486
Down in KO, Up with training (41.5%)
Up in KO, Up with training (9.6%)
Down in KO, Down with training (17%)
Up in KO, Down with training (31.9%)
Log2 FC
iMSBmal1KO vs. iMSBmal1KO Exercise Trained
Log2 FC
Vehicle Control vs. iMSBmal1KO Control
J
Npas2 Clock Rorc Cry1 Rorb Nfil3 Bhlhe41 Nr1d1 Ppargc1a Per1 Per3 Rora Bhlhe40 Nr1d2 Per2 Dbp Cry2
Vehicle Control
Vehicle Exercise Trained
iMSBmal1KO Control
iMSBmal1KO Exercise Trained
Circadian Clock/Clock Output Genes
Pdk4 Hk1 Slc2a4 Rab10 Hk2 Tbc1d1 Slc2a3 Gbe1 Pgm2 Pygm Pgm1 Phka1 Fbp2 Aldoc
Vehicle Control
Vehicle Exercise Trained
iMSBmal1KO Control
iMSBmal1KO Exercise Trained
Glucose/Glycogen Homeostasis
Log2 Z-Score

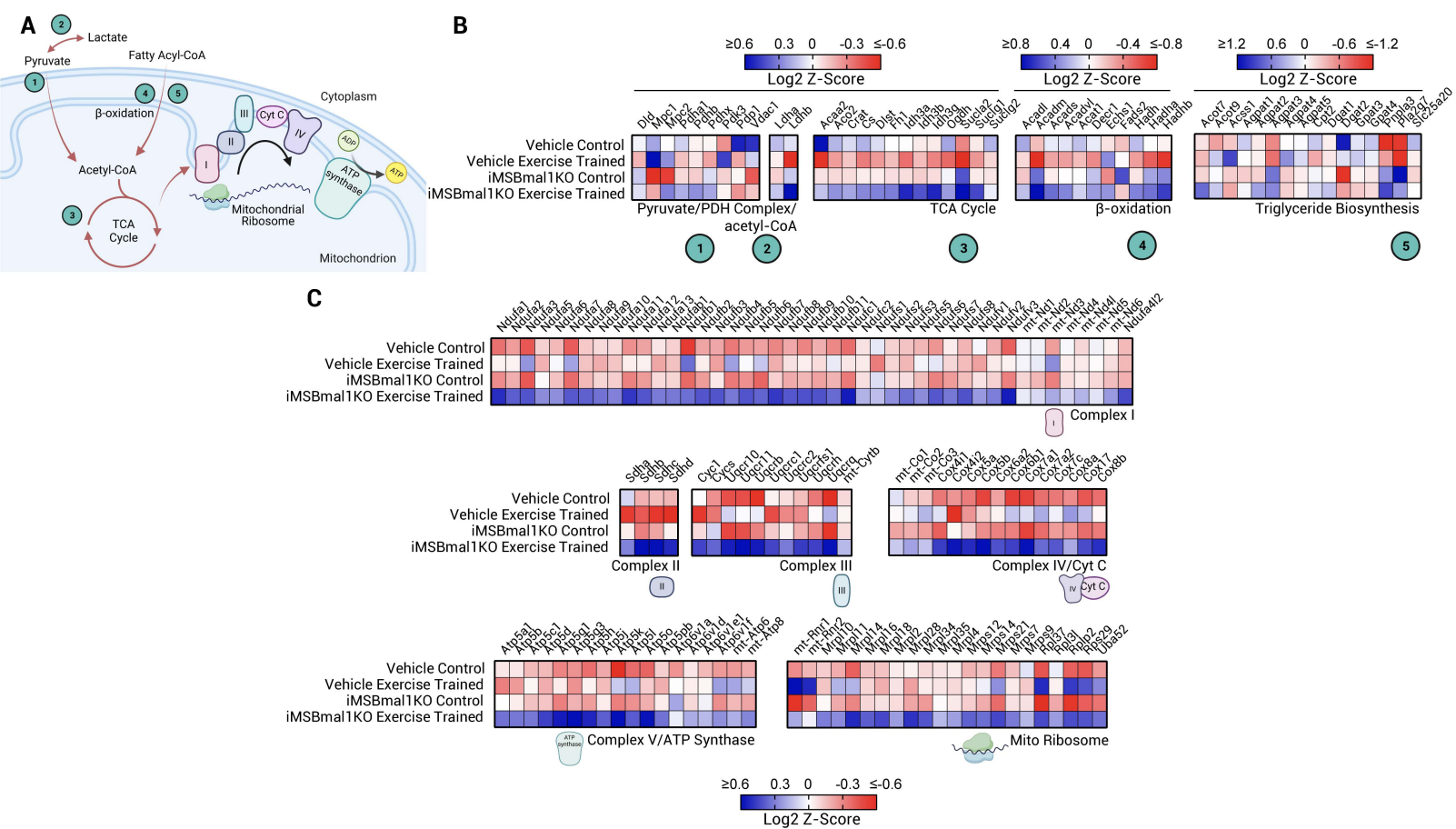
A
Lactate
Pyruvate
Fatty Acyl-CoA
β-oxidation
Cytoplasm
Acetyl-CoA
TCA Cycle
Mitochondrial Ribosome
ATP synthase
ADP
ATP
Mitochondrion
B
Log2 Z-Score
Vehicle Control
Vehicle Exercise Trained
iMSBmal1KO Control
iMSBmal1KO Exercise Trained
Pyruvate/PDH Complex/ acetyl-CoA
TCA Cycle
β-oxidation
Triglyceride Biosynthesis
C
Complex I
Complex II
Complex III
Complex IV/Cyt C
Complex V/ATP Synthase
Mito Ribosome

A

Comparison	Number of Altered Metabolites
Vehicle Control vs iMSBmal1KO Control	47
Vehicle Exercise Training Response	19
iMSBmal1KO Exercise Training Response	116

B

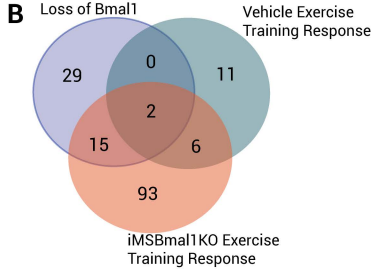

C

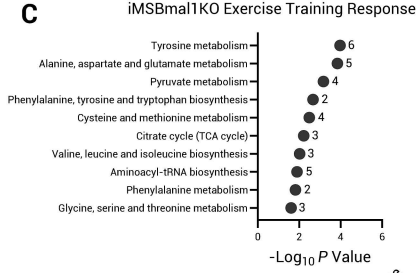

D

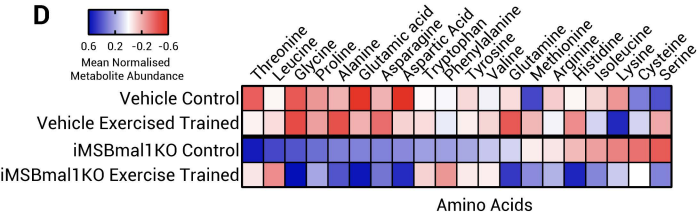

E

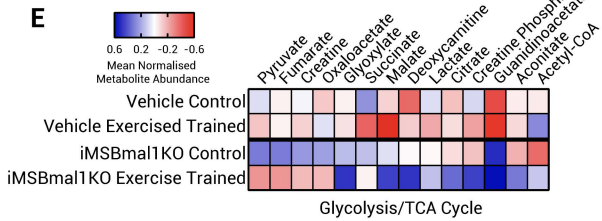

F

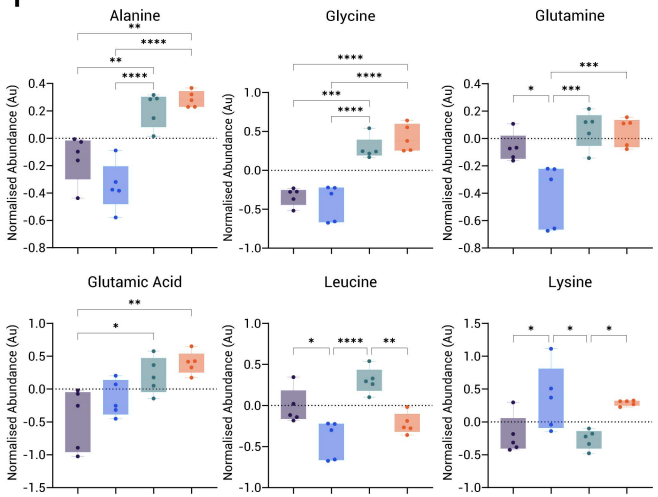

G

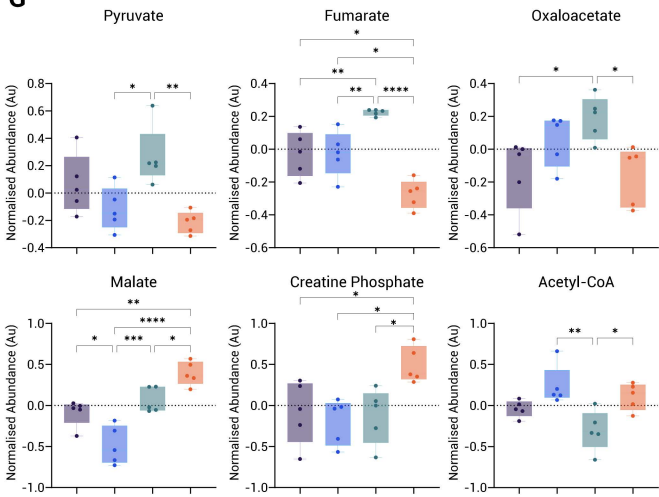

H

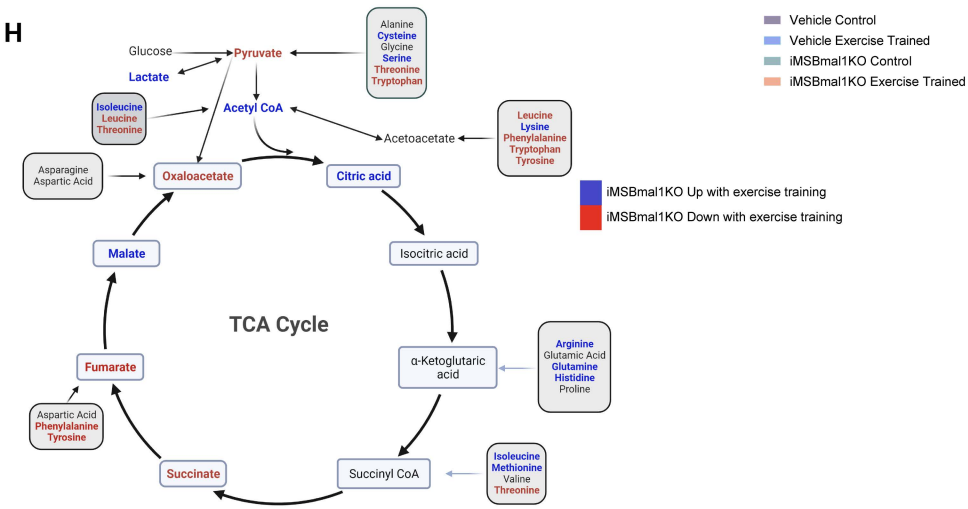

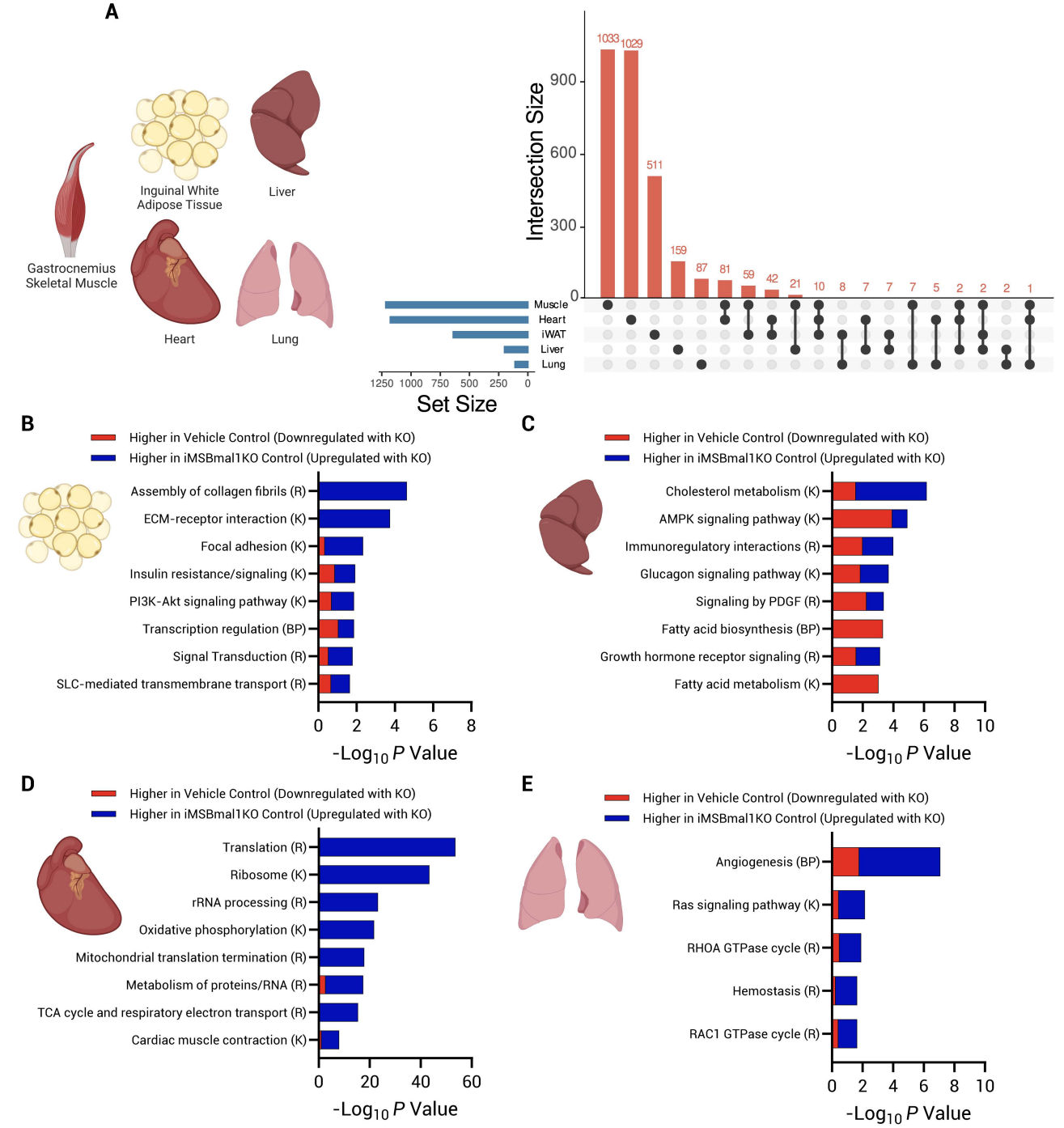
A
Gastrocnemius Skeletal Muscle
Inguinal White Adipose Tissue
Liver
Heart
Lung
Intersection Size
1033
1029
511
159
87
81
59
42
21
10
8
7
7
7
5
2
2
2
1
Muscle
Heart
iWAT
Liver
Lung
Set Size
B
Higher in Vehicle Control (Downregulated with KO)
Higher in iMSBmal1KO Control (Upregulated with KO)
Assembly of collagen fibrils (R)
ECM-receptor interaction (K)
Focal adhesion (K)
Insulin resistance/signaling (K)
PI3K-Akt signaling pathway (K)
Transcription regulation (BP)
Signal Transduction (R)
SLC-mediated transmembrane transport (R)
-Log10 P Value
C
Higher in Vehicle Control (Downregulated with KO)
Higher in iMSBmal1KO Control (Upregulated with KO)
Cholesterol metabolism (K)
AMPK signaling pathway (K)
Immunoregulatory interactions (R)
Glucagon signaling pathway (K)
Signaling by PDGF (R)
Fatty acid biosynthesis (BP)
Growth hormone receptor signaling (R)
Fatty acid metabolism (K)
-Log10 P Value
D
Higher in Vehicle Control (Downregulated with KO)
Higher in iMSBmal1KO Control (Upregulated with KO)
Translation (R)
Ribosome (K)
rRNA processing (R)
Oxidative phosphorylation (K)
Mitochondrial translation termination (R)
Metabolism of proteins/RNA (R)
TCA cycle and respiratory electron transport (R)
Cardiac muscle contraction (K)
-Log10 P Value
E
Higher in Vehicle Control (Downregulated with KO)
Higher in iMSBmal1KO Control (Upregulated with KO)
Angiogenesis (BP)
Ras signaling pathway (K)
RHOA GTPase cycle (R)
Hemostasis (R)
RAC1 GTPase cycle (R)
-Log10 P Value

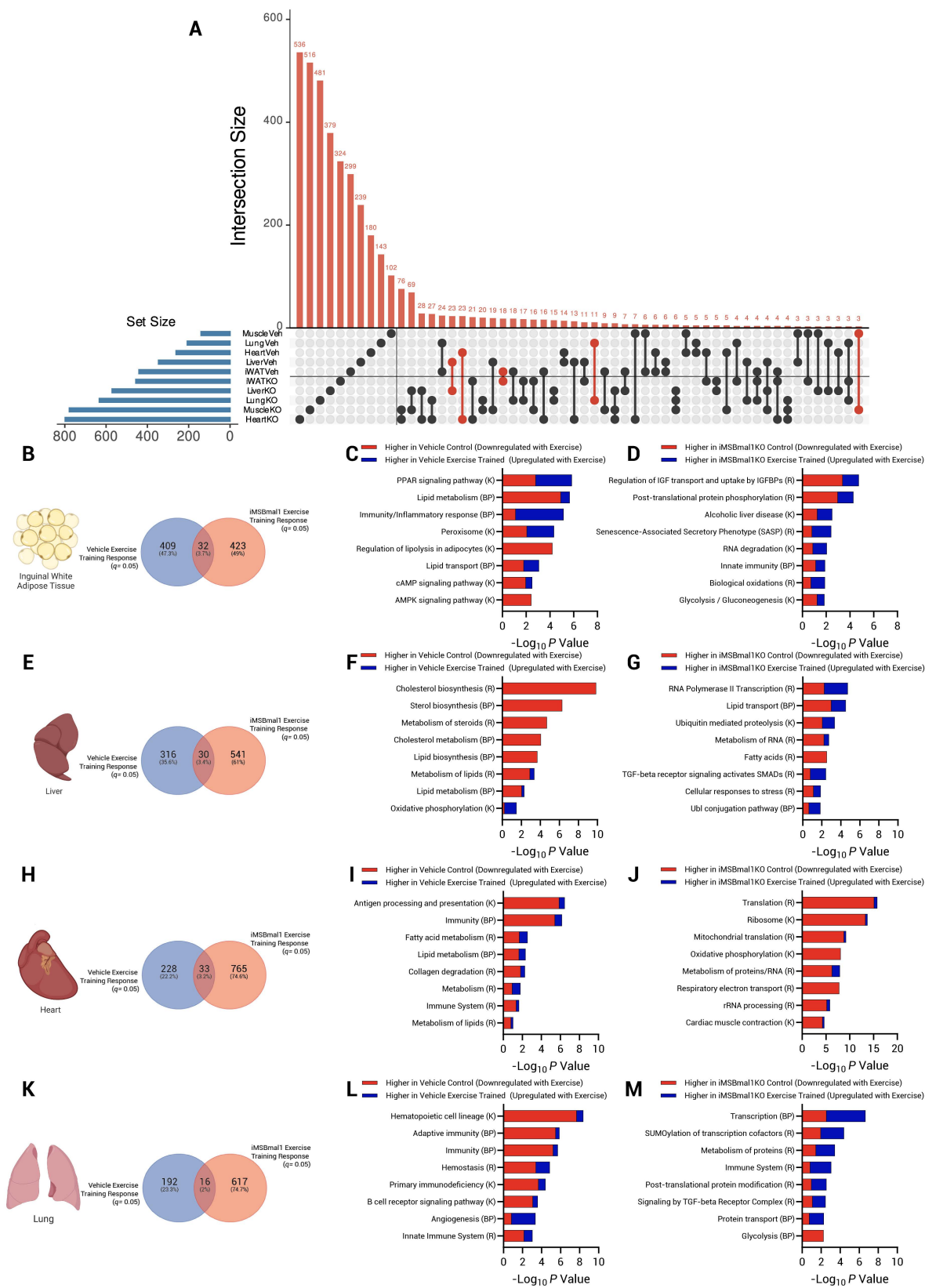
A
Intersection Size
Set Size
MuscleVeh
LungVeh
HeartVeh
LiverVeh
iWATVeh
iWATKO
LiverKO
LungKO
MuscleKO
HeartKO
B
Inguinal White Adipose Tissue
Vehicle Exercise Training Response (q= 0.05)
iMSBmal1 Exercise Training Response (q= 0.05)
409 (47.3%)
32 (3.7%)
423 (49%)
C
Higher in Vehicle Control (Downregulated with Exercise)
Higher in Vehicle Exercise Trained (Upregulated with Exercise)
PPAR signaling pathway (K)
Lipid metabolism (BP)
Immunity/Inflammatory response (BP)
Peroxisome (K)
Regulation of lipolysis in adipocytes (K)
Lipid transport (BP)
cAMP signaling pathway (K)
AMPK signaling pathway (K)
-Log10 P Value
D
Higher in iMSBmal1KO Control (Downregulated with Exercise)
Higher in iMSBmal1KO Exercise Trained (Upregulated with Exercise)
Regulation of IGF transport and uptake by IGFBPs (R)
Post-translational protein phosphorylation (R)
Alcoholic liver disease (K)
Senescence-Associated Secretory Phenotype (SASP) (R)
RNA degradation (K)
Innate immunity (BP)
Biological oxidations (R)
Glycolysis / Gluconeogenesis (K)
-Log10 P Value
E
Liver
Vehicle Exercise Training Response (q= 0.05)
iMSBmal1 Exercise Training Response (q= 0.05)
316 (35.6%)
30 (3.4%)
541 (61%)
F
Higher in Vehicle Control (Downregulated with Exercise)
Higher in Vehicle Exercise Trained (Upregulated with Exercise)
Cholesterol biosynthesis (R)
Sterol biosynthesis (BP)
Metabolism of steroids (R)
Cholesterol metabolism (BP)
Lipid biosynthesis (BP)
Metabolism of lipids (R)
Lipid metabolism (BP)
Oxidative phosphorylation (K)
-Log10 P Value
G
Higher in iMSBmal1KO Control (Downregulated with Exercise)
Higher in iMSBmal1KO Exercise Trained (Upregulated with Exercise)
RNA Polymerase II Transcription (R)
Lipid transport (BP)
Ubiquitin mediated proteolysis (K)
Metabolism of RNA (R)
Fatty acids (R)
TGF-beta receptor signaling activates SMADs (R)
Cellular responses to stress (R)
Ubl conjugation pathway (BP)
-Log10 P Value
H
Heart
Vehicle Exercise Training Response (q= 0.05)
iMSBmal1 Exercise Training Response (q= 0.05)
228 (22.2%)
33 (3.2%)
765 (74.6%)
I
Higher in Vehicle Control (Downregulated with Exercise)
Higher in Vehicle Exercise Trained (Upregulated with Exercise)
Antigen processing and presentation (K)
Immunity (BP)
Fatty acid metabolism (R)
Lipid metabolism (BP)
Collagen degradation (R)
Metabolism (R)
Immune System (R)
Metabolism of lipids (R)
-Log10 P Value
J
Higher in iMSBmal1KO Control (Downregulated with Exercise)
Higher in iMSBmal1KO Exercise Trained (Upregulated with Exercise)
Translation (R)
Ribosome (K)
Mitochondrial translation (R)
Oxidative phosphorylation (K)
Metabolism of proteins/RNA (R)
Respiratory electron transport (R)
rRNA processing (R)
Cardiac muscle contraction (K)
-Log10 P Value
K
Lung
Vehicle Exercise Training Response (q= 0.05)
iMSBmal1 Exercise Training Response (q= 0.05)
192 (23.3%)
16 (2%)
617 (74.7%)
L
Higher in Vehicle Control (Downregulated with Exercise)
Higher in Vehicle Exercise Trained (Upregulated with Exercise)
Hematopoietic cell lineage (K)
Adaptive immunity (BP)
Immunity (BP)
Hemostasis (R)
Primary immunodeficiency (K)
B cell receptor signaling pathway (K)
Angiogenesis (BP)
Innate Immune System (R)
-Log10 P Value
M
Higher in iMSBmal1KO Control (Downregulated with Exercise)
Higher in iMSBmal1KO Exercise Trained (Upregulated with Exercise)
Transcription (BP)
SUMOylation of transcription cofactors (R)
Metabolism of proteins (R)
Immune System (R)
Post-translational protein modification (R)
Signaling by TGF-beta Receptor Complex (R)
Protein transport (BP)
Glycolysis (BP)
-Log10 P Value

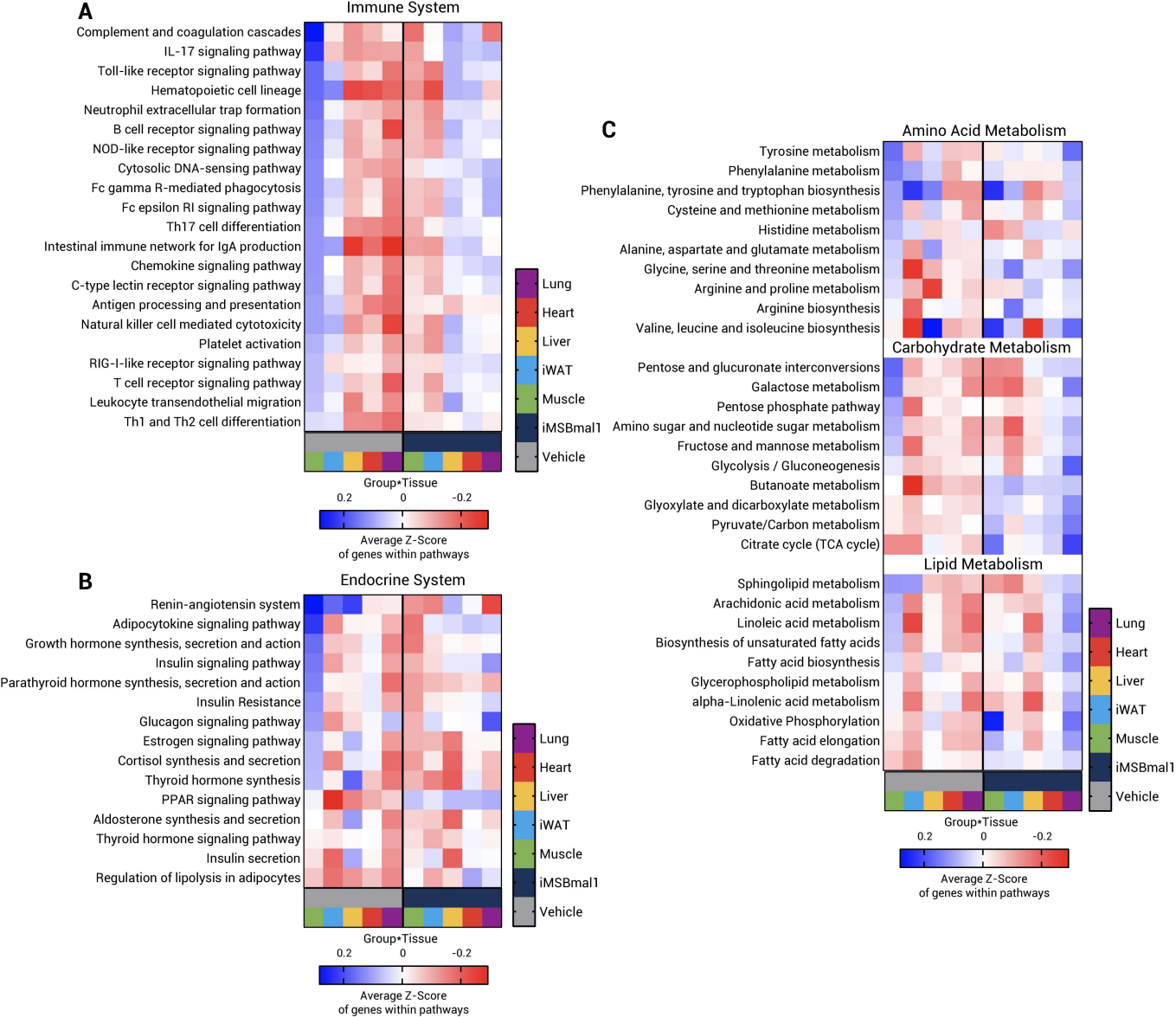
A
Immune System
Complement and coagulation cascades
IL-17 signaling pathway
Toll-like receptor signaling pathway
Hematopoietic cell lineage
Neutrophil extracellular trap formation
B cell receptor signaling pathway
NOD-like receptor signaling pathway
Cytosolic DNA-sensing pathway
Fc gamma R-mediated phagocytosis
Fc epsilon RI signaling pathway
Th17 cell differentiation
Intestinal immune network for IgA production
Chemokine signaling pathway
C-type lectin receptor signaling pathway
Antigen processing and presentation
Natural killer cell mediated cytotoxicity
Platelet activation
RIG-I-like receptor signaling pathway
T cell receptor signaling pathway
Leukocyte transendothelial migration
Th1 and Th2 cell differentiation
Lung
Heart
Liver
iWAT
Muscle
iMSBmal1
Vehicle
Group*Tissue
0.2
0
-0.2
Average Z-Score
of genes within pathways
B
Endocrine System
Renin-angiotensin system
Adipocytokine signaling pathway
Growth hormone synthesis, secretion and action
Insulin signaling pathway
Parathyroid hormone synthesis, secretion and action
Insulin Resistance
Glucagon signaling pathway
Estrogen signaling pathway
Cortisol synthesis and secretion
Thyroid hormone synthesis
PPAR signaling pathway
Aldosterone synthesis and secretion
Thyroid hormone signaling pathway
Insulin secretion
Regulation of lipolysis in adipocytes
Lung
Heart
Liver
iWAT
Muscle
iMSBmal1
Vehicle
Group*Tissue
0.2
0
-0.2
Average Z-Score
of genes within pathways
C
Amino Acid Metabolism
Tyrosine metabolism
Phenylalanine metabolism
Phenylalanine, tyrosine and tryptophan biosynthesis
Cysteine and methionine metabolism
Histidine metabolism
Alanine, aspartate and glutamate metabolism
Glycine, serine and threonine metabolism
Arginine and proline metabolism
Arginine biosynthesis
Valine, leucine and isoleucine biosynthesis
Carbohydrate Metabolism
Pentose and glucuronate interconversions
Galactose metabolism
Pentose phosphate pathway
Amino sugar and nucleotide sugar metabolism
Fructose and mannose metabolism
Glycolysis / Gluconeogenesis
Butanoate metabolism
Glyoxylate and dicarboxylate metabolism
Pyruvate/Carbon metabolism
Citrate cycle (TCA cycle)
Lipid Metabolism
Sphingolipid metabolism
Arachidonic acid metabolism
Linoleic acid metabolism
Biosynthesis of unsaturated fatty acids
Fatty acid biosynthesis
Glycerophospholipid metabolism
alpha-Linolenic acid metabolism
Oxidative Phosphorylation
Fatty acid elongation
Fatty acid degradation
Lung
Heart
Liver
iWAT
Muscle
iMSBmal1
Vehicle
Group*Tissue
0.2
0
-0.2
Average Z-Score
of genes within pathways

A

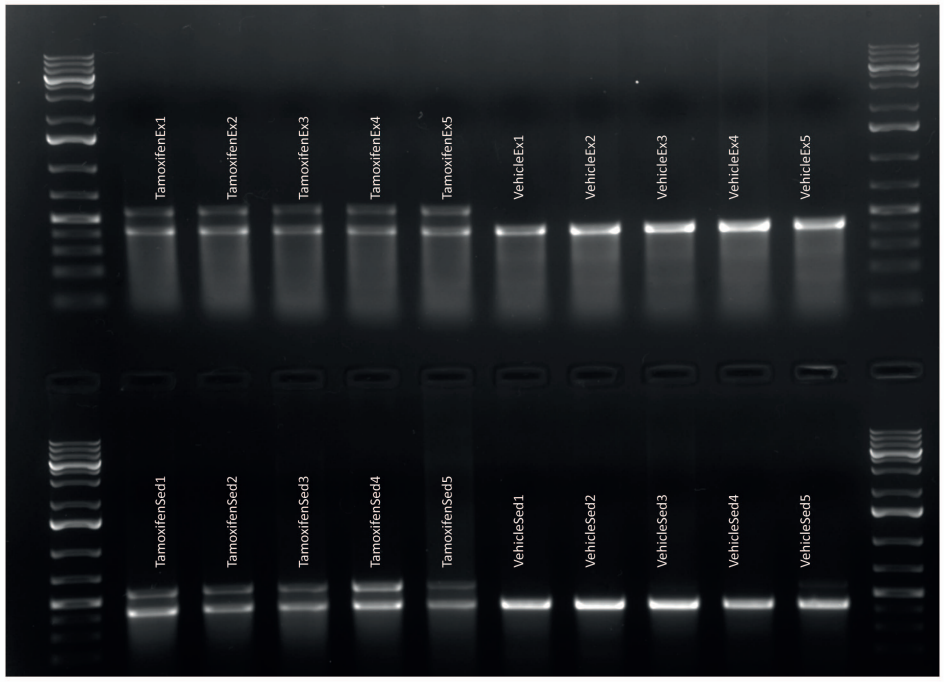
TamoxifenEx1
TamoxifenEx2
TamoxifenEx3
TamoxifenEx4
TamoxifenEx5
VehicleEx1
VehicleEx2
VehicleEx3
VehicleEx4
VehicleEx5
TamoxifenSed1
TamoxifenSed2
TamoxifenSed3
TamoxifenSed4
TamoxifenSed5
VehicleSed1
VehicleSed2
VehicleSed3
VehicleSed4
VehicleSed5

B

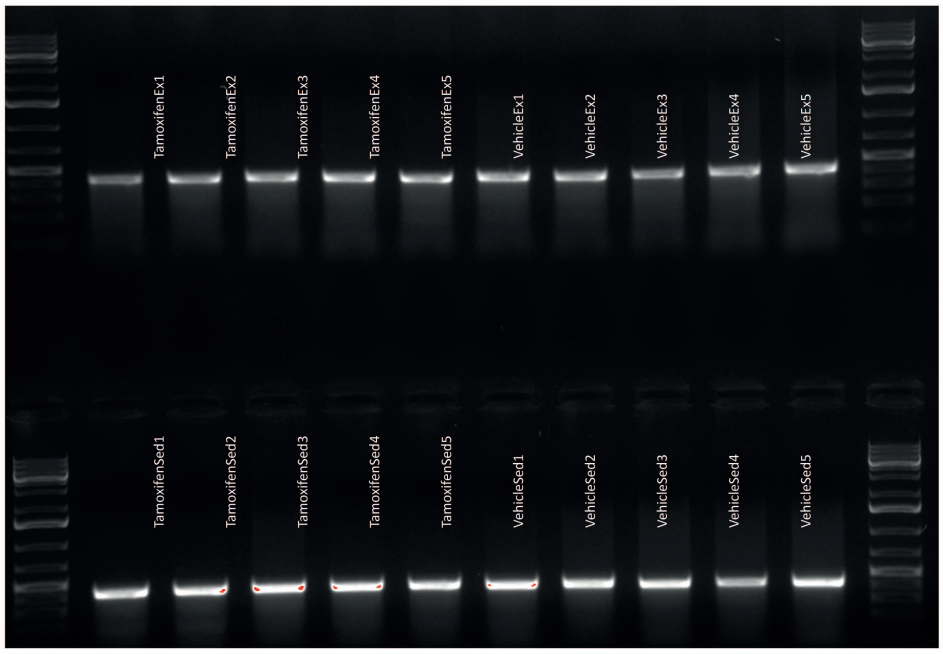
TamoxifenEx1
TamoxifenEx2
TamoxifenEx3
TamoxifenEx4
TamoxifenEx5
VehicleEx1
VehicleEx2
VehicleEx3
VehicleEx4
VehicleEx5
TamoxifenSed1
TamoxifenSed2
TamoxifenSed3
TamoxifenSed4
TamoxifenSed5
VehicleSed1
VehicleSed2
VehicleSed3
VehicleSed4
VehicleSed5

C

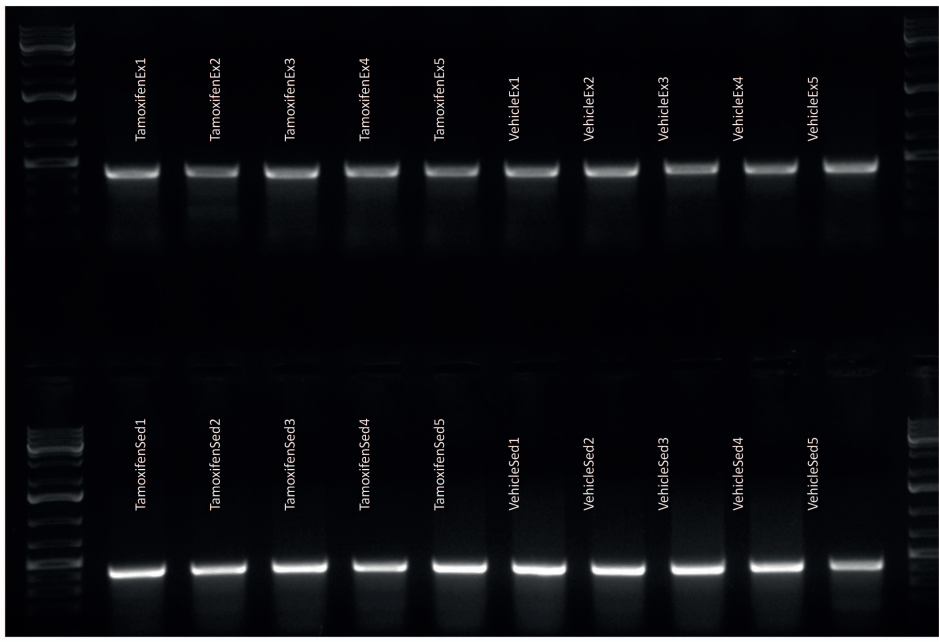
TamoxifenEx1
TamoxifenEx2
TamoxifenEx3
TamoxifenEx4
TamoxifenEx5
VehicleEx1
VehicleEx2
VehicleEx3
VehicleEx4
VehicleEx5
TamoxifenSed1
TamoxifenSed2
TamoxifenSed3
TamoxifenSed4
TamoxifenSed5
VehicleSed1
VehicleSed2
VehicleSed3
VehicleSed4
VehicleSed5

D

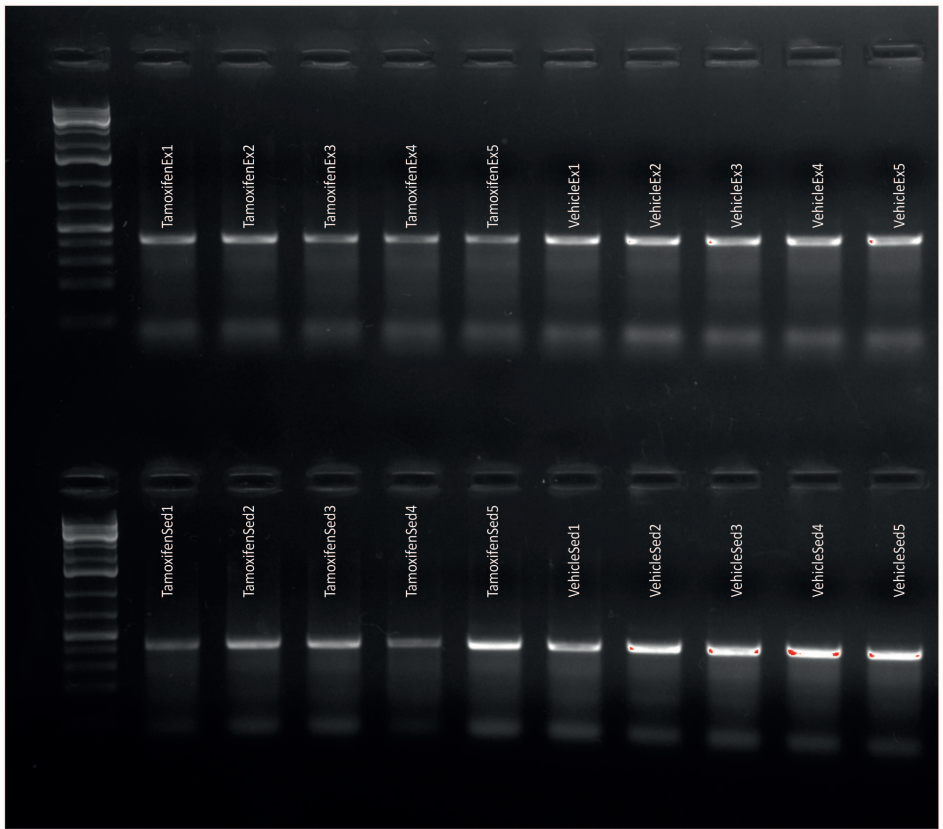
TamoxifenEx1
TamoxifenEx2
TamoxifenEx3
TamoxifenEx4
TamoxifenEx5
VehicleEx1
VehicleEx2
VehicleEx3
VehicleEx4
VehicleEx5
TamoxifenSed1
TamoxifenSed2
TamoxifenSed3
TamoxifenSed4
TamoxifenSed5
VehicleSed1
VehicleSed2
VehicleSed3
VehicleSed4
VehicleSed5

E

TamoxifenEx1
TamoxifenEx2
TamoxifenEx3
TamoxifenEx4
TamoxifenEx5
VehicleEx1
VehicleEx2
VehicleEx3
VehicleEx4
VehicleEx5
TamoxifenSed1
TamoxifenSed2
TamoxifenSed3
TamoxifenSed4
TamoxifenSed5
VehicleSed1
VehicleSed2
VehicleSed3
VehicleSed4
VehicleSed5

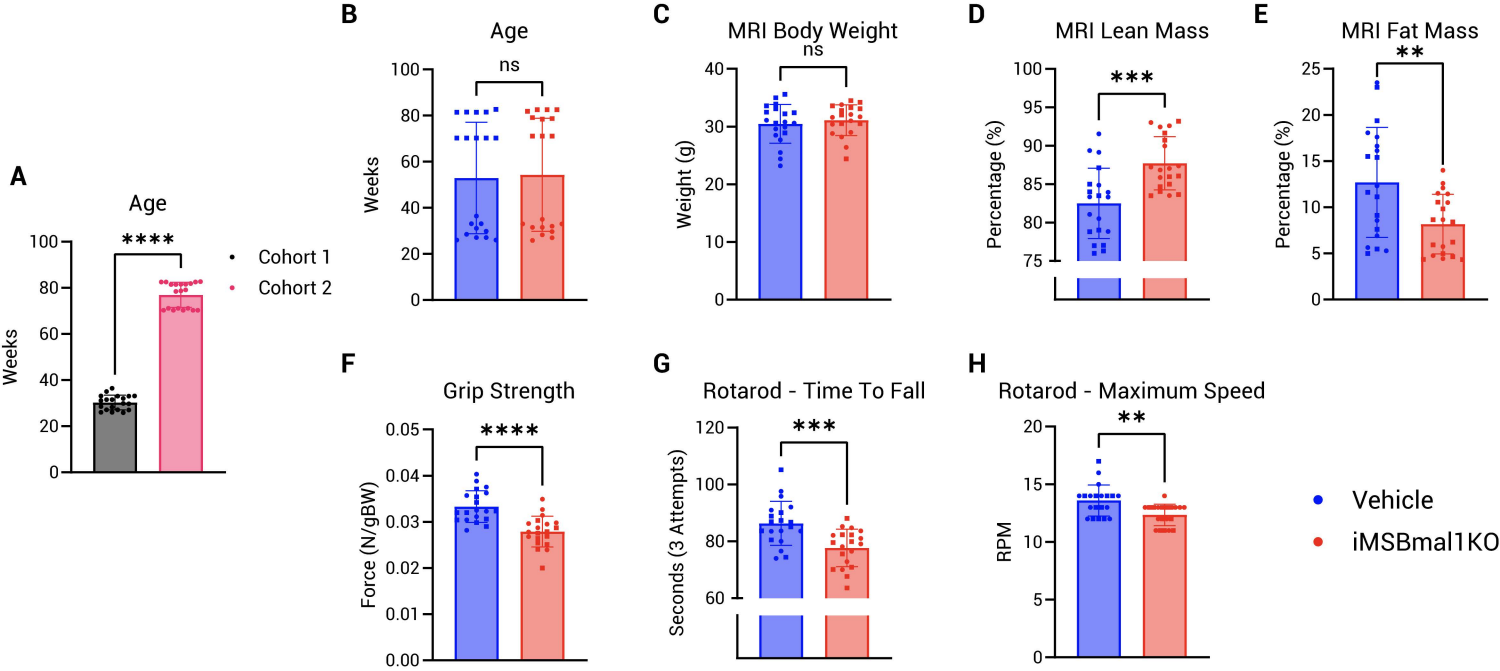
A
Age
****
Weeks
Cohort 1
Cohort 2
B
Age
ns
Weeks
C
MRI Body Weight
ns
Weight (g)
D
MRI Lean Mass
***
Percentage (%)
E
MRI Fat Mass
**
Percentage (%)
F
Grip Strength
****
Force (N/gBW)
G
Rotarod - Time To Fall
***
Seconds (3 Attempts)
H
Rotarod - Maximum Speed
**
RPM
Vehicle
iMSBmal1KO

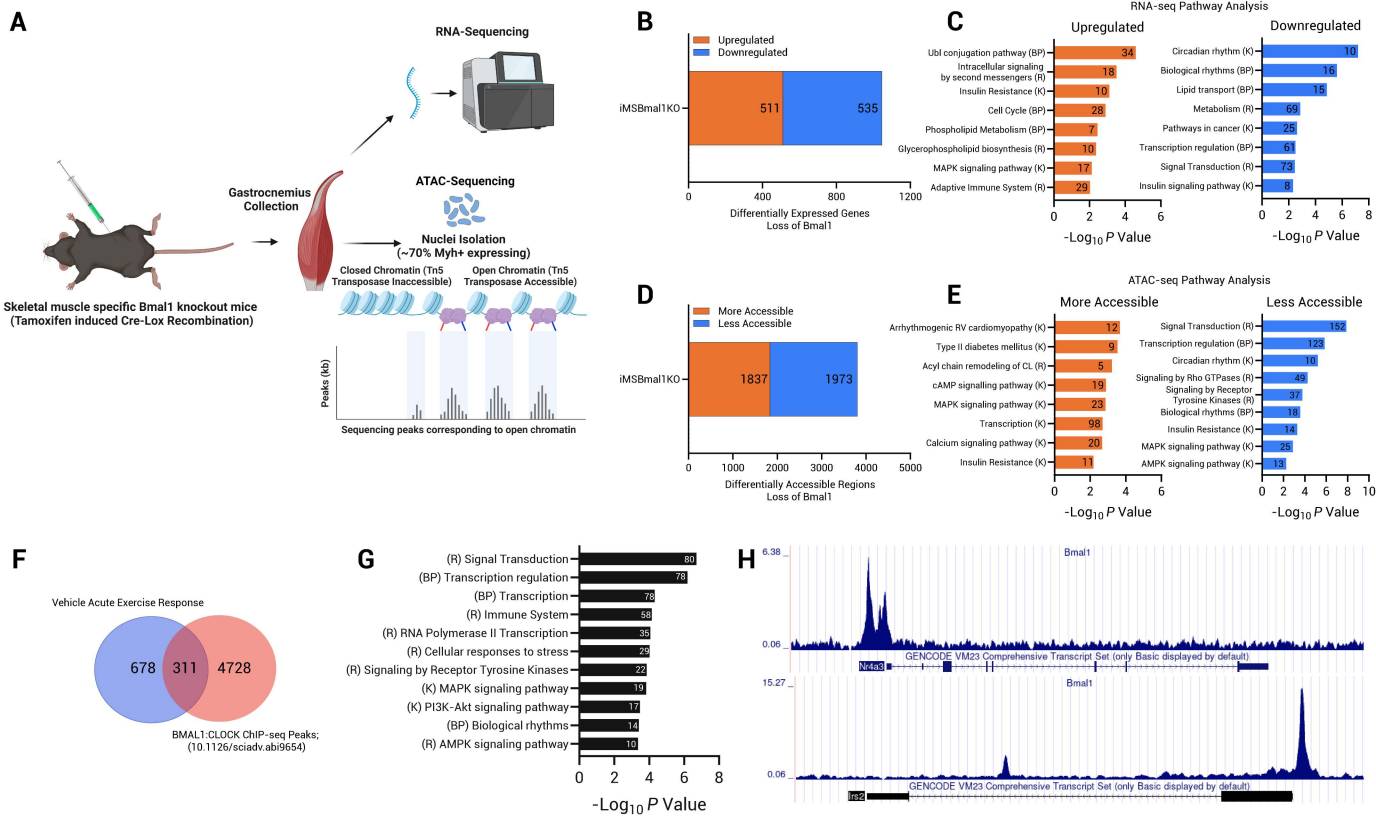
A
RNA-Sequencing
ATAC-Sequencing
Gastrocnemius Collection
Nuclei Isolation (~70% Myh+ expressing)
Closed Chromatin (Tn5 Transposase Inaccessible)
Open Chromatin (Tn5 Transposase Accessible)
Peaks (kb)
Sequencing peaks corresponding to open chromatin
Skeletal muscle specific Bmal1 knockout mice (Tamoxifen induced Cre-Lox Recombination)
B
Upregulated
Downregulated
iMSBmal1KO
511
535
0
400
800
1200
Differentially Expressed Genes Loss of Bmal1
C
RNA-seq Pathway Analysis
Upregulated
Ubl conjugation pathway (BP) 34
Intracellular signaling by second messengers (R) 18
Insulin Resistance (K) 10
Cell Cycle (BP) 28
Phospholipid Metabolism (BP) 7
Glycerophospholipid biosynthesis (R) 10
MAPK signaling pathway (K) 17
Adaptive Immune System (R) 29
Downregulated
Circadian rhythm (K) 10
Biological rhythms (BP) 16
Lipid transport (BP) 15
Metabolism (R) 69
Pathways in cancer (K) 25
Transcription regulation (BP) 61
Signal Transduction (R) 73
Insulin signaling pathway (K) 8
0 2 4 6
0 2 4 6 8
-Log10 P Value
D
More Accessible
Less Accessible
iMSBmal1KO
1837
1973
0
1000
2000
3000
4000
5000
Differentially Accessible Regions Loss of Bmal1
E
ATAC-seq Pathway Analysis
More Accessible
Arrhythmogenic RV cardiomyopathy (K) 12
Type II diabetes mellitus (K) 9
Acyl chain remodeling of CL (R) 5
cAMP signalling pathway (K) 19
MAPK signaling pathway (K) 23
Transcription (K) 98
Calcium signaling pathway (K) 20
Insulin Resistance (K) 11
Less Accessible
Signal Transduction (R) 152
Transcription regulation (BP) 123
Circadian rhythm (K) 10
Signaling by Rho GTPases (R) 49
Signaling by Receptor Tyrosine Kinases (R) 37
Biological rhythms (BP) 18
Insulin Resistance (K) 14
MAPK signaling pathway (K) 25
AMPK signaling pathway (K) 13
0 2 4 6
0 2 4 6 8 10
-Log10 P Value
F
Vehicle Acute Exercise Response
678
311
4728
BMAL1:CLOCK ChIP-seq Peaks; (10.1126/sciadv.abi9654)
G
(R) Signal Transduction 80
(BP) Transcription regulation 78
(BP) Transcription 78
(R) Immune System 58
(R) RNA Polymerase II Transcription 35
(R) Cellular responses to stress 29
(R) Signaling by Receptor Tyrosine Kinases 22
(K) MAPK signaling pathway 19
(K) PI3K-Akt signaling pathway 17
(BP) Biological rhythms 14
(R) AMPK signaling pathway 10
0 2 4 6 8
-Log10 P Value
H
6.38
Bmal1
0.06
GENCODE VM23 Comprehensive Transcript Set (only Basic displayed by default)
Nr4a3
15.27
Bmal1
0.06
GENCODE VM23 Comprehensive Transcript Set (only Basic displayed by default)
Ttr-2

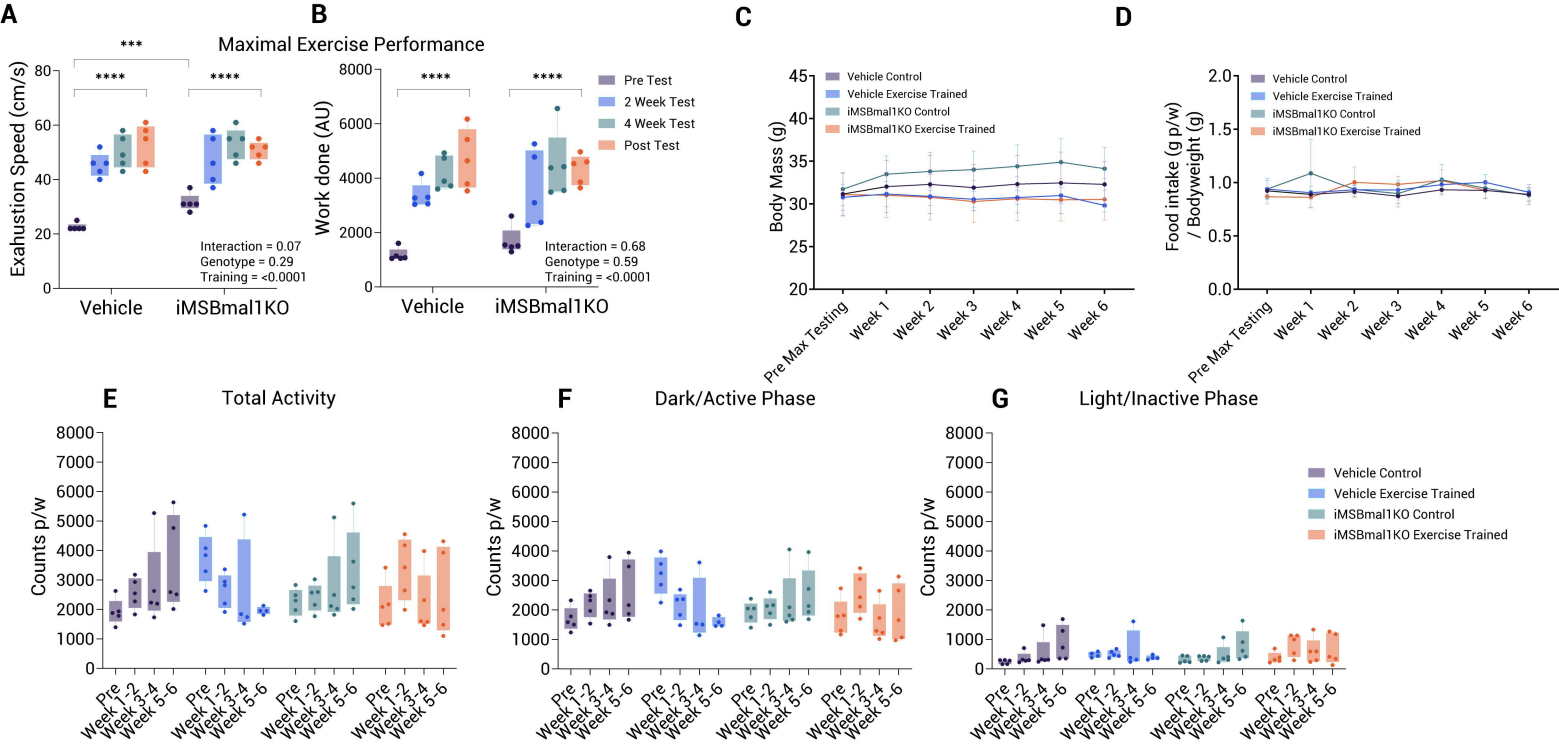
A
B
C
D
Maximal Exercise Performance
Exahustion Speed (cm/s)
Work done (AU)
***
****
Interaction = 0.07
Genotype = 0.29
Training = <0.0001
Interaction = 0.68
Genotype = 0.59
Training = <0.0001
Vehicle
iMSBmal1KO
Pre Test
2 Week Test
4 Week Test
Post Test
Body Mass (g)
Food intake (g p/w) / Bodyweight (g)
Vehicle Control
Vehicle Exercise Trained
iMSBmal1KO Control
iMSBmal1KO Exercise Trained
Pre Max Testing
Week 1
Week 2
Week 3
Week 4
Week 5
Week 6
E
F
G
Total Activity
Dark/Active Phase
Light/Inactive Phase
Counts p/w
Pre
Week 1-2
Week 3-4
Week 5-6

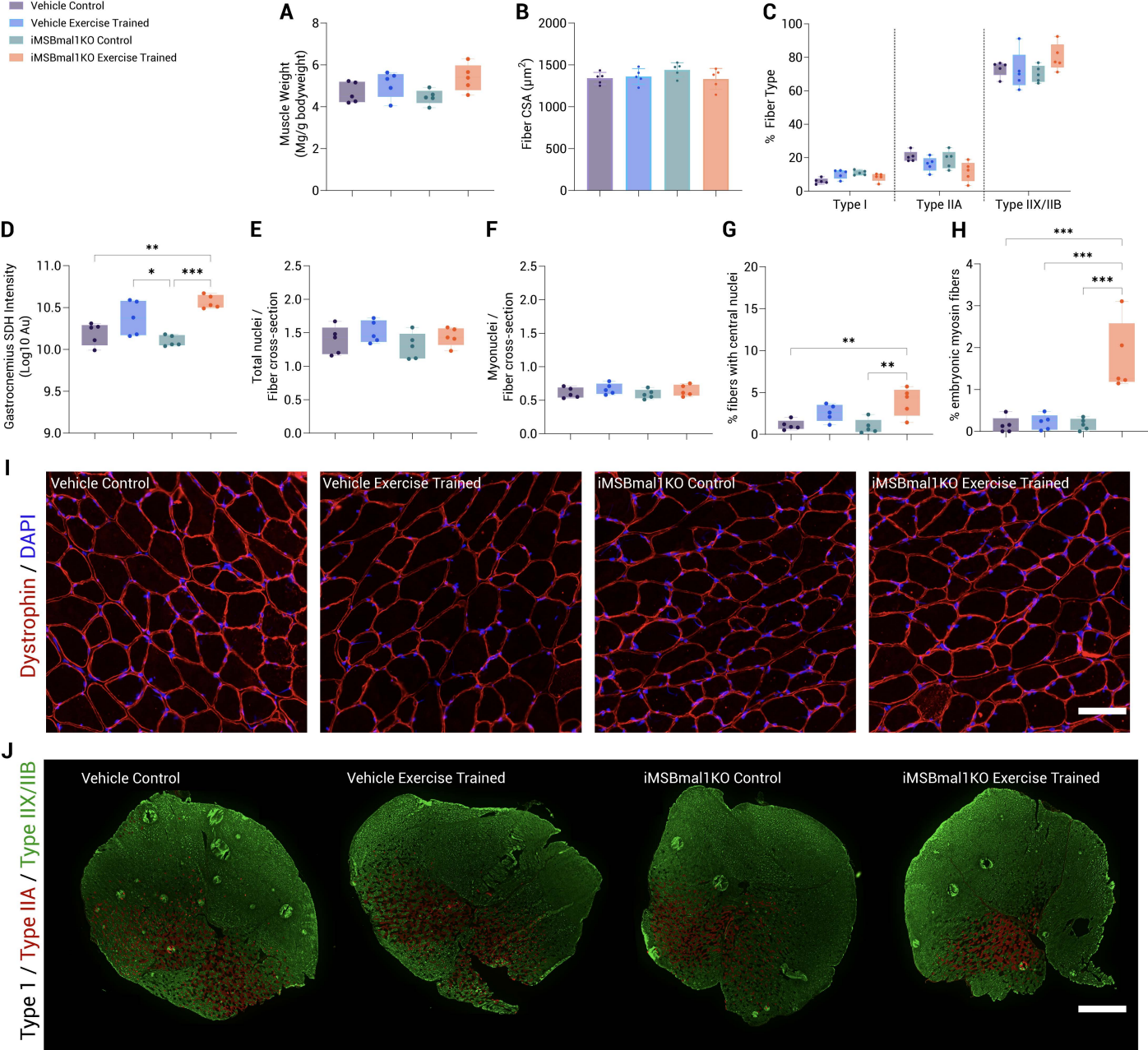
Vehicle Control
Vehicle Exercise Trained
iMSBmal1KO Control
iMSBmal1KO Exercise Trained
A
Muscle Weight (Mg/g bodyweight)
B
Fiber CSA (μm²)
C
% Fiber Type
Type I
Type IIA
Type IIX/IIB
D
Gastrocnemius SDH Intensity (Log10 Au)
E
Total nuclei / Fiber cross-section
F
Myonuclei / Fiber cross-section
G
% fibers with central nuclei
H
% embryonic myosin fibers
I
Dystrophin / DAPI
Vehicle Control
Vehicle Exercise Trained
iMSBmal1KO Control
iMSBmal1KO Exercise Trained
J
Type 1 / Type IIA / Type IIX/IIB
Vehicle Control
Vehicle Exercise Trained
iMSBmal1KO Control
iMSBmal1KO Exercise Trained

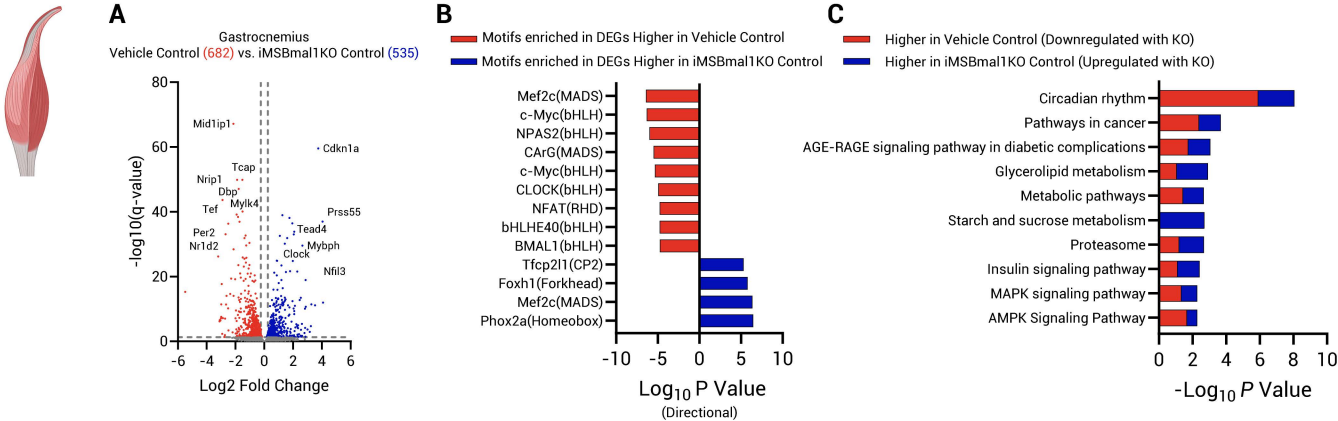
A
Gastrocnemius
Vehicle Control (682) vs. iMSBmal1KO Control (535)
-log10(q-value)
Log2 Fold Change
Mid1ip1
Cdkn1a
Tcap
Nrip1
Dbp
Mylk4
Tef
Prss55
Tead4
Per2
Nr1d2
Mybph
Clock
Nfil3
B
Motifs enriched in DEGs Higher in Vehicle Control
Motifs enriched in DEGs Higher in iMSBmal1KO Control
Mef2c(MADS)
c-Myc(bHLH)
NPAS2(bHLH)
CArG(MADS)
c-Myc(bHLH)
CLOCK(bHLH)
NFAT(RHD)
bHLHE40(bHLH)
BMAL1(bHLH)
Tfcp2l1(CP2)
Foxh1(Forkhead)
Mef2c(MADS)
Phox2a(Homeobox)
Log10 P Value
(Directional)
C
Higher in Vehicle Control (Downregulated with KO)
Higher in iMSBmal1KO Control (Upregulated with KO)
Circadian rhythm
Pathways in cancer
AGE-RAGE signaling pathway in diabetic complications
Glycerolipid metabolism
Metabolic pathways
Starch and sucrose metabolism
Proteasome
Insulin signaling pathway
MAPK signaling pathway
AMPK Signaling Pathway
-Log10 P Value

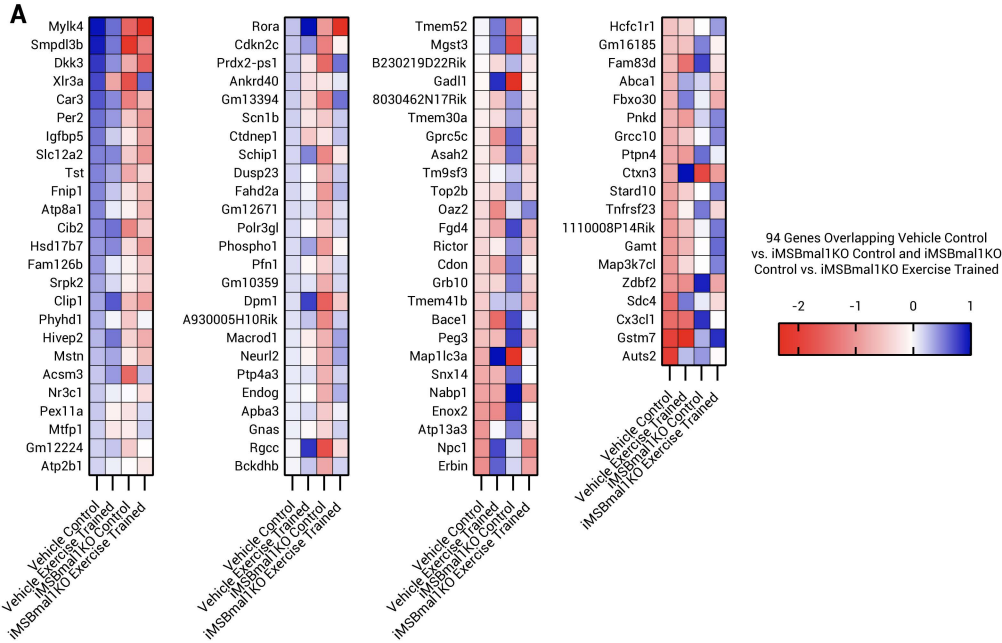
A
Mylk4
Smpdl3b
Dkk3
Xlr3a
Car3
Per2
Igfbp5
Slc12a2
Tst
Fnip1
Atp8a1
Cib2
Hsd17b7
Fam126b
Srpk2
Clip1
Phyhd1
Hivep2
Mstn
Acsm3
Nr3c1
Pex11a
Mtfp1
Gm12224
Atp2b1
Rora
Cdkn2c
Prdx2-ps1
Ankrd40
Gm13394
Scn1b
Ctdnep1
Schip1
Dusp23
Fahd2a
Gm12671
Polr3gl
Phospho1
Pfn1
Gm10359
Dpm1
A930005H10Rik
Macrod1
Neurl2
Ptp4a3
Endog
Apba3
Gnas
Rgcc
Bckdhb
Tmem52
Mgst3
B230219D22Rik
Gadl1
8030462N17Rik
Tmem30a
Gprc5c
Asah2
Tm9sf3
Top2b
Oaz2
Fgd4
Rictor
Cdon
Grb10
Tmem41b
Bace1
Peg3
Map1lc3a
Snx14
Nabp1
Enox2
Atp13a3
Npc1
Erbin
Hcfc1r1
Gm16185
Fam83d
Abca1
Fbxo30
Pnkd
Grcc10
Ptpn4
Ctxn3
Stard10
Tnfrsf23
1110008P14Rik
Gamt
Map3k7cl
Zdbf2
Sdc4
Cx3cl1
Gstm7
Auts2
Vehicle Control
Vehicle Exercise Trained
iMSBmal1KO Control
iMSBmal1KO Exercise Trained
94 Genes Overlapping Vehicle Control vs. iMSBmal1KO Control and iMSBmal1KO Control vs. iMSBmal1KO Exercise Trained
-2
-1
0
1

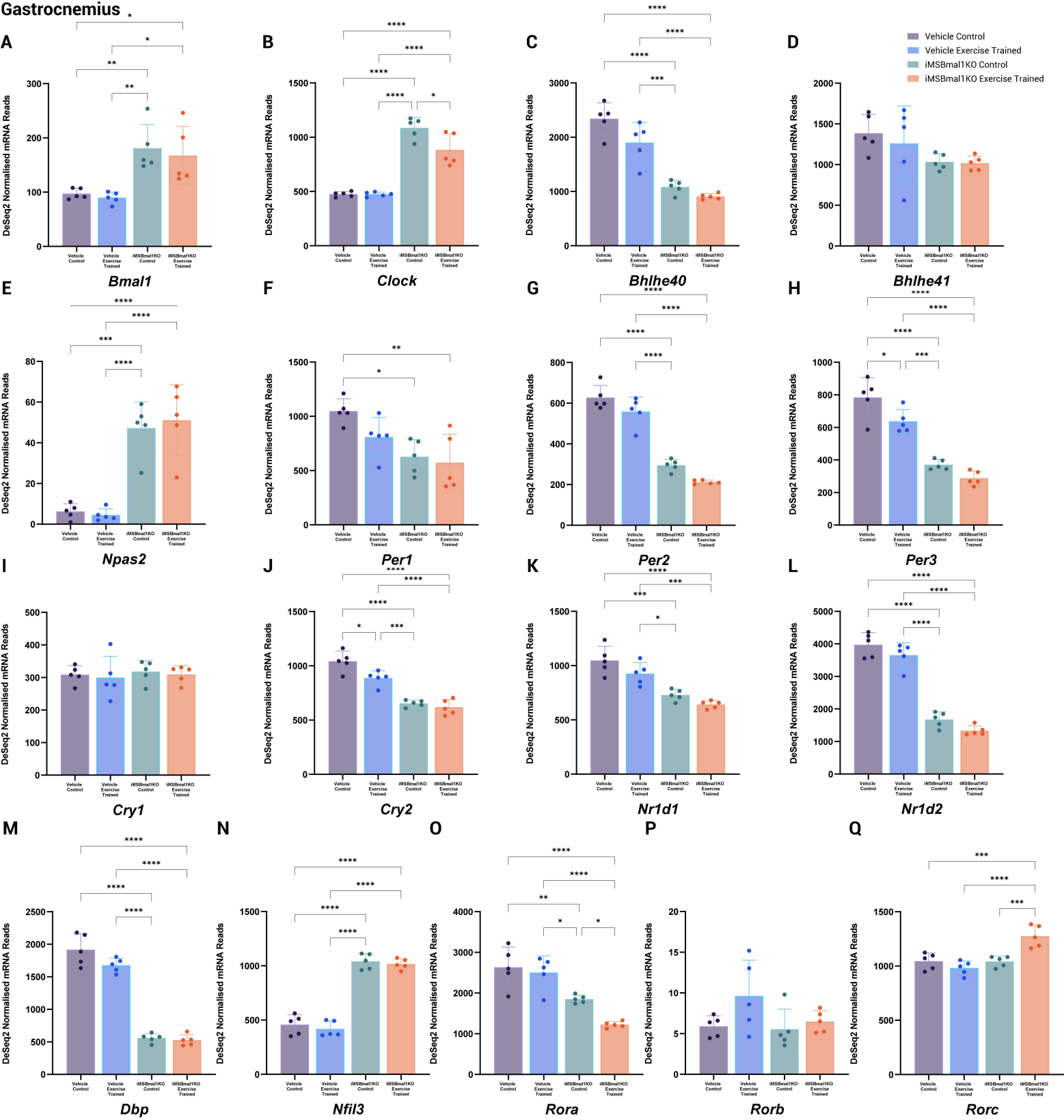
Gastrocnemius
Vehicle Control
Vehicle Exercise Trained
iMSBmal1KO Control
iMSBmal1KO Exercise Trained
DeSeq2 Normalised mRNA Reads
A
Bmal1
B
Clock
C
Bhlhe40
D
Bhlhe41
E
Npas2
F
Per1
G
Per2
H
Per3
I
Cry1
J
Cry2
K
Nr1d1
L
Nr1d2
M
Dbp
N
Nfil3
O
Rora
P
Rorb
Q
Rorc

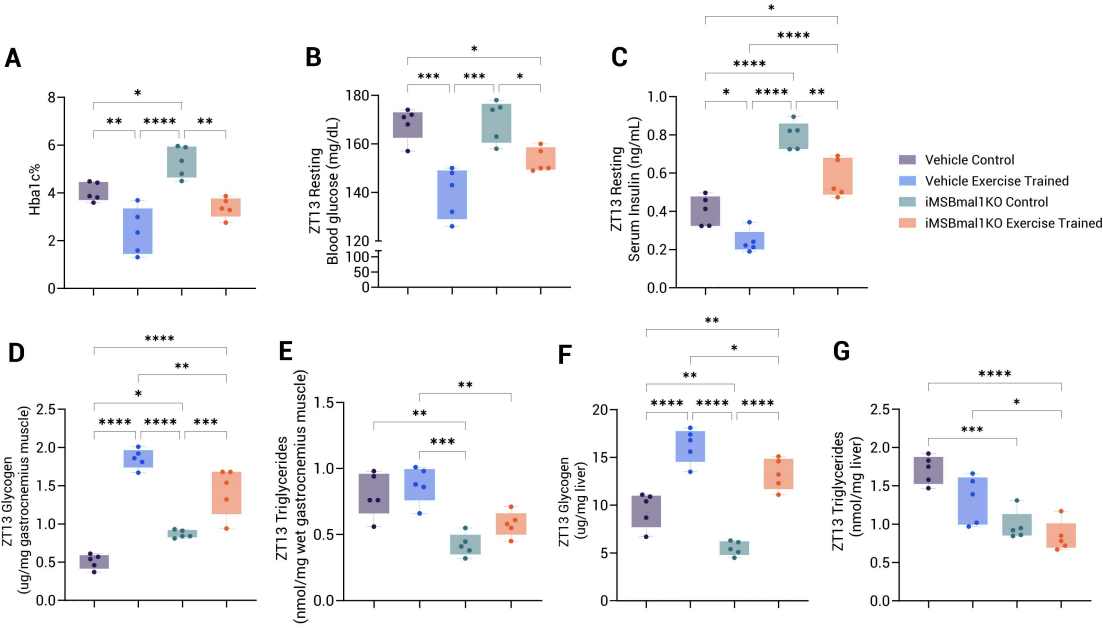
A
Hba1c%
B
ZT13 Resting
Blood glucose (mg/dL)
C
ZT13 Resting
Serum Insulin (ng/mL)
Vehicle Control
Vehicle Exercise Trained
iMSBmal1KO Control
iMSBmal1KO Exercise Trained
D
ZT13 Glycogen
(ug/mg gastrocnemius muscle)
E
ZT13 Triglycerides
(nmol/mg wet gastrocnemius muscle)
F
ZT13 Glycogen
(ug/mg liver)
G
ZT13 Triglycerides
(nmol/mg liver)

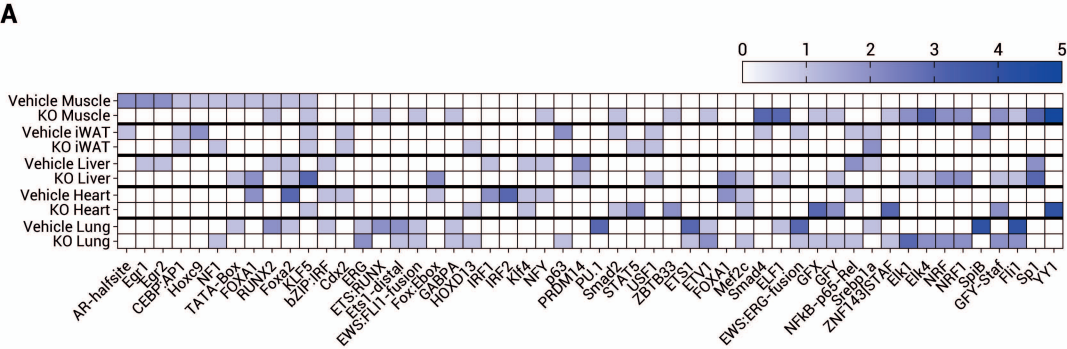
A
0
1
2
3
4
5
Vehicle Muscle
KO Muscle
Vehicle iWAT
KO iWAT
Vehicle Liver
KO Liver
Vehicle Heart
KO Heart
Vehicle Lung
KO Lung
AR-halfsite
Egr1
Egr2
CEBPAP1
Hoxc9
NF1
TATA-Box
FOXA1
RUNX2
Foxa2
KLF5
bZIP:IRF
Cdx2
ERG
ETS:RUNX
Ets1-distal
EWS:FLI1-fusion
Fox:Ebox
GABPA
HOXD13
IRF1
IRF2
Klf4
NFY
p63
PRDM1.4
PU.1
Smad2
STAT5
USF1
ZBTB33
ETS1
ETV1
FOXA1
Mef2c
Smad4
ELF1
EWS:ERG-fusion
GFX
GFY
NFkB-p65-Rel
Sreb1a
ZNF143:STAF
Elk1
Elk4
NRF1
NRF1
SpiB
GFY:Staf
Fli1
Sp1
YY1

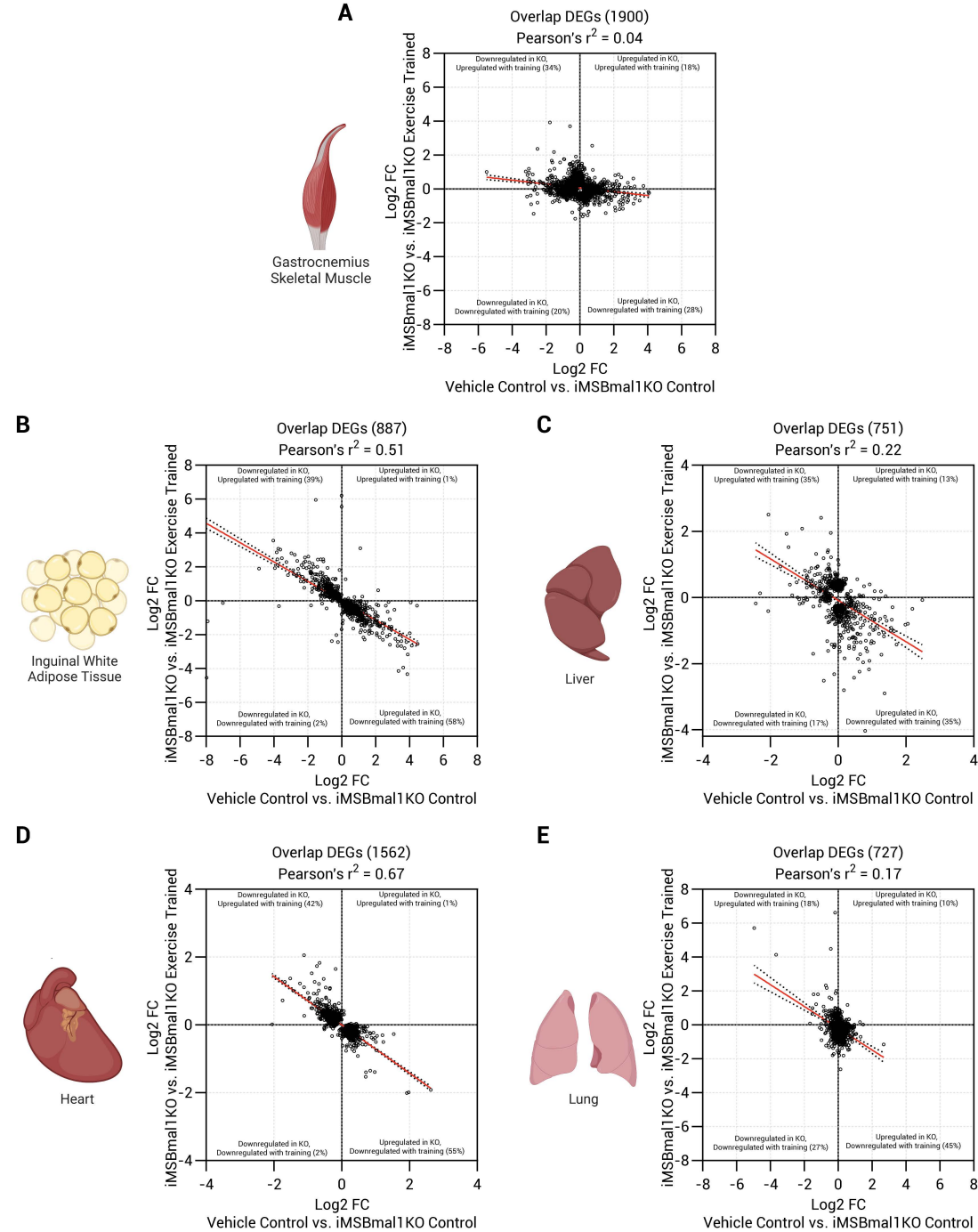
A
Overlap DEGs (1900)
Pearson's r2 = 0.04
Gastrocnemius Skeletal Muscle
Downregulated in KO, Upregulated with training (34%)
Upregulated in KO, Upregulated with training (18%)
Downregulated in KO, Downregulated with training (20%)
Upregulated in KO, Downregulated with training (28%)
Log2 FC iMSBmal1KO vs. iMSBmal1KO Exercise Trained
Log2 FC Vehicle Control vs. iMSBmal1KO Control
B
Overlap DEGs (887)
Pearson's r2 = 0.51
Inguinal White Adipose Tissue
Downregulated in KO, Upregulated with training (39%)
Upregulated in KO, Upregulated with training (1%)
Downregulated in KO, Downregulated with training (2%)
Upregulated in KO, Downregulated with training (58%)
C
Overlap DEGs (751)
Pearson's r2 = 0.22
Liver
Downregulated in KO, Upregulated with training (35%)
Upregulated in KO, Upregulated with training (13%)
Downregulated in KO, Downregulated with training (17%)
Upregulated in KO, Downregulated with training (35%)
D
Overlap DEGs (1562)
Pearson's r2 = 0.67
Heart
Downregulated in KO, Upregulated with training (42%)
Upregulated in KO, Upregulated with training (1%)
Downregulated in KO, Downregulated with training (2%)
Upregulated in KO, Downregulated with training (55%)
E
Overlap DEGs (727)
Pearson's r2 = 0.17
Lung
Downregulated in KO, Upregulated with training (18%)
Upregulated in KO, Upregulated with training (10%)
Downregulated in KO, Downregulated with training (27%)
Upregulated in KO, Downregulated with training (45%)